University of Kentucky Doctoral Dissertations   Graduate School

2011

DEVELOPMENT OF LUMINESCENT SENSING SYSTEMS WITH CLINICAL APPLICATIONS

Daniel F. Scott
University of Kentucky, dfs0112@aol.com

Right click to open a feedback form in a new tab to let us know how this document benefits you.

ABSTRACT OF DISSERTATION

Daniel F. Scott

The Graduate School

University of Kentucky

2011

DEVELOPMENT OF LUMINESCENT SENSING SYSTEMS WITH CLINICAL
APPLICATIONS

ABSTRACT OF DISSERTATION

A dissertation submitted in partial fulfillment of the
requirements for the degree of Doctor of Philosophy in the
College of Arts and Sciences
at the University of Kentucky

By

Daniel F. Scott

Lexington, Kentucky

Director: Dr. Sylvia Daunert, Professor of Chemistry

Lexington, Kentucky

2011

ABSTRACT OF DISSERTATION

DEVELOPMENT OF LUMINESCENT SENSING SYSTEMS WITH CLINICAL
APPLICATIONS

As the move towards the miniaturization of many diagnostic and detection systems continues, the need for increasingly versatile yet sensitive labels for use in these systems also grows. Luminescent reporters provide us with a solution to many of the issues at hand through their unique and favorable characteristics. Bioluminescent proteins offer detection at extremely low concentrations and no interference from physiological fluids leading to excellent detection limits, while the vast number of fluorescent proteins and molecules available allows the opportunity to select a tailored reporter for a specific task. Both provide relatively simply instrumentation requirements and have exhibited great promise with many of the miniaturized systems such as lab-on-a-chip and lab-on-a-CD designs. Herein, we describe the novel employment of luminescent reporters for four distinct purposes. First off, by combining both time and wavelength resolution we have expanded the multiplexing capabilities of the photoprotein aequorin beyond duel-analytes, demonstrating the ability to simultaneously detect three separate analytes. Three semi-synthetic aequorin proteins were genetically conjugated to three pro-inflammatory cytokines (interleukins 1β, 6, and 8) resulting in aequorin labeled cytokines with differing emission maxima and half lives to allow for the simultaneous detection of all three in a single solution through the elevated physiological concentration range. Secondly a semi-synthetic aequorin variant has been genetically enhanced to serve as an immunolabel and exhibited the ability to sensitively detect the acute myeloid leukemia marker, CD33, down to the attomole level in addition to improving aequorin imaging capabilities. In the third example, the aequorin complex was rationally, genetically split into two parts and attached to the termini of the cAMP selective cAMP receptor protein (CRP) creating a genetically fused molecular switch. The conformational change experienced by CRP upon the binding of cAMP translates into a loss of bioluminescent signal from aequorin and has shown the ability to respond linearly to cAMP over several orders of magnitude. Lastly, through custom design, a reagentless, portable, fluorescent fiber optic detection system has been developed, capable of being integrated into the body through a heart catheter. The system was able to respond to changes in potassium concentration selectively, reproducibly and reversibly with a fast response time of one minute.

_____
Daniel F. Scott

Daniel F. Scott
            3/28/2011
_____
Date

DEVELOPMENT OF LUMINESCENT SENSING SYSTEMS WITH CLINICAL
APPLICATIONS

By

Daniel F. Scott

_____

Sylvia Daunert

Director of Dissertation

John Anthony

_____

Director of Graduate Studies

3/28/2011

_____

Date

RULES FOR THE USE OF DISSERTATIONS

Unpublished dissertations submitted for the Doctor's degree and deposited in the University of Kentucky Library are as a rule open for inspection, but are to be used only with due regard to the rights of the authors.
Bibliographical references may be noted, but quotations or summaries of parts maybe published only with the permission of author, and with the usual scholarly acknowledgements.

Extensive copying or publication of the dissertation in whole or in part also requires the consent of the Dean of the Graduate School of the University of Kentucky.

A library that borrows this dissertation for use by its patrons is expected to secure the signature of each user.

Name   Date

_____

_____

_____

_____

_____

_____

_____

_____

_____

_____

_____

DISSERTATION

Daniel F. Scott

The Graduate School

University of Kentucky

2011

DEVELOPMENT OF LUMINESCENT SENSING SYSTEMS WITH CLINICAL
APPLICATIONS

DISSERTATION

A dissertation submitted in partial fulfillment of the
requirements for the degree of Doctor of Philosophy in the
College of Arts and Sciences
at the University of Kentucky

By

Daniel F. Scott

Lexington, Kentucky

Director: Dr. Sylvia Daunert, Professor of Chemistry

Lexington, Kentucky

2011

ACKNOWLEDGMENTS

TABLE OF CONTENTS

CHAPTER THREE:SIMULTANTIOUS MULTIPLEXED CYTOKINE ANALYSIS

VIA SEMI-SYNTHETIC AEQUORIN FUSION PROTEINS

CHAPTER FOUR:GENETICALLY ENHANCED SEMI-SYNTHETIC AEQUORIN

VARIANT WITH IMPROVED DETECTION AND IMAGING CAPABILITIES

CHAPTER FIVE:CYCLIC AMP RECEPTOR PROTEIN- AEQUORIN

MOLECULAR SWITCH FOR CYCLIC AMP

LIST OF TABLES

LIST OF FIGURES

CHAPTER ONE

STATEMENT OF RESEARCH

Luminescent sensing systems offer many advantages in a clinical, diagnostic, and research setting. To that end, the first goal of this work was to employ and expand the use of the photoprotein aequorin for novel analytical applications. The second goal of this work was to develop a compatible system for the fluorescent, real time monitoring of a desired analyte in a clinically relevant setting. The overall hypothesis for this work is that: *By altering, combining, and applying luminescent molecules in a new environment, novel luminescent sensing systems are developed that find relevance in a diversity of clinical and investigative areas. More specifically the photoprotein aequorin can be genetically manipulated and combined with chromophoric alterations to expand the number and type of detection platforms possible. Additionally by incorporating luminescent optode membranes on the tip a fiber optic, new monitoring applications are made possible.*

-Chapter 3 describes the development of a competitive assay for three clinically relevant cytokines of interest through the use of three different semi-synthetic aequorin complexes to expand aequorin's multiplexing capabilities beyond dual-analytes.

1

-Chapter 4 shows how genetic engineering can enhance the ability of aequorin to be used as a label through the addition of a unique cysteine to an aequorin mutant. The feasability was demonstrated through the detection and imaging of the acute myeloid leukemia cells and its surface antigen CD33.

-Chapter 5 demonstrates aequorin's unique ability to be genetically split and then structurally reformed. The bioluminescence can be modulated through a cAMP assisted conformational change of cAMP receptor protein.

-Chapter 6 details the development of a potassium ion sensor that is capable of being incorporated through a heart catheter to monitoring blood potassium changes *in vivo*, in real time.

CHAPTER TWO

INTRODUCTION

Adapted with permission from: Scott, D., Dikici, E., Ensor, C., Danuert, S., 2011. Bioluminescence and its Impact on Bioanalysis, *Annual Reviews of Analytical Chemistry*, 4, 297-319. Copyright 2011, Annual Reviews.

Bioluminescence Background

Bioluminescence is a natural phenomenon that has captivated the attention of mankind throughout human history. The Greeks had a fascination with bioluminescence and Aristotle reported detailed observations of bioluminescence in nature. Even earlier accounts of bioluminescence can be found in the legends of a number of ancient civilizations such as the Polynesian and Siberian (*1-2*). Bioluminescence has been at the center of various types of legends and superstitions, a part of religious beliefs and ceremonies, and more recently, the focus of scientific explorations.

Bioluminescence is the production and emission of light by a living organism. It has been observed in a diverse collection of organisms including insects, bacteria, fish, fungi, plants and an assortment of marine invertebrates (see figure 1). The functions of bioluminescence are just as varied, ranging from defense, predation, and communication to metabolic, in which it acts as a terminal oxidase (*3*). In general, the basis for the generation of bioluminescent light stems from a biochemical internal reaction whereas the substrate of an enzyme or the chromophore of a photoprotein undergoes a reaction that results
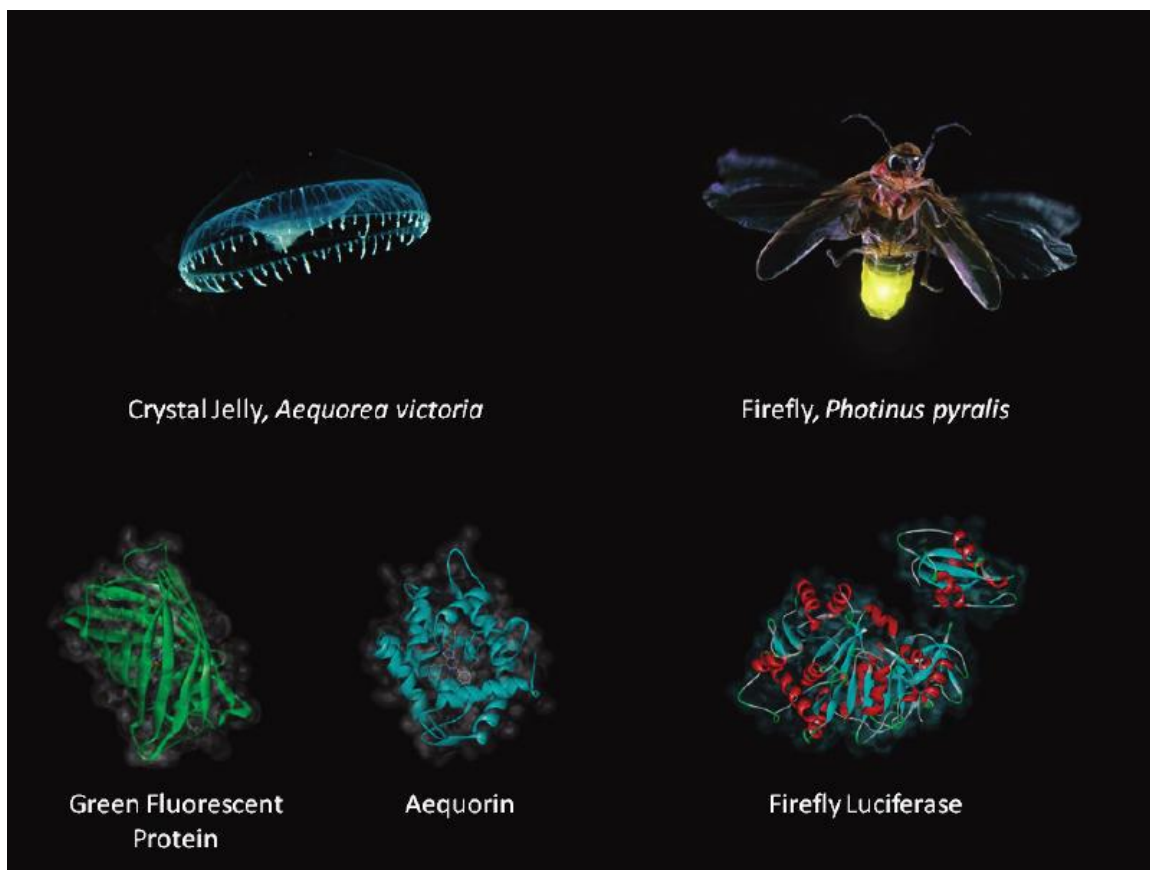
Figure 1. Several bioluminescent proteins are isolated from different organisms such as *Photinus pyralis,* and *Aequorea victoria.* Reprinted with permission from: Laura Rowe, Emre Dikici and Sylvia Daunert, 2009. Engineering Bioluminescent Proteins: Expanding the Analytical Potential. *Anal. Chem.*, 81 (21), pp 8662–8668. Copyright American Chemical Society, 2009.

in the excitation of the electrons into a higher energy level, which upon relaxation results in the emission of a photon.

Although the phenomenon of bioluminescence has been observed for thousands of years, it was not until more recently, roughly in the last 50 years, that the true analytical potential of bioluminescence started to be realized. A renewed interest in bioluminescence was prompted by the discovery and isolation of aequorin and the green fluorescent protein (GFP) from the jellyfish *Aequorea victoria* by Osamu Shimomura in 1962 (4). Later on, Martin Chalfie cloned GFP(*5*), making it widely available to researchers for a multitude of chemical and biological applications, and Roger Tsien prepared a series of mutants with an array of wavelengths of emission that resulted in proteins fluorescing in most of the colors of the spectrum (*6*). The applications that these proteins have found in biomedical research and bioanalysis are unprecedented. The importance and contribution of this discovery to major advances in science was recognized in 2008 when Osamu Shimomura, along with Martin Chalfie and Roger Tsien were awarded the Nobel Prize in Chemistry for the discovery and development of GFP (*7*).

Advancement in photonics instrumentation has also enabled the use of bioluminescence proteins in a number of detection and imaging applications. Bioluminescence offers marked advantages in this area, exhibiting efficient quantum yields (*8*). Moreover, given that the light generation is the result of a biochemical reaction, there is no need for an external excitation source, thus eliminating background noise associated with scattering from the source as well

as from autofluorescent molecules present in the sample (especially in physiological fluids). Therefore, the use of bioluminescent proteins has been especially successful in applications and fields requiring high sensitivity.

Advances in molecular biology have also greatly diversified the potential uses of bioluminescent proteins, which include their use as reporters and labels in intracellular ATP and Ca^{2+} detection, DNA and RNA hybridization assays, immunoassays, gene expression, whole-cell biosensors, bioluminescence resonance energy transfer (BRET) assays, and as labels for miniaturized systems such as lab-on-a-chip and lab-on-a-CD based instruments.

Bioluminescent proteins

Bioluminescent proteins are typically divided into two subgroups consisting of luciferases and photoproteins. The mechanism of bioluminescence emission of luciferases is characterized by an enzyme-substrate reaction where, in the presence of oxygen, the luciferase oxidizes luciferin (substrate) resulting in the formation of a product that is in an electronically excited state, and whose subsequent relaxation is responsible for the emission of a photon (*9*) (figure 2). Thus, the amount of light emitted is proportional to the concentration of the luciferin present.

Photoproteins, on the other hand, are capable of emitting light in a manner that is proportional to the concentration of the protein present. This type of protein could be considered as a very stable form of an enzyme-substrate complex where the dissociated forms are not energetically favorable and thus,

6
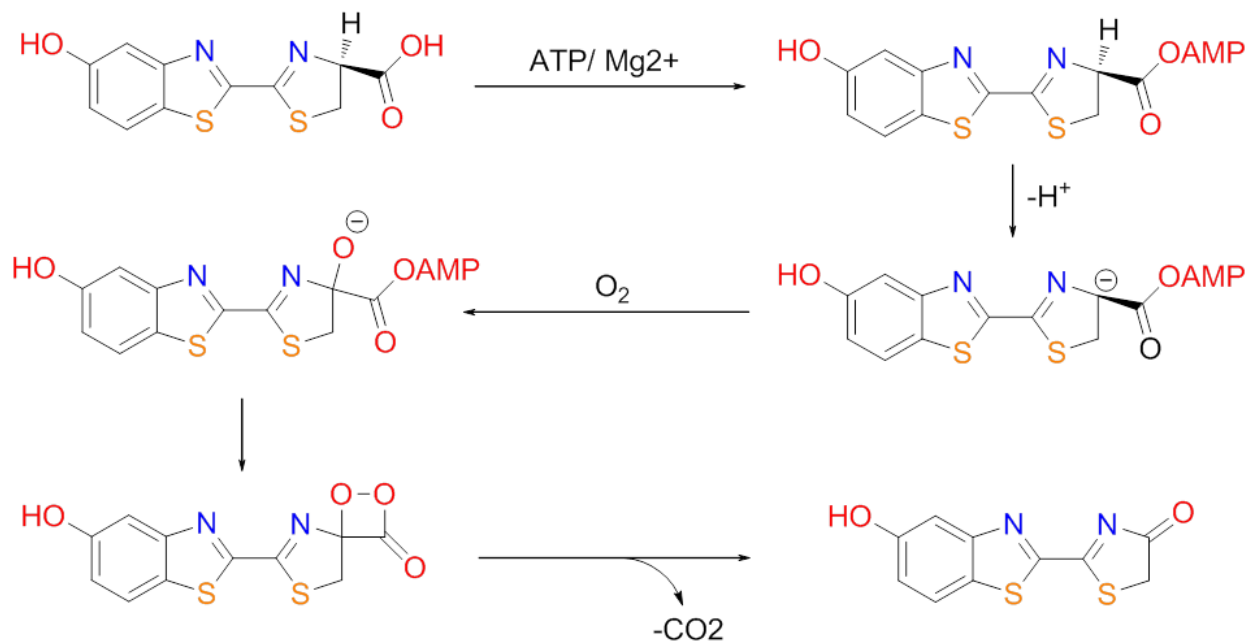
Figure 2. The ATP dependent reaction mechanism for the bioluminescence of firefly luciferase. With ATP and Mg^{2+} as co-factors, luciferase catalyzes the oxidation of luciferin which results in an excited state luciferin. When this excited state luciferin relaxes back down to the ground state, light is emitted corresponding the difference in the engery levels.

stay complexed and represent the primary light emitting component (*10*). Both, bioluminescent enzymes and photoproteins have distinct advantages and the preferential use of one type over the other often depends on the need at hand.

As mentioned above, bioluminescence occurs in a variety of terrestrial and marine organisms and, in vivo, bioluminescence serves numerous biological functions.   These functions range from feeding, mating, communication and concealment from predators (*11*).   Despite the abundance of bioluminescent organisms in the oceans, the number of bioluminescent proteins isolated and characterized from these organisms is surprisingly low, and consequently, their use in analytical applications is still fairly meager. This review will focus on the known proteins and their use and contributions and advancements in bioanalysis.

Some of the first and most extensively studied bioluminescent proteins are the luciferases found in certain beetles, particularly the firefly luciferase from the Lampyridaefamily. This group of luciferases from terrestrial insects also includes the railroad worm (Phengodidae family) and click beetle (Elateridae family) luciferases.   These luciferases generate bioluminescent light emission by catalyzing a reaction where oxidation of D-luciferin in the presence of ATP and O_2 results in an excited state, oxyluciferin, which upon relaxation emits a photon (*12*). The bioluminescence light produced by firefly luciferase is observed as a broad band with a wavelength of emission that peaks at 560 nm (3). These luciferases have found uses as labels in such applications as ATP assays for the estimation of total biomass, contamination of microorganisms, cell viability and

8

enzyme assays, and as a reporter gene in a variety of cellular and physiological investigations (*13*).

The most abundant source of bioluminescent organisms, however, is undoubtedly, the marine environment. A broad range of marine organisms exhibit bioluminescence (*11, 14*), but only a few of the bioluminescent proteins from these organisms have been employed in analytical applications. Among those are the luciferases found in the marine copepod *Gaussia princeps* and the sea pansy *Renilla reniformis*. These luciferases use coelenterazine as a substrate which, in the presence of molecular oxygen, undergoes an oxidation step that results in an excited form of coelenterazine, coelenteramide, that upon relaxation emits light (*14*). The wavelength of emission maxima of the *Renilla* and *Gaussia* luciferases are almost identical, at 485 and 490 nm, respectively (*15*). These luciferases have been employed in protein-protein interaction studies, BRET assays, and whole-cell biosensors, to name a few (*16-18*).

As with their terrestrial counterparts, marine luciferases are the bioluminescent proteins better characterized. In the marine bacterial luciferase from *Vibrio fischeri* and *Vibrio harvey*, the production of light is due to a two-step mechanism where the first step involves the reaction of luciferase bound to reduced flavin mononucleotide with oxygen to produce a peroxyflavin intermediate. This intermediate then reacts with an aldehyde luciferin endogenous in the bacteria to form a second intermediate, whose decay generates the emission of bioluminescent light at a wavelength of ~490 nm (see

figure 3) (*19*). An interesting aspect of this bioluminescent system is that the *lux*

cassette gene (*luxCDABE*) is responsible for coding for not only the luciferase,

but also the enzymes able to synthesize the necessary substrates for the

bioluminescence reaction, as opposed to the luciferin synthesizing enzymes of

other organisms, which are controlled by separate genes.   The incorporation of

the entire *lux* cassette as a reporter gene in biosensor applications, results in

systems where there is no need for the addition of the external luciferase

substrate, thus creating self-reporting systems.   Such technology has been

employed in the design and development of whole cell and protein-based

biosensing systems capable of monitoring water toxicity, heavy metals, quorum

sensing molecules (*20*), and organic compounds among others (*21-24*).

The photoproteins aequorin (figure 4) found in the jellyfish *Aequorea*

victoria, and obelin native of the hydromedusa *Obelia longissima*, differ from the

luciferase proteins in their mechanism of bioluminescence emission.   The

bioluminescence-emitting aequorin and obelin are formed by the apoprotein and

an imidazo-pyrazine chromophore, coelenterazine.   In these photoproteins, the

amount of bioluminescence generated is, therefore, proportional to the

concentration of the protein.   In both proteins, coelenterazine resides in a

hydrophobic pocket of the protein, and is oxidized in the presence of molecular

oxygen to form an excited coelenteramide (see figure 5). However, in aequorin,

for example, the coelenterazine in the hydroperoxide form is tightly bound in a

hydrophobic pocket that does not allow this oxidation. Upon binding Ca^{2+}, the

protein undergoes a conformational change, allowing the oxidation of the
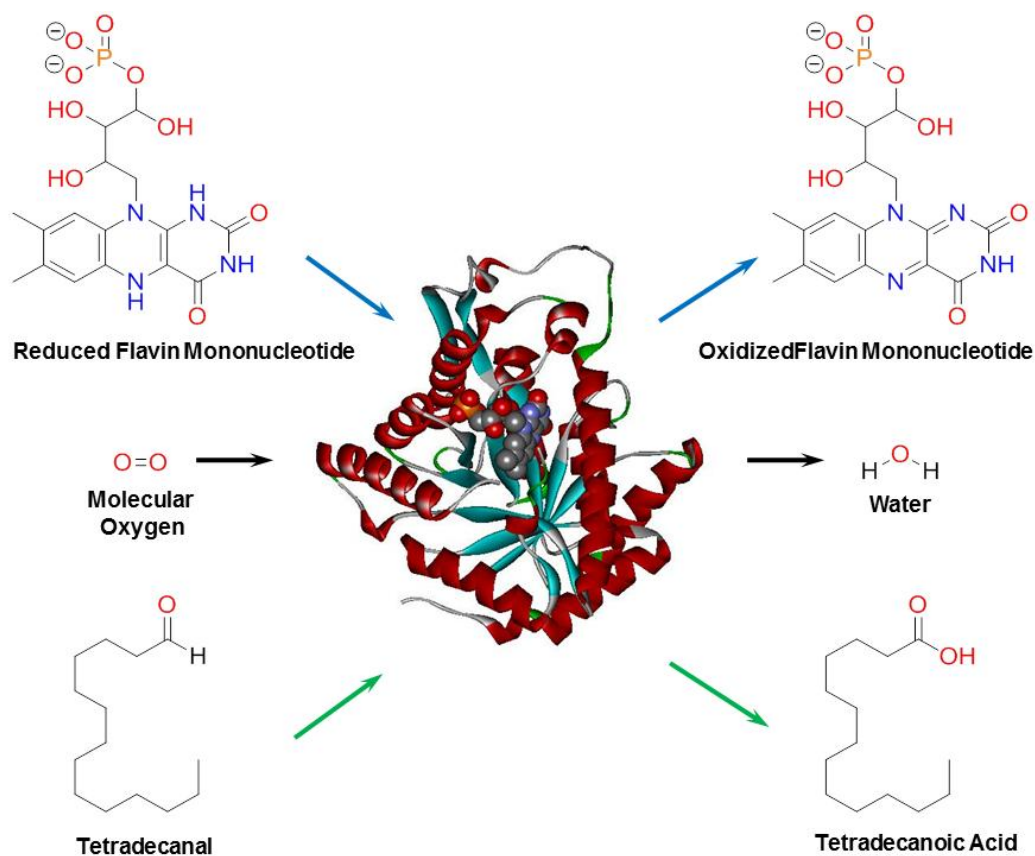
Figure 3. The reaction mechanism for the bioluminescence of bacterial luciferase. The production of light is due to a two-step mechanism where the first step involves the reaction of luciferase bound to reduced flavin mononucleotide with oxygen to produce a peroxyflavin intermediate. This intermediate then reacts with an aldehyde luciferin endogenous in the bacteria to form a second intermediate, whose decay generates the emission of bioluminescent light at a wavelength.
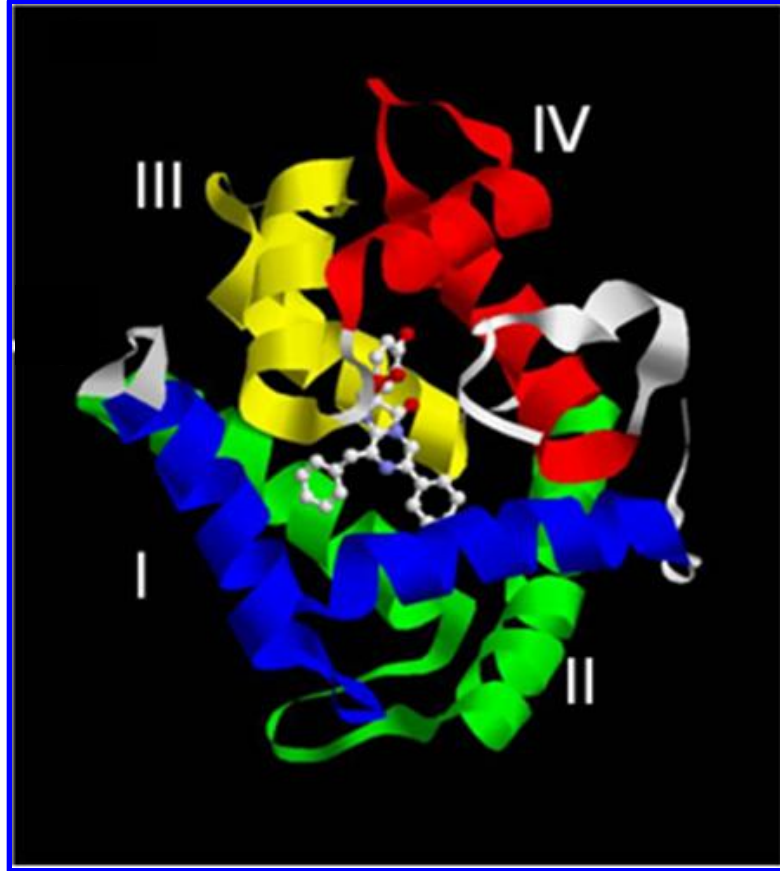
Figure 4. The ribbon structure of the photoprotein aequorin. The protein is composed of 4 EF hands highlighted by the different colors.
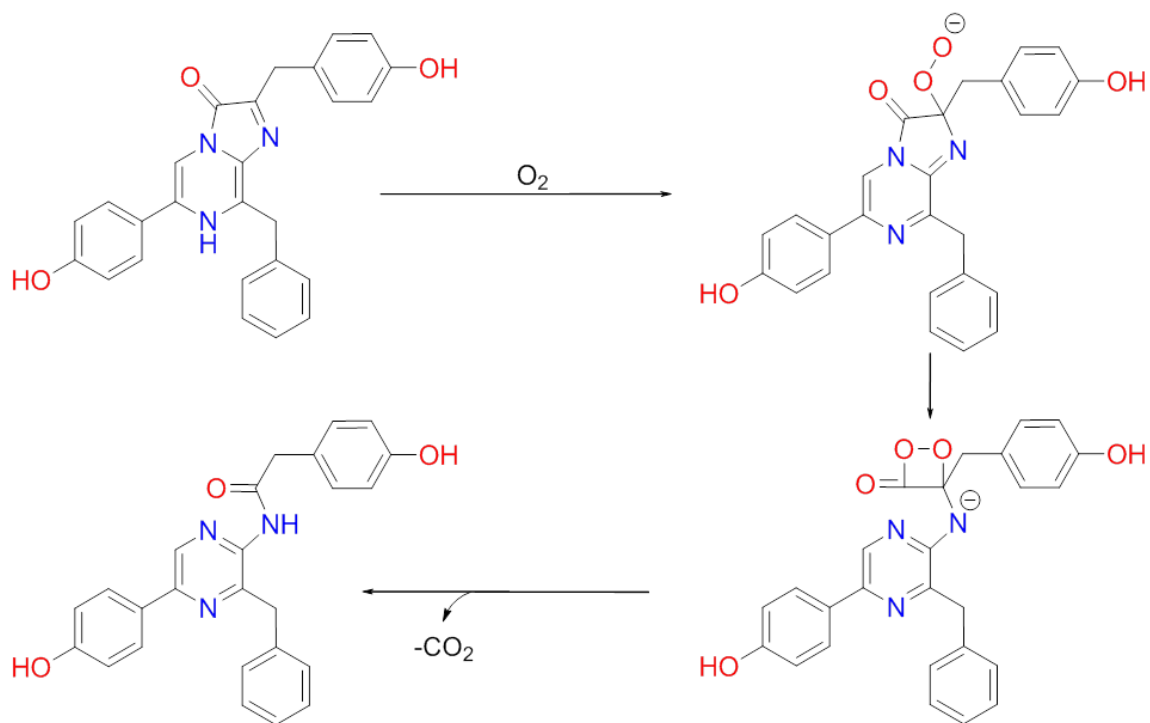
Figure 5. The reaction mechanism for the bioluminescence of aequorin. In the presence of Ca^{2+}- aequorin undergoes a conformational change, oxidizing coelenterazine in the process, which results in an excited state coelenteramide. The relaxation of this coelenteramide back to the ground state is accompanied by the release of a photon.

coelenterazine and subsequent conversion into a highly unstable dioxetanone intermediate. This intermediate then loses CO_2 yielding an excited enolate anion of coelenteramide, which upon relaxation produces a flash of light at 469 nm (*25-26*). The relaxed coelenteramide is still held by the photoprotein and is releasedvery slowly; if excess coelenterazine is added to the initial solution, the resulting light intensity will be directly proportional only to the amount of photoprotein in the sample (*25*). Since aequorin is a Ca^{2+}-regulated photoprotein, it was initially employed as a probe for monitoring of intracellular Ca^{2+}, but recently its use has been greatly expanded to other applications, among those hybridization and binding assays (*10, 27*).

Analytical Applications of Bioluminescence

As mentioned previously, bioluminescent proteins can provide the technology necessary to quantify extremely low concentrations of a desired analyte with the required sensitivity and reproducibility essential to today's scientists. Thus, it comes as no surprise that the use of these proteins has exploded recently in an abundance of different detection systems and methods. These includeassays for Ca^{2+} and ATP, as well as nucleic acid quantification and hybridization assays, and immunoassays, among other binding assays. In addition, bioluminescence has also been employed in resonance energy transfer and protein-protein interaction studies.

ATP Assays: Quantifying Energy Production

Many luciferase enzymes require ATP to catalyze the oxidation reaction of the luciferin substrate. In these cases, the absence of ATP blocks the bioluminescence reaction. Based on this premise, researchers have developed highly sensitive bioluminescent assays for the detection of ATP. For example, it has been shown that by employing firefly luciferase, ATP can be measured down to 0.01 fmol (*28*). A variety of different format assays have been implemented to date. A rapid screening test for to determine levels of ATP produced by contaminating fungi, bacteria, and yeast in food and feeds was developed by employing firefly luciferase. In this assay, the amount of light emitted was shown to directly correspond to the microbial number (*29*). With the increasing prevalence of multidrug resistant organisms, the ability to quickly screen a number of drugs for their effectiveness against different organisms would provide valuable information in the clinical setting (*30-31*). Lafond et al. have worked towards using bioluminescent assays for ATP for the rapid determination of antibiotic susceptibility. They were able to use the ATP assay in conjunction with adenylate kinase and quinine:NAD(P)H oxidoreductase in a parallel assay to demonstrate the ability to rapidly check for antibiotic resistance, shortening the investigation time to 6 hr while 24 hr of incubation is currently required. The future prospects include the automation of the system in a microplate format to allow for more high throughput screening applications (*32*). These are just a few of the examples of the bioluminescence ATP assays, as they have also been

employed for other hygiene (*33*), cytotoxicity (*34*), microbiological, drug discovery (*35*) and enzymatic assay applications (*13*).

Intracellular Calcium Ion Detection: Illuminating Signal Transduction Pathways

Similar to the initial use of luciferase for ATP measurements, the photoprotein aequorin was also first employed for the detection of its cofactor, Ca^{2+}. Aequorin was both injected into cells and expressed in vivo to monitor intracellular Ca^{2+} fluctuations in a variety of different cellular locations and in response to different external stimuli (*27, 36*). Two recently published book chapters by Michelini et al. and Villalobos et al. discuss, in detail, the methodologies and the instrumentation required for the imaging of Ca^{+2} in vivo (*37-38*). The determination of Ca^{2+} concentrations in physiological fluids and cells is important because of the role that this ion plays in cellular signaling events. The release of Ca^{2+} can be triggered by the activation of G-protein receptors and ion channels in the initiation of signal transduction mechanism in the cell. It is important to understand the mechanism of action of these receptors and ion channels and their interaction with Ca^{2+} to elucidate signaling pathways as well as to design and develop new drug targets (*39*). Thus, as the need for faster, more efficient detection methods capable of high throughput screening continues to progress, the inherent advantages of bioluminescence have been recognized by the recent use of aequorin in a high throughput screening for Ca^{2+} with a microplate reader setup. Menon et al. (*40*) intracellularly expressed apo-aequorin alongside a chimeric G-protein and a G-protein-coupled dopamine

receptor and used the cells to screen 8,106 compounds as potential drugs targeting G-protein coupled receptors and ion channels. Validation of this method and comparison with the current high throughput screening method of choice for the Ca^{2+} ion, a fluorescence based system, demonstrated similar performance with regard to the identification of positive hits. However, the bioluminescent-based system presents some advantages in that it is more cost-effective, has better reproducibility and a decreased number of false positives, most probably due to the lack of interference from autofluorescent compounds and excitation source.

Bioluminescence in Genetics: The Importance of DNA Detection.

Nucleic acids are the building blocks of the macromolecules DNA and RNA, and as such, they play a vital role in the function and replication of living organisms. DNA forms the basis of the genetic code that defines both our genotype, and later on our phenotype. In other words, DNA dictates, for example, what we look like and whether or not we may be carriers of a genetic disorder. In order to determine whether an individual is a carrier of a hereditary disease, it is necessary to establish the presence of harmful mutations in the DNA present in the affected chromosomes and determine their concentrations. Nucleic acids are present and experience changes at extremely low concentrations, which prompt the development of new emerging technologies based on bioluminescent detection. These methods afford the low detection limits needed for measuring nucleic acids (*41-42*). There are methods based on luminescence, i.e., real-time quantitative polymerase chain reaction (Q-PCR),

17

that have provided significant advances to the field. Briefly, Q-PCR consists of designing an oligonucleotide probe specific for the target DNA labeled with both a fluorescent probe and a related quencher molecule. The labeled oligonucleotide anneals to the target DNA, and as the polymerase progresses along the DNA strand it cleaves off the labeled probe, thus increasing the distance between the fluorescent probe and the attached quencher, which results in a subsequent increase in the observed fluorescent intensity (see figure 6). Drawbacks of this method include its costs, and the need for the preparation and labeling of the specific fluorescent nucleotide probes. A bioluminescent alternative has been developed utilizing the bioluminescence regenerative cycle (BRC). The premise behind the method involves the quantification of the pyrophosphate molecules released during the polymerization of the nucleic acids by the respective polymerase, which directly corresponds to the number of target molecules present. The released pyrophosphate is converted to ATP by an ATP-sulfurylaseenzyme, which then firefly luciferase can use to generate bioluminescence in the presence of luciferin (see figure 7). Additionally, after the ATP is used for the emission of light by the luciferase it is regenerated back to a pyrophosphate molecule making the recycling and amplification of the signal from one pyrophosphate molecule possible. It was shown that at a concentration of 1×10^{-8} M pyrophosphate, the amount of light produced at a given time interval is proportional to the number of nucleic acid molecules in a sample. This translates to a detection limit of 1 amol of DNA in a solution, allowing potential
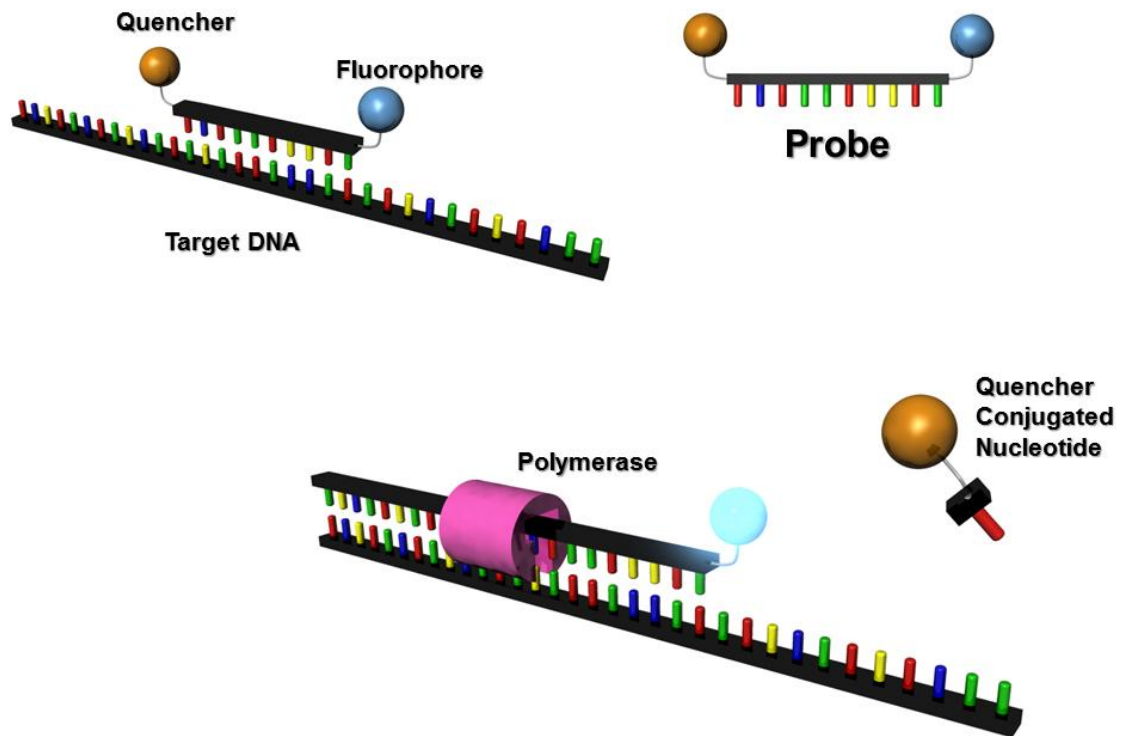
Figure 6. Schematic depiction of real time PCR the fluorescent equivalent to Q-PCR. The polymerization of the DNA cleaves off the quencher molecule, which allows the fluorescence from the fluorophore to be observed. The intensity of light from the fluorophore will be proportional to the amplification of the DNA.
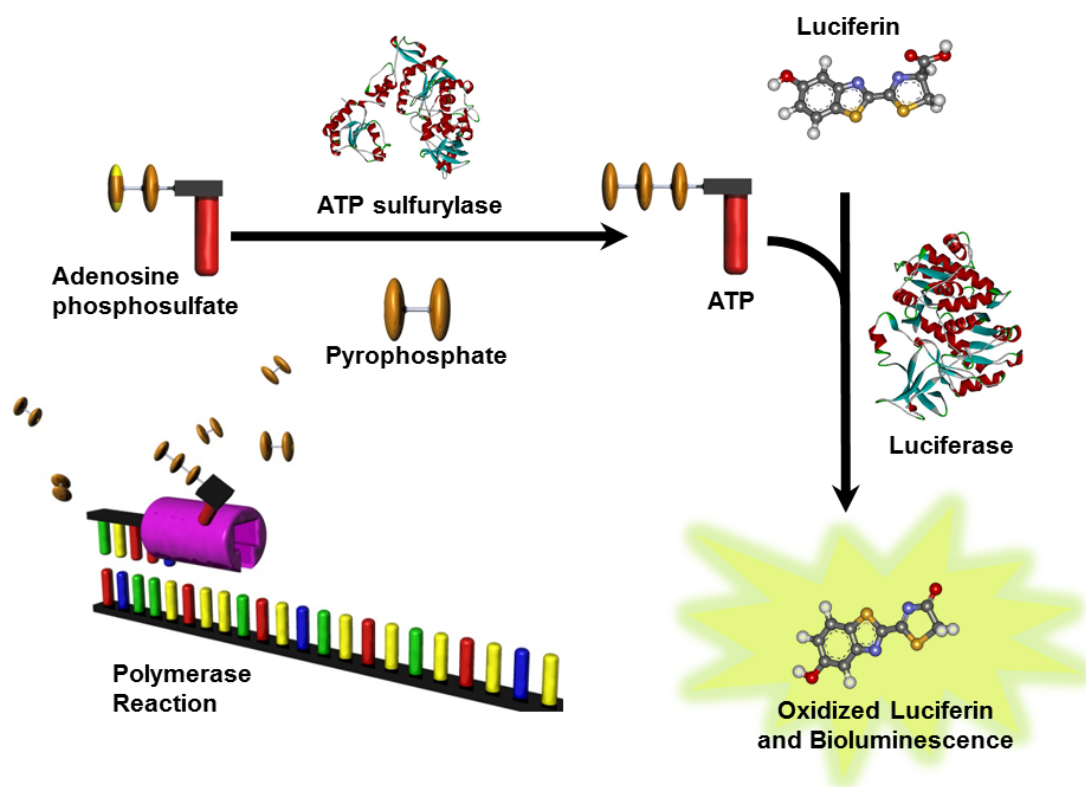
Figure 7.   Schematic depiction of bioluminescence regenerative cycle (BRC). The premise behind the method involves the quantification of the pyrophosphate molecules released during the polymerization of the nucleic acids by the respective polymerase, which directly corresponds to the number of target molecules present. The released pyrophosphate is converted to ATP by an ATP-sulfurylaseenzyme, which then firefly luciferase can use to generate bioluminescence in the presence of luciferin.

applications in gene expression, DNA and RNA quantification and single nucleotide polymorphism detection assays (*43*).

Additionally, with the sequencing of the human genome in 2003, single-nucleotide polymorphisms (SNPs) have recently surfaced as a potential marker for disease susceptibility and have been shown to be useful for monitoring drug effectiveness and side effects. Thus, the ability to quickly monitor and recognize the SNPs is valuable with applications in clinical medicine, genome drug discovery and personalized medical treatment (*44-45*). In a method similar to the previously mentioned BRC, a bioluminescence pyrophosphate assay has also been used for SNP detection. Here the pyrophosphate released by the DNA polymerization from a specific primer after the polymerization to the target DNA is converted to ATP by pyruvate phosphate dikinase, which can also be quantified by firefly luciferase bioluminescence. This method was capable of the identification of SNPs in both the p53 and K-ras genes (*46*). Variations in the mannose-binding lectin gene, a genetic defect associated with increased susceptibility to infection and autoimmune disorders, have also been identified using aequorin as the reporter in genotyping tests (*45*).

During the late 20$^{\text{th}}$ century, the popularity of solution hybridization assays along with the need to replace radioisotopes as labels in DNA and RNA detection, non-radiometric labeling options became preferred over the traditional radiolabels. As mentioned earlier, bioluminescence offers the sensitive detection desired without the safety issues that radioisotopes impose (*47-48*). In general, a bioluminescent protein is attached to the oligonucleotide of interest that is

21

complementary to an immobilized or target oligonucleotide sequence. A potential limitation of this method is inactivation of the bioluminescent protein upon conjugation to the oligonucleotide. However, a recent study has shown that this limitation can be overcome by using site-specific attachment methods. For example, Nagatsuki et al attached an oligonucleotide to a cysteine of luciferase without adversely affecting the luminescent activity or the selectivity of the probe (*49*). In another study, the photoprotein aequorin was employed for the sensitive detection of the malaria parasite *Plasmodium falciparum*. The assay was based on a competition between free target DNA and an aequorin-labeled DNA molecule. A genetically engineered aequorin was attached to the DNA oligonucleotide through a biotin-streptavidin interaction. Detection limits of 3 pg/µL in human serum were achieved, which fall within the range needed for diagnosis and management of malaria. The most important advantage of this method is that there is no need for PCR amplification of the target DNA, thus rendering an assay that can be prepackaged and used in a microtiter plate format allowing faster throughput analysis of a large number of samples. In addition, this assay offers advantages in terms of automation and the capability of use in developing regions and remote locations as compared to the current light microscopy technique for the parasite detection (*50*).

Driving the Detection of Biomolecules to the Lower Limits: Highly Sensitive Bioluminescence Immuno- and Binding Assays in Biomedical Analysis

In simple terms, an immunoassay is a method that measures the concentration of a species of interest within a complex biological matrix by employing biological reagents that display molecular recognition toward each other. In order to achieve the detection of a target analyte in a complex biological matrix, the method employed needs to be exceptionally selective. In immunoassays this selectivity is usually achieved by using antibodies raised against the analyte of interest, while in competitive binding assays the selectivity is provided by a binding partner, often a binding protein or a receptor, that displays high affinity for the analyte-ligand. Another issue to be taken into account when performing analysis in biological matrices is the potential low concentrations of analyte in the sample, which drives the choice for use of exceedingly sensitive labeling strategies. In the early times of immunoassays development, the required high sensitivity was reached by employing radionucleotides. Given the undesirable properties of radioactivity, researchers started to search for less dangerous alternatives by using electrochemical and optical methods. To that end, the number of applications of bioluminescent proteins as sensitive labels in immunoassays has increased dramatically in recent years (*8, 47, 51-53*). Bioluminescent proteins can be used for immunoassays either in a sandwich type or competitive assay format. The sandwich immunoassay consists of an antibody labeled with a bioluminescent protein which is used to quantify a target analyte bound by a separate antibody

attached to a solid support. As the amount of analyte in the solution increases so does the observed bioluminescent signal, as more labeled antibodies are able to bind to the analyte. In a competitive immunoassay format, the analyte of interest is labeled directly with the bioluminescent protein and competes with free unlabeled analyte in solution for a limited number of analyte-binding sites on the antibody. Thus, the amount of light produced is indirectly proportional to the amount of analyte present in a given sample. An increased amount of analyte results in fewer free sites on the antibody for the binding of the labeled analyte, which results in a smaller bioluminescent signal. In both cases, dose-response or calibration curves can be generated that correlate the amount of bioluminescence signal produced with the concentration of analyte present in the sample.

The conjugation of the bioluminescent protein to the analyte or antibody can be accomplished by either chemical or genetic conjugation methods. Chemical conjugation offers the convenience of the ability to use a single protein label for a broader range of applications by only altering the molecule to which the bioluminescent protein is attached, without having to express and purify a different protein each time. Traditionally, using chemical conjugation to label luciferases has been limited due to resulting loss of luciferase activity. However, conjugation through a biotin-streptavidin binding pair has been shown to be an effective method for maintaining the bioluminescence activity of luciferase. A biotinylated *Cypiridina* luciferase was used for a sandwich immunoassay for α-interferon with a linear range of detection of 7.8-500 pg/mL, demonstrating the

ability of the enzyme to provide sensitive and versatile detection (*54*). Interestingly, aequorin is more amenable to chemical conjugation than some of the other bioluminescent proteins. Although the activity can be adversely affected by chemical modification, the residual bioluminescence activity still allows for its effective use as a label in assay development. One such example involves the use a genetically modified aequorin with a unique cysteine that was recently used to chemically label α-fetoprotein antibody, a serological marker of liver cancer. The assay developed was capable of α-fetoprotein detection in the 0.02-200 ng/mL range (*55*). There are numerous other examples where aequorin has been incorporated as a label in immunoassays and has yield excellent methods for the determination of a variety of physiologically relevant analytes such as cortisol, thyroxine, and 6-keto-prostaglandin-F1-α, thus demonstrating the broad applications of aequorin in bioanalysis (*56*).

Genetic conjugation offers advantages such as a known one to one conjugation ratio and reproducible batch-to-batch production of the labeled probe. To accomplish this, the bioluminescent protein's coding gene is placed in frame with the target protein or peptide's coding sequence. Thus, after transcription and translation a single fusion protein consisting of the two proteins is created. An example of such a strategy can be seen in the angiotensin II assay in which an angiotensin II-aequorin fusion protein competed with free angiotensin in human serum and resulted in a detection limit of 1 pg/mL (*57*). Fusion proteins with obelin and luciferases have also been developed for a

variety of applications including streptavidin fusion proteins for biotin conjugations and assays for IgGs and other proteins of interest (*52*).

Designer Proteins: Split Bioluminescent Proteins and Molecular Switches

Proteins can be genetically manipulated by using an array of strategies encompassing fusions, site-directed and random mutagenesis, insertions, deletions, incorporation of unnatural amino acids into their structures, and even splicing. For the latter strategy, a protein is spliced or split in two fragments, which usually causes total or significant loss of its original activity, which is regained when the two fragments recombine. The proteins selected need to be able to regain their original activity or close to it, by either spontaneously reassemble or by coming in close contact via the help of a second protein. Researchers have utilized these strategies to split bioluminescent proteins into fragments and employed them to prepare molecular switches, protein complementation and protein-protein interaction assays (*58-61*). In all these assays, an external process such as analyte binding or protein interaction to reposition the fragments, modulating the bioluminescence emission of the protein, which can be related to the concentration of analyte present, and thereby allowing quantification or visualization of the event (see figure 8). The discovery of theinteraction between the split bioluminescent proteins and other analytes and/or proteins is an interesting and versatile one as it can form the basis for the design of a plethora of assays by choosing different methods to split and recombine the proteins.
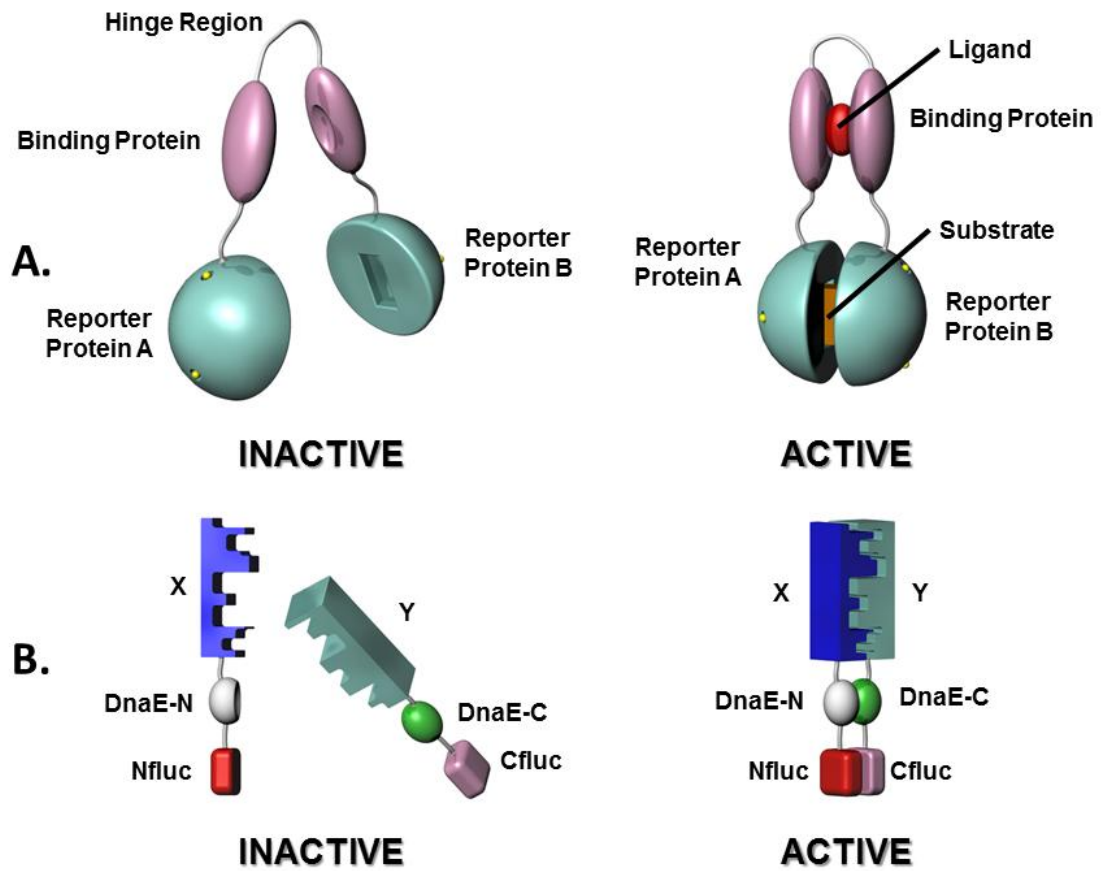
Figure 8. Schematics of bioluminescent A. molecular switches and B. split complementation assays. Molecular switches utilize a molecular recognition mediated conformational change of a binding protein to alter the position of the two fragments a reporter protein to modify the output signal. Split complementation assays rely on protein-protein interactions to facilitate the positioning of the reporter protein fragments into close proximity.

Many proteins in their natural environment require specific interaction and recognition of other protein complexes to be activated or to perform a function. Much still needs to be learned about these processes, as they are key to many fundamental events such as cellular functions, energy storage, on-set of disease, etc. Thus, new technologies that can provide insight into these interactions and mechanisms of action of proteins should advance the understanding of cellular events. To that end, protein complementation assays and protein-protein interactionshave been developed. An interesting example, albeit somewhat complicated with respect to its design involves splitting firefly luciferase and attaching, by genetic means, the N-terminal and C-terminal of the luciferase fragments to the N- and C-termini of the split intein containing DnaE, respectively to develop an assay for insulin. These fusion proteins were linked to a protein of interest, in this case the insulin receptor substrate 1 (IRS-1), which was attached to the N-terminal luciferase-DnaE and its target protein, the SH2 domain of PI 3-kinase, which was linked to the C-terminal luciferase-DnaE. The DnaE intein is known to excise out and ligate the flanking external proteins together, in this case the N- and C-terminal luciferase complexes. It was shown that the insulin induced phosphorylation of IRS-1 led to the recognition of the SH2 domain, bringing the DnaE fragments together, followed by the splicing of the luciferase fragments to reform the bioluminescently active luciferase. The corresponding light can then be directly correlated with the concentration of insulin in a dose-dependent manner (*62*). A similar mechanism with *Renilla* luciferase further demonstrated the versatility of such systems (*63*).

The study of protein-protein interaction employing protein splicing is not limited to intein-mediated reassembly as in the case described above. Indeed, *Renilla* luciferase has also been employed for such studies without the intein excision. Specifically, a genetically modified *Renilla* luciferase was split and attached to the Y941 peptide of the aforementioned IRS-1 and N-terminal SH2 domains, demonstrating an ability to detect low levels of insulin from pM to nM range (*64*). Small molecule mediated protein-protein interaction has also been investigated using the rapamycin-mediated interaction between the human FK506-binding protein and the FKBP12-rapamycin binding domain (*65*). Given the large number of potential target proteins for these types of assays, potential applications are limitless and include high throughput drug screening and investigation of specific pathways in signaling events, among others.

More recently, a molecular switch that employs the bioluminescent protein aequorin as its signal generator has been reported. This molecular switch differs from the protein complementation in that both components of the split bioluminescent proteins are attached to a single recognition protein. The two fragments of aequorin are genetically attached to the termini of the recognition protein, which upon the specific binding of a target analyte undergoes a conformational change, altering the orientation of the two aequorin fragments. This leads to an "on-off" type switch where the binding of the analytes can either turn the bioluminescence on or off, allowing for the quantification of the specific analytes. To this end an aequorin molecular switch for the detection of glucose was developed by inserting the DNA coding sequence of glucose galactose

binding protein (GBP) into the aequorin coding sequence, yielding a unique fusion protein with the two fragments of aequorin attached to the N- and C-termini of GBP. GBP, upon the selective binding of glucose, undergoes a conformational change to bring the two fragments of aequorin in close enough proximity to reassemble the bioluminescence complex, turning the bioluminescence on. The switch showed selective response to glucose over other sugars, and responded linearly at physiological levels of glucose (*66*).

Sensing with Living Cells: Whole-Cell Biosensors Based on Bioluminescent Reporters

Protein- based assays and biosensing systems have a proven record of excellent performance in the detection and quantification of analytes in different types of samples, those being biomedical or environmental toxins (*67*). A disadvantage of these systems is that they are not poised to indicate the bioavailability of said toxins, and therefore, researchers cannot gain information regarding information related to cytotoxicity, genotoxicity, or the synergistic toxic effects of these environmental pollutants upon living systems. Bioavailability and effect on cellular functions can only be obtained when employing whole-cell biosensors, which can gain insight into living cells, and help understand how a particular substance or group of substances will impact living organisms (*68-70*). In general, bioluminescent whole cell sensors are based on the principle that either a specific analyte or group of analytes will interact with living cells containing a gene for a bioluminescent protein. The interaction of the analytes with the cells will then either "turn" the bioluminescent property of the cells on or

off, depending on the type of system employed. Systems employing the "lights off" approach are typically applied in toxicity assays. In this assay format, a naturally bioluminescent species, such as *V. fisherii*, is exposed to a water sample. The premise of this type of toxicity assays, also known as cell-death based assays, is the known sensitivity of *V. fisherii* to a variety of environmental toxins. The presence of a toxin in the water sample can interfere with the metabolic pathway of the cell or block the expression of luciferase, which is observed as a decrease in the bioluminescence signal generated by the bioluminescent organism. Similar strategies have incorporated the luxCDABE cassette into different microorganisms including *E. coli, P. fluorescens*, and cyanobacteria, increasing the versatility of the whole cell sensing systems (*71*). For the "lights on" systems the expression of a bioluminescent gene, such as the luxCDABE cassette, is controlled by a selective promoter or a regulatory gene. Thus, when the target analyte is present, the expression of Lux proteins and subsequent bioluminescence is turned on to produce the bioluminescent signal (see figure 9). The specific DNA promoters allow the cells to be engineered to detect specific toxins, including heavy metals such as cadmium, lead, copper, and mercury among others, antibiotics, aromatic and other organic compounds, and quorum sensing molecules to name a few (*20, 72-78*). These types of biosensing systems have had an important impact in environmental analysis as well as in drug and cell screening in pharmacological and biomedical applications.
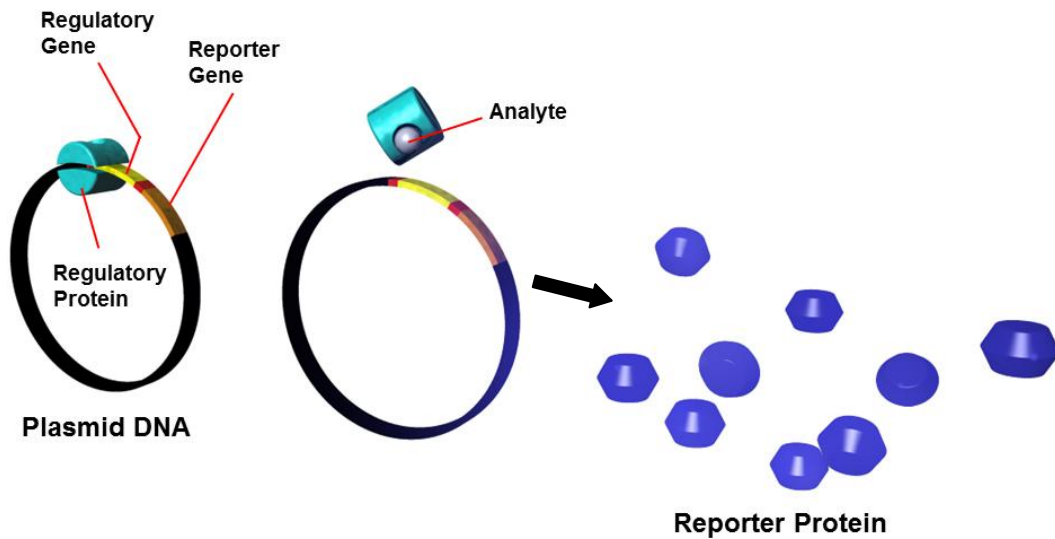
Figure 9. A schematic of whole cell bioluminescent sensors.The binding of an analyte to the regulatory protein turns on the transcription of the lux cassette gene and translation of the light producing proteins. Thus, the amount of light produced will be directly proportional to the concentration of analyte.

The Achilles' heel of living cell biosensing systems, which limits their field applications, is their long-term stability and the somewhat difficulty of their transport. To overcome these problems, the Daunert group proposed the use of sporulating microorganisms as the living cells that harbor the chosen sensing system. For that, they used sporulating bacteria such as *B. subtilis*and *B. megaterium*for the development of these sensing systems for arsenic and zinc. Spores can be stored for very long periods of time preserving its genetic material intact. Under favorable environmental conditions, spores can be germinated to generate viable and metabolically active cells during many cycles. To validate their hypothesis they employed a whole cell bioluminescent biosensing system based on reporter gene strategies capable of detecting arsenite. The data obtained demonstrated that after either six-months of storage or three cycles of sporulation/regermination, the sensing system retained its analytical performance in terms of detection limit, dynamic range and reproducibility, thus demonstrating the feasibility of employing spores as a means of long term storage and transportation of whole-cell biosensors(*79-80*). Storage strategies of this type could play a key role in enabling the use of whole cell sensing systems in on-site and field applications where the systems risk exposure to harsh or suboptimal conditions.

Taking a Cue from Nature: Bioluminescence Resonance Energy Transfer Assays

Bioluminescence resonance energy transfer (BRET) is a naturally occurring phenomenon which was first discovered in marine organisms (*81*). In

nature, there are plenty of examples of bioluminescence as a source of excitation of an acceptor protein that results in the emission of light at a different wavelength than that of the donor protein. Perhaps the best example of a bioluminescent protein emitting light to excite a second protein is that of the pairing of the photoprotein aequorin and GFP. In nature, in the jellyfish of the *Aequorea* family, aequorin and GFP reside in photocytes located in the umbrella of the jellyfish. Under certain circumstances that cause stress to the organism and when in cold deep dark locations of the ocean, the aequorin of the jellyfish emits bioluminescent light, which in turn via a radiationless energy transfer it excites GFP, which causes the now well-known and characterized typical emission of green fluorescence. Taking a cue from nature, researchers have designed BRET based systems that resemble those found in nature, where the energy produced by a bioluminescent protein is transferred from this donor molecule, to an acceptor over short distances. For the transfer to be effective this distance must typically be 10 nanometers and the bioluminescent donor protein emission profile must have good spectral overlap with the fluorescent acceptor molecule's absorption profile (*15*). BRET offers advantages over fluorescence resonance energy transfer (FRET) because it does not require an external excitation source. Therefore, it can be used in cells that are photosensitive, and also in cells exhibiting autofluorescence. The application of BRET also reduces the photobleaching problems associated with the fluorophores due to constant bombardment with high intensity sources. Since the donor and acceptor must be in close proximity, BRET has been employed for

the study of various protein-protein interactions (*82-84*), receptor-ligand interactions (*16*), conformational change studies (*85-86*), and RNA detection and quantification (*47*) in a variety of applications. The analytical applications of BRET have been the subject of recent reviews, and therefore, herein, will only be briefly covered (*15, 87-88*).

An interesting recent report described a novel biomineralization approach for the development of a near-infrared (NIR) light-emitting BRET complex. The emission of NIR light is advantageous in deep tissue imaging, thus, a NIR BRET complex should have a plethora of applications in medicine. Biomolecules have been used previously as a bottom-up control of inorganic nanostructure synthesis, however, in the biomineralization approach proposed the biomolecules serve a dual function, (1) as a template for nanostructure formation, and (2) as an active participant in the production of NIR light. In this work, a mutant *Renilla reniformis* luciferase acted as a template for the growth of PbS quantum dots. It was shown that the presence of luciferase was necessary as a template for the quantum dot configuration. The luciferase activity was preserved during this process, so that the addition of coelenterazine light was produced in the NIR region. The purified *Renilla reniformis* luciferase typically shows an emission maximum ~480 nm. This emission wavelength was still observed in the quantum dot complex; however, the intensity of the emission was significantly reduced compared to that of luciferase outside of the quantum dot, while emission in the NIR region appeared. This confirmed that there was a radiationless transfer of the energy from luciferase to the PbS quantum dot that yield the NIR emission.

This is an important example of coupling biological materials with inorganic ones, and broadens the scope of use of these types of hybrid structures in a wide range of fields (*89*).

Killing Two Birds (or More) with One Stone: Multianalyte Detection

One area where the use of bioluminescence has been limited in relation to other optical methods, such as fluorescence, is in multiplex detection. Multiplexing, or detecting multiple analytes within a given sample simultaneously has received much attention in recent years. To date, the reporters most utilized for multiplex assays are fluorescent compounds. Fluorescent reporters are available throughout the visible light region making the differentiation of signals from several different sources possible. Many of the bioluminescent proteins, however, exhibit broad emission profiles in similar regions impeding the discernment of multiple signals. The ability to use bioluminescent labels for multiplexing assays would offer advantages for many technologies requiring high sensitivity and low detection limits, such as miniaturized devices and high throughput screening assays. Great strides have recently been made in this area due to extensive mutagenesis studies performed on the bioluminescent proteins aequorin and luciferase as well as with the combination of multiple proteins. Firefly luciferase natively emits light with a maximum at around 560 nm (3). Through site directed mutagenesis, key amino acids were altered, shifting the emission maximum towards the red region at 615 nm and in the blue direction to 549 nm (*90*). With a 66 nm difference in emission maxima, the development of a dual analyte assay was possible. Further detailed

36

investigations on the mechanism of bioluminescence emission of the protein led to the understanding that the wavelength of light emitted is a result of the degree of molecular rigidity of the excited state species, affected by the interacting amino acids. This gained information laid the foundation for further tuning of the emission characteristics of luciferase (*91*). Another method of altering the emission maximum through the incorporation of non-natural amino acids has also shown promise, shifting the maximum to 603 nm (*92*).

An interesting approach to multianalyte detection is the so called "self-illuminating quantum dot conjugates". This methodology developed at the Gambhir laboratory at Stanford University involves the conjugation of different quantum dots to *Renilla* luciferase. The bioluminescence energy transfer between the luciferase and the quantum dots results in different colors of luminescence, which can be used to image cellular events or detect more than one analyte simultaneously (*93-94*).

The deep oceans are full of bioluminescent organisms that are not fully studied, catalogued, or are yet to be discovered. The growing collection of available bioluminescent proteins with different wavelengths of emission will offer an alternative to use genetic engineering to create proteins for use in multiplex analysis. Ito et al. employed two natural proteins, namely aequorin and luciferase that emit at different wavelengths, in the development of a dual analyte sandwich immunoassay for prostate specific antigen/α-fetoprotein and prostate specific antigen/prostatic acid phosphatase pairs. The assay utilized aequorin to label one antibody and firefly luciferase to label the other. The bioluminescence

of both proteins was triggered simultaneously by adding Ca^{2+} and D-luciferase to the wells in a microtiter plate. The signal emitted by aequorin was measured individually first, followed by that of luciferase detection. Both measurements were completed in 4 s. The assay showed high sensitivity and its performance correlated well with that of commercially available detection kits (*95*).

It has been also reported that the photoprotein obelin has also been spectrally tuned by altering the amino acid interactions with its chromophore, coelenterazine. Obelin, which natively emits light at a 491 nm wavelength of emission, was genetically engineered to emit at 493 and 390 nm. Mutations of positions W92F and H22E of the protein sequence yielded the obelin mutant with the 390 nm maximum, and a Y193F mutation resulted in the 493 nm variant. The proteins were used to label antibodies for the detection of the hormones hFSH and hLH, which are useful for the evaluation and diagnosis of diseases dealing with gonadal function. The light emitting reactions were triggered by the addition of Ca^{2+}, and the assay was able to achieve comparable detection levels to those obtained with radioimmunoassay techniques (*96*).

Similarly, aequorin has undergone extensive genetic modifications in the form of random and rational mutagenesis in the search for aequorin variants with a wide range of spectral characteristics. It should be noted that variations in the chemical structure of aequorin's chromophore, coelenterazine, also play a major role in affecting the mechanism of bioluminescence emission, and ultimately in altering the wavelength of emission of aequorin. Pairing aequorin with different natural and synthetic coelenterazines offers another avenue, in addition to

mutagenesis of the protein, by which the spectral characteristics of aequorin can be tuned (*97*). A large library of such semi-synthetic aequorin variants has been prepared and catalogued that display bioluminescence emission wavelengths that range from 448 nm to 519 nm (*98*). It is noteworthy to point out that because aequorin has a bioluminescence emission with flash-type kinetics, altering the structure of the protein and pairing it with different celenterazines results in an alteration of the decay lives of the protein. Wild type aequorin paired with native coelenterazine typically exhibits flash-type kinetics with a short half-life of ~ 2s. In contrast, aequorin mutants paired with the coelenterazine i analog showed half-lives ranging from 11.8 to 50.1 s, which are significantly longer than the majority of the other semi-synthetic aequorin combinations (*98*).

Non-natural amino acid incorporation into aequorin has also recently been reported as an alternative method of spectral tuning showing a shift in the emission maximum up to 517 nm (*99*). In this case, four non-natural amino acids were site-specifically incorporated into aequorin at amino acid positions 82 through the use of a specially designed tRNA and an amber codon. The introduction of the non-natural amino acid at a critical position within the aequorin's hydrophobic pocket where coelenterazine resides, resulted in altering the protein's interaction with coelenterazine, and as explained above this alteration resulted in a shift of the bioluminescence emission wavelength. An array of bioluminescence emissions with diverse spectral characteristics were recorded when the non-natural aequorin variants were combined with synthetic coelenterazines.

The aequorin variants paired with different coelenterazine analogues have been employed to develop a simultaneous, dual analyte assay in a single well for two important cardiovascular molecules, 6-keto-prostaglandin-FI-αand angiotensin II. A cysteine-free aequorin mutant was chemically conjugated to 6-keto-prostaglandin-FI-αand genetically fused to angiotensin II. The 6-keto-prostaglandin-FI-α aequorin complex was paired the native coelenterazine and showed a half-life of 0.5 s, while the angiotensin II-aequorin construct was paired with coelenterazine i and showed a half-life of 11.7 s. Two distinct time intervals of 0-6 s and 6-25 s were then used to differentiate the signals and allow for simultaneous detection (*100*) (See figure 10).

Fluorescence in Analytical Chemistry

Very similarly to bioluminescence, fluorescence has also been widely applied in analytical chemistry and aided in many scientific advances and breakthroughs. The major difference between bioluminescence and fluorescence lies in the requirement for an excitation source. While bioluminescence undergoes a chemical reaction to achieve an excited species, fluorescence relies on an outside light source to promote the chromophore to an elevated energy level. The chromophore will then relax back to the ground state, releasing a photon of light corresponding to the energy difference. Fluorescence offers some advantages over bioluminescence in that the intensity and duration of light emission can be adjusted by the excitation light. Along with this however comes the need for the incorporation of an excitation source into the instrumental setup and also the possibility of high background fluorescence from unintended
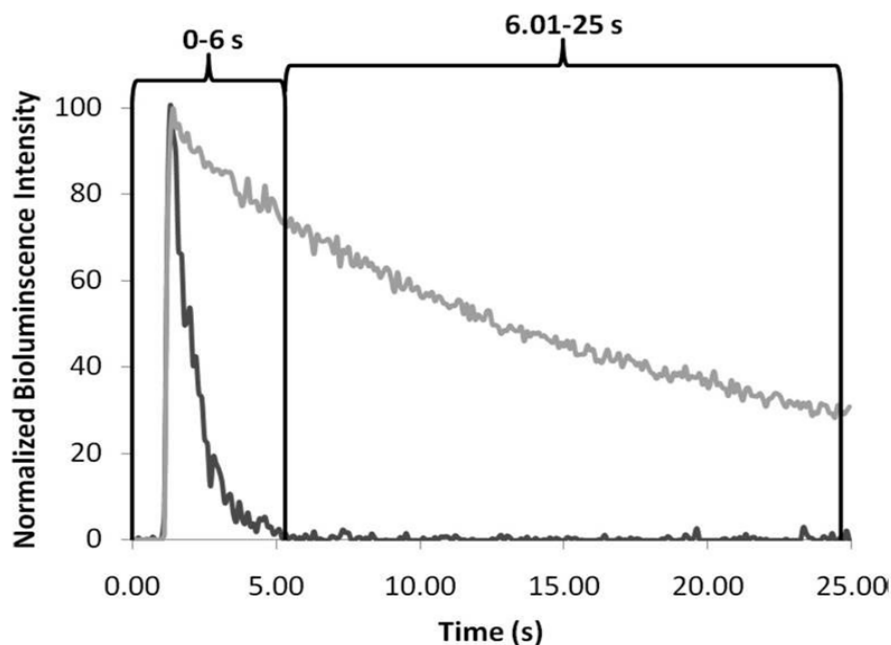
Figure 10. A visualization of the two kinetic windows used for the the duel analyte bioluminescent assay relying on half life difference for signal resolution. The signal windows were separated into a 0-6s window and a 6-25 window to allow the differientiation of the individual signals. Reprinted with permission from:Rowe, L., Combs, K., Deo, S., Ensor, C., Daunert, S., Qu, X., 2008. Genetically Modified Semisynthetic Bioluminescent Photoprotein Variants: Simultaneous Dual-Analyte Assay in a Single Well Employing Time Resolution of Decay Kinetics. Analytical Chemistry 80(22), 8470-8476.. Copyright 2008 American Chemical Society.

molecules, particular prevalent with physiological fluids, and the scattering of incident light. Despite these limitations fluorescence has been and continues to allow for very versatile and sensitive detection systems. Fluorescence is observed from a large population of sources including, but not limited to, small molecules, nanoparticles, amino acids, and proteins (*101-103*) (see figure 11). This diverse offering of fluorescent species catersto an increasing number of applications by allowing the selection of specific fluorescent molecules that can be optimized for the differing requirements of individual applications. Additionally,an assorted pallet of colors is also available enhancing the multiplexing capabilities (*101, 104-105*). The fluorescent labeling applications are nurmerous but include functions such as immunoassays, molecular tagging, imaging, protein-protein interactions, and forensics to name a few (*83, 103, 106*).

Fiber Optic Sensors

Fiber optics are traditionally associated with their use in the telecommunications industry, but over the years fiber optics have become a popular choice for the transduction oflight in a plethora of biosensors and detection systems. This wide spread used is merited by the many favorable characteristics they possess including chemical passiveness, small and customizable dimensions, immune to electromagnetic pickup, unaffected by harsh environments, and can carry light over vast distances (*107*). Fiber optics are composed of a cylindrical silica core surrounded by a silica cladding. The
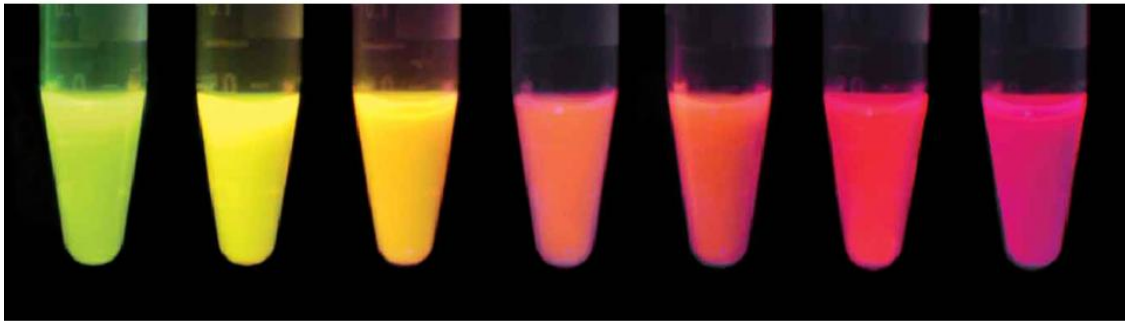
Figure 11. Different fluorescent proteins showing an example of the multiple colors avaible with fluorescent proteins.Reprinted by permission from Macmillan Publishers Ltd: [Nature Biotechnology] Shaner, N.C., Campbell, R.E., Steinbach, P.A., Giepmans, B.N., Palmer, A.E., Tsien, R.Y., 2004. Improved monomeric red, orange and yellow fluorescent proteins derived from Discosoma sp. red fluorescent protein. Nat Biotechnol 22(12), 1567-1572., copyright 2004.

refractive index of the core is slightly higher than that of the cladding which is what allows the total internal reflections and the ability to carry light extremely long distances with a minimal loss of intensity. As mentioned, fiber optic sensors have been used in a variety of circumstanses, including luminescent, reflectance and absorption based systems. Among the specific applications of fiber optic sensors include examples such as sensors for gases including hydrogen, oxygen, and hydrocarbons, pH, inorganic ions, glucose, DNA, and the employment with immunosensor and bacterial biosensing systems (*108-116*).

CHAPTER THREE

SIMULTANTIOUS MULTIPLEXED CYTOKINE ANALYSIS VIA SEMI-SYNTHETIC AEQUORIN FUSION PROTEINS

INTRODUCTION

Effective disease diagnosis depends largely on the knowledge of disease-specific biomarkers. In a majority of the cases, multiple biomarkers are necessary to accurately diagnose a disease. In addition, the levels of biomarkers can be very low in physiological fluids adding to the complexity of the problem. Thus, the knowledge of biomarkers complemented with a rapid, highly sensitive, and multiplex detection method is one of the challenges in medicine. Movement towards the miniaturization of many systems in order to save time, money and resources has also lead to the requirement for not only more sensitive, but also more versatile labels. Therefore, highly sensitive labels with multiplexing capabilities that can be employed in miniaturized systems are desired in clinical analysis. Luminescent proteins encompass many of these favorable characteristics and have the potential to unlock a vast new array of detection technologies. Bioluminescent proteins, including luciferases and photoproteins, have established themselves as vital components of the biosensing toolbox and have been used for an assortment of applications including gene expression, drug discovery, binding assays, *in vivo* indicators, and the study of protein-protein interactions (*5, 10, 117-121*). Bioluminescence offers distinct advantages over alternate detection methods, such as fluorescence or absorbance, including

lower detection limits due to essentially zero background signal in physiological fluids, no complications from an excitation source, simple instrumentation, the ability to be produced *in vivo,* biocompatibility, and lack of toxicity to living organisms (*8, 122*). Recent advances in instrumentation for the luminescence detection has also aided in the advancement of luminescent labels (*8*). However, unlike fluorescence-based detection, which can be performed at multiple emission wavelengths using different fluorophores or fluorescent proteins, bioluminescent proteins have lagged in this area. This issue has been tackled in a number of ways in current research that has expanded the utility of bioluminescent proteins in multiplex assays. Recent progress in this area includes using two different naturally available luminescent proteins to achieve resolved signals (*123-125*), genetically engineered bioluminescent proteins exhibiting shifted emission profiles (*96, 126*), and genetically mutated photoproteins, specifically aequorin, differentiated through time resolution (*100*). The previous studies, although greatly advancing bioluminescent assays, are limited to two analytes. These approaches have multiplexing capabilities but are limited by the availability of spectrally distinct or time-resolved mutants. In this study, we have demonstrated that by combining both the spectrally distinct mutants and time resolved mutants we can extend the multiplexing capability of the bioluminescent protein, aequorin. To that end, the photoprotein aequorin has been employed for the simultaneous detection of three separate analytes in a single well, the signals of which will be differentiated through the use of three discrete time/wavelength windows (figure 12). The three analytes of interest will

46

be conjugated to three different semi-sythetic aequorin proteins to create a competitive assay.   The aequorin labeled analytes will compete with free analytes in solution for a limited number of analyte binding sites. Thus, as the concentration of free analyte increases the number of aequorin labeled analytes able to bind will decrease, decreasing the observered bioluminescent signal.

Aequorin, native of the jellyfish *Aequorea victoria*, is a 22 kDa bioluminescent photoprotein with the active complex consisting of the apoaequorin, the imidazopyrazine chromophore coelenterazine contained in the protein's hydrophobic core, and molecular oxygen. The binding of calcium by aequorin triggers a conformational change in the protein leading to the oxidation of the coelenterazine to an excited state, which upon relaxation results in the emission of light with a λ_{max}~ 469 nm (*25, 127*). Aequorin has been mutated both site-specifically and randomly to generate mutant aequorin proteins displaying altered emission maxima, emission decay half-lives, and thermostability(*128- 132*).   Additionally, introducing synthetic coelenterazine analogues creating "semi-synthetic" aequorin have also shown altered bioluminescent properties (*97, 133-139*).   Thus, by combining both strategies of the mutated aequorin proteins and synthetic coelenterazines, an even greater diversity can be achieved (*98*). Herein we describe the simultaneous analysis of interleukins 1β (IL-1β), 6 (IL-6), and 8 (IL-8) in a single well through the genetic conjugation of the interleukins with semi-synthetic aequorin mutant proteins. These pro-inflammatory cytokines can serve as markers for the diagnosis and monitoring of a variety of diseases, including diabetes, prostate cancer, lupus, and hyperalgesia, but are present in
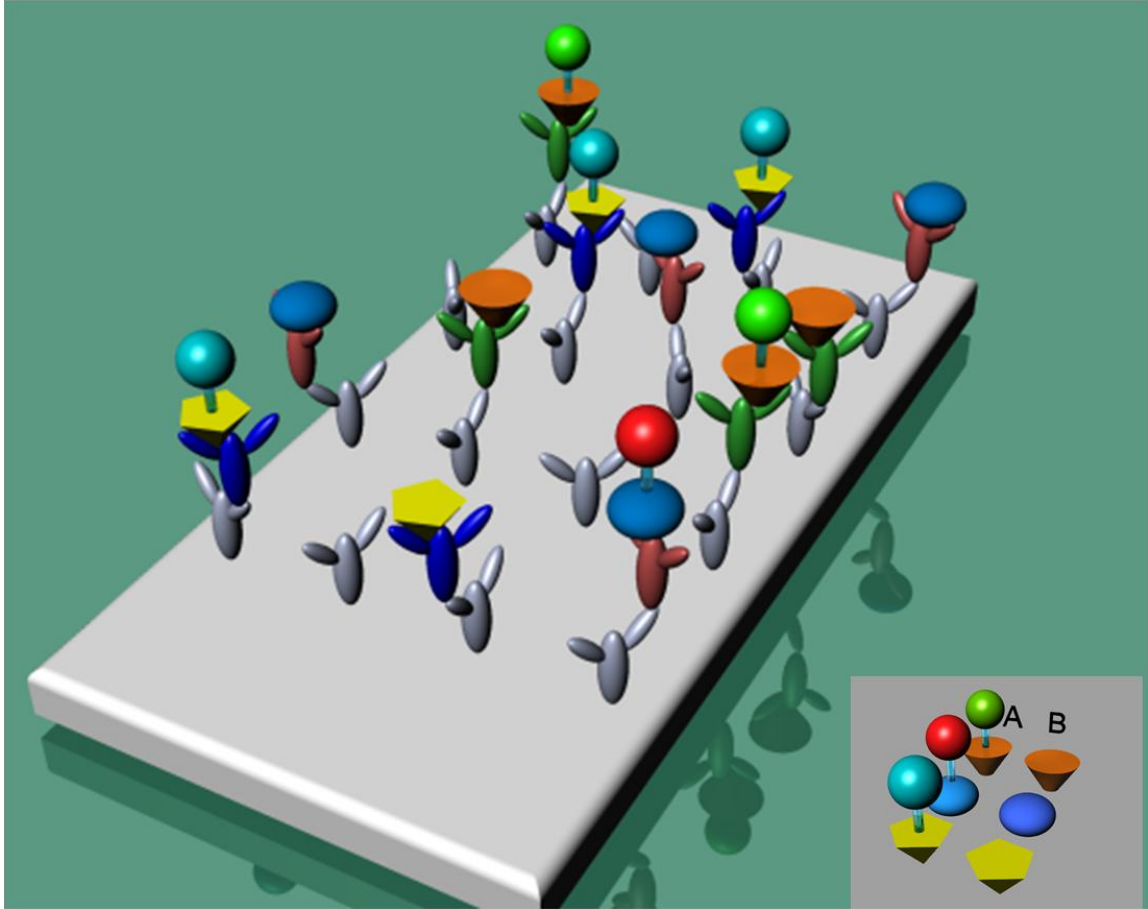
Figure 12. A schematic of the simultaneous competitive assay for IL1β, IL6 and IL8. The grey Y-shaped structures represent the anti-mouse IgG antibodies coated on the microtiter plates. Anti-human IL1β, IL6, and IL8 antibodies are represented by the green, red, and blue Y-shaped structures respectively. Column A in the lower right hand corner represents the interleukin-aequorin fusion proteins while column B represents the free interleukin proteins. IL1β is the orange cone and is attached to the Y82F aequorin mutant paired with ctz f (lime green sphere, detected in the 0-6 s and 515 nm window). The blue ellipsoid represents IL6 and the red sphere Y82F aequorin mutant paired with ctz i (detected in the 6-25 s and 515 nm window). The yellow triangle is IL8 and is fused with the F113W aequorin mutant (cyan sphere, detected in the 0-6 s and 410 nm window).

very low concentrations in physiological fluids (*140-145*). A rapid, sensitive, and multiplex assay systemswould be highly advantageous in the detection of biomarkers such as interleukins.

EXPERIMENTAL PROCEDURES

Reagents. Disodium ethylenediaminetetraacetate (EDTA), Luria-Bertani (LB) agar, and LB broth were purchased from Fischer Scientific (Fair Lawn, NJ). Diethylaminoethyl (DEAE) Fast Flow was obtained from GE Life Sciences. Poros 50 HQ was from AB Applied Biosystems (Foster City, CA). The Bradford protein assay kit was purchased from Bio-Rad Laboratories (Hercules, CA). Sodium dodecyl sulfate (SDS) was purchased from Curtin Mathesin Scientific (Houston, TX). Plasmid mini-prep kits and gel extraction kits were obtained from Qiagen (Valencia, CA). T4 DNA ligase, alkaline phosphatase, and EcoRI,HindIII, and BamHI, restriction enzymes were purchased from Promega (Madison, WI). Pfu Ultra polymerase and Taq polymerase were from Stratagene (Ceder Creek, TX). Tris(hydroxymethyl)amino methane (Tris) free base, ampicillin, Tween-20, sodium phosphate, sodium chloride, and bovine serum albumin (BSA) were purchased from Sigma Aldrich (St. Louis, MO). The cDNA clones of human IL-1β, IL-6, and IL-8 were purchased from ATCC (Manassas, VA). The standard human IL-1β, IL-6, and IL-8 proteins, Top10, Top10F, JM101 chemical competent cells and human serum were obtained from Invitrogen (Carlsbad, CA). Human IL-1β/IL-1F2 monoclonal antibody, human IL-6 monoclonal antibody, and human CXCL8/ IL-8 monoclonal antibody were purchased from R&D systems (Minneapolis, MN). Reacti-Bind goat anti-mouse IgG coated white 96-well plates

49

were from Pierce Biotechnology (St. Louis, MO). All chemicals were reagent grade or better and all aqueous solutions were prepared using 16 MΩ deionized distilled water produced by a Milli-Q water purification system (Millipore, Bedford, MA).

Apparatus. Polymerase chain reactions (PCR) were performed using an Eppendorf Mastercycler Personal thermocycler (AG, Hamburg). DNA electrophoresis was performed using a FB105 Fischer Biotech Electrophorese Power Supply (Pittsburgh, PA) and the gels were visualized using a UV Transilluminator (UVP, Upland, CA). OD_{600} readings were taken using a Spectronic 21D UV-vis Spectrophotometer (Milton Roy, Ivy Land, PA). Bacteria employed for the expression of the interleukin-aequorin fusion proteins were incubated in a Fisher Scientific incubator orbital shaker and Fisher Scientific open air orbital shaker (Fair Lawn, NJ) and harvested by a Beckman J2-M1 centrifuge (Palo Alto, CA). All chromatographical purifications were performed on a BioCAD SPRINT perfusion chromatography system from Perceptive Biosciences (Framingham, MA). Purity of the fusion proteins were verified by sodium dodecyl sulfate-polyacrylamide gel electrophoresis (SDS-PAGE) using Invitrogen 10-20% Tris-glycine gels in an Invitrogen X Cell Sure Lock Mini Cell (Carlsbad, CA). Bioluminescence measurements were made on a Polarstar Optima luminometer from BMG Labtech (Cary, NC) and decay kinetics analyzed with GraphPad Prism 5.0 (San Diego, CA). Emission spectra were taken on a custom made SpectroScan instrument from Sciencewares (Farmingham, MA).

Construction of Interleukin-Aequorin Mutant Fusion Proteins. Three different

fusion protein constructs were developed for assaying interleukin 1 (IL-1),

interleukin 6 (IL-6) and interleukin 8 (IL-8), simultaneously. Previously, aequorin

mutants when combined with synthetic coelenterazine analogs have been shown

to exhibit altered emission spectra (*98*). For this study, the genetic sequence

coding for the Y82F and F113W aequorin mutants were utilized (*135*). The

interleukin coding sequences were genetically attached to the aequorin mutants

of choice via overlap polymerase chain reaction (PCR) (figure 13). Each fusion

protein was also designed to contain a SGGGGS spacer sequence between

theaequorin mutant and interleukin. Aequorin mutant F113W was genetically

attached to the 3´ end of IL-8 (IL8F113W) and aequorin mutant Y82F was

genetically attached to the 3´ end of both IL-1β (IL1βY82F) and IL-6 (IL6Y82F).

The specifics for each over lap PCR are as follows (See Table 1 for primer

sequences):

The IL-1β genetic coding sequence was amplified with the IL-1β forward

primer which also introducedan*EcoRI* restriction site on the 5´ end, and the IL-1β

reverse primer. Meanwhile, the aequorin mutant Y82F coding sequence was

amplified using the Aequorin forward primerand the BamHI aequorin reverse

primer. This amplification introduced a BamHI restriction site on the 3´ end of the

aequorin gene sequence. The two sequences were combined and then

amplified with IL-1β forward and the BamHI aequorin reverse primer to yield the

IL1βY82F coding sequence. Similar genetic manipulations were performed with

the IL-6 coding sequence as a template and using the IL-6 forward and reverse

51
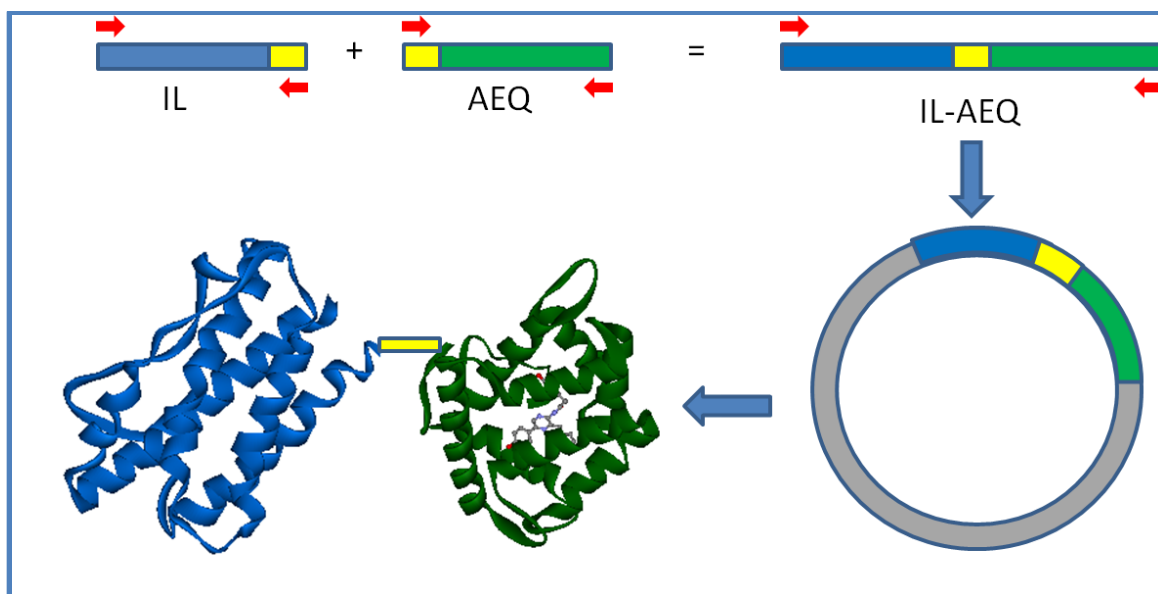
Figure 13. A schematic of the overlap PCR method used to create the IL-aequorin fusion proteins. Briefly, individual PCR reactions were performed to amplify the IL and aequorin gene separately while introducing a common linker region (represented by the yellow boxes). The individual products were then combined in a single PCR reaction and amplified with the IL forward and aequorin reverse primers to produce the conjugated fusion protein gene.

Primer	Sequence (5´-3´)
Aequorin Forward	TCTGGCGGTGGCGGTTCTGTGAAACTGACCAGCGACTTC
Aequorin Reverse BamHI	ATCGGATCCTTAGGGGACAGCTCCACCGTAGAGCTTTTCGGAAGCAGG GTCCATGGTGTA
Aequorin Reverse HindIII	ATCAAGCTTTTAGGGGACAGCTCCACCGTAGAGCTTTTCGGAAGCAGGG TCCATGGTGTA
IL-1β Forward	GAGGAATTCCAGATGCACCTGTACGATCA
IL-1β Reverse	TTTCACAGAACCGCCACCGCCAGAGGAAGACACAAATTGCATGGT
IL-6 Forward	GAGGAATTCCAAACTCCTTCTCCACAAGC
IL-6 Reverse	TTTCACAGAACCGCCACCGCCAGACATTTGCCGAAGAGCCCTCAG
IL-8 Forward	GAGGAATTCCAAGTGCTAAAGAACTTAGA
IL-8 Reverse	TTTCACAGAACCGCCACCGCCAGATGAGTTCTCAGCCCTCTTCAA

Table 1. The primer sequences used for the creation of the interleukin-aequorin

fusion proteins.

primers. This introduced an EcoRI restriction site on the 5′ end of IL-6. The Y82F aequorin mutant was amplified similarly with aequorin forward primer and the HindIII aequorin reverse primer to introduce the HindIII restriction site on the 3′ end of the aequorin gene. The IL-6 and aequorin sequences were combined and amplified with the IL-6 forward and HindIII aequorin reverse primers to yield the IL6Y82F coding sequence. Finally, the IL-8 forward and reverse primers were used in conjunction with the IL-8 coding sequence to introduce the EcoRI restriction site on the 5′ end. The aequorin forward and BamHI aequorin reverse primers were used to create a BamHI restriction site on the 3′ end of the F113W aequorin mutant. This sequence was combined with the newly created IL-8 coding sequence and the aequorin forward and IL-8 reverse primers were used to yield the IL8F113W coding sequence. The PCR reaction conditions were 95 ^{o}C for 30 s, 55 ^{o}C for 30 s, followed by 72 ^{o}C for 1 min/1000 base pairs and repeated for 30 cycles.

All of the fusion protein coding sequences were then inserted into an ompA containing pIN4 plasmid by using restriction digestions and subsequent ligations. The DNA sequencing was performed by the Advanced Genetic Technologies Center at the University of Kentucky to confirm the gene for the fusion proteins. Then, the plasmids containing the gene for IL1βY82F and IL6Y82F were transformed into JM101 *Escherichia coli* cells and grown while shaking at 250 rpm at 37°C in 500 mL LB broth containing 100 µg/mL ampicillin overnight to an OD$_{600}$ ~ 1.5. The proteins were expressed in the periplasmic space, thus they were isolated from the cells through osmotic shock and then

purified through ion-exchange chromatography. The proteins were loaded onto a DEAE Sepharose fast flow column in a 30 mM Tris/HCl pH 7.5, 2mM EDTA buffer. A gradient was then run from 0-50 % of 30 mM Tris/HCl pH 7.5, 2 mM EDTA, 1 M NaCl over 10 column volumes.   Four fractions of one mL volume were collected and fractions containing the highest concentration of the fusion proteins, determined by SDS-PAGE and aequorin activity, were pooled. The plasmid containing the IL8F113W gene was transformed into Top10F' *Escherichia coli* cells and grown with shaking at 250 rpm at 4^oC in 500 mL of LB broth containing 100 μg/mL ampicillin to an OD_{600} ~ 1.5. The fusion protein was expressed in the periplasmic space and was isolated from the cells through osmotic shock followed by the purification through ion-exchange chromatography using the same procedure as above. Protein concentration was determined by Bradford protein assay from Bio-Rad Laboratories (Hercules, CA). All purified proteins were stored at 4^oC until further use.

Decay Half-Life of Interleukin-Aequorin Fusion Proteins. The decay kinetics of each interleukin-aequorin fusion protein was examined with an array of coelenterazine analogues (ctz *ntv, i, f, cp, hcp, fcp, n, fcp, h*). A three molar excess of each coelenterazine analog was added to aliquots of each of the three interleukin-aequorin fusion proteins and incubated 18 h at 4^oC. The fusion proteins were then diluted with 30 mM Tris/HCl, containing 2 mM EDTA, 150 mM NaCl, 1 mg/mL BSA pH 7.5 (buffer A) until the maximal bioluminescent intensities were between 50,000 and 500,000 relative light units (RLUs) when analyzed on the Polarstar Optima luminometer. For the analysis, a volume of 10

μL of the coelenterazine bound fusion protein solution was added to the well of a microtiter plate and the bioluminescent light reaction was initiated by injecting 100 μL of 30 mM Tris/HCl pH 7.5 buffer containing 100 mM $CaCl_2$ (buffer B). The light intensity was then monitored for 25 s, with readings taken every 100 ms. The data was analyzed by GraphPad Prism 5.0 software using a non-linear, one phase exponential decay kinetics half-life equation.

Bioluminescent Emission Spectra of Interleukin-Aequorin Fusion Proteins. The bioluminescent emission spectral profile was observed for each of the fusion proteins again with same array of coelenterazine analogues as used for the half-life study. The emission spectra were collected on the SpectroScan, a custom made instrument based on the Thermo-Labsystems Luminoskan Ascent luminometer. The instrument is capable of recording the spectra of flash bioluminescence reactions in the range of 400-700 nm. Again, a three molar excess of each coelenterazine was added to aliquots of each fusion protein and incubated for 18 h at 4^oC. A volume of 10 μL of the coelenterazine bound fusion protein solution was then added to a well on a 96 well microtiter plate. A volume of 100 μL of buffer B was then injected in the well and the light was collected for 6 s.

Concentration Optimization of Fusion Proteins. Each fusion protein was incubated for 18 h at 4^oC with a three molar excess of a selected coelenterazine. The fusion protein IL1βY82F was incubated with coelenterazine *f*, IL6Y82F with coelenterazine *i*, and IL8F113W with coelenterazine *cp*. The fusion proteins were then serially diluted with buffer A. A volume of 50 μL of each protein of

selected concentration was added to a well on a 96 well microtiter plate, 100 µL of buffer B was injected into the well and bioluminescent signal was determined. The concentration optimization was performed on both the SpectroScan and Polarstar Optima. For fusion proteins IL1βY82F and IL8F113W the SpectroScan CCD exposure time was set to 6 s and the Polarstar Optima also collected light for 6 s. For IL6Y82F the SpectroScan CCD exposure time was set to 19 s with a 6 s delay and the Polarstar Optima collected light from 6-25 s in a 25 s collection window. The intensity at 452 nm for IL8F113W and 504 nm for IL1βY82F and IL6Y82F were plotted when analyzing SpectroScan data.

Binder Dilution Plots for Fusion Proteins with Interleukin Specific Antibody. Monoclonal anti-human IL1β, anti-human IL6, and anti-human IL8 antibodies, isolated from mice, were purchased from R&D Systems (Minneapolis, MN). Binder dilution studies were performed in identical fashion for all antibodies with exception to the exposure times as noted below. All antibodies were serially diluted in PBS buffer pH 7.4 containing 2 mM EDTA, 1 mg/mL BSA (buffer C) starting at an initial concentration of 10 µg/mL antibody. Anti-mouse IgG precoated 96 well microtiter plates were used for all experiments performed with antibodies. Prior to incubation each well of the anti-mouse IgG precoated 96 well plate was washed three times with 100 µL of 30 mM Tris/HCl, pH 7.4 containing 2 mM EDTA, 150 mM NaCl, 0.05% Tween-20 (buffer D). Next, an aliquot of 50 µL of each antibody concentration was added to the wells of the plate and allowed to incubate at 4°C with shaking at ~100 rpm for 2 h. The antibody solution was removed from the wells and the wells were washed three times with

buffer D. An aliquot of 50 µL of the corresponding fusion protein solution was then added to the wells and allowed to incubate with shaking at ~100 rpm, 4 $^{\circ}$C for 1 h. For the IL-1β antibody a concentration of 2.98 x 10^{-8} M IL1βY82F was used, 5.62 x 10^{-6} M concentration of IL6Y82F was employed with the IL6 antibody, and 2.39 x 10^{-7} M of IL8F113W fusion protein was used with the IL-8 antibody as determined from the concentration optimization studies of the fusion proteins. The wells were then emptied and washed again three times with buffer D. The microtiter plate was then loaded into the respective instrument and 100 µL of buffer B was injected into each well and the emitted luminescence light was collected. Binder dilutions plots were examined for both the SpectroScan and Polarstar Optima. For fusion proteins IL1βY82F and IL8F113W the SpectroScan CCD exposure time was set to 6 s and the Polarstar Optima collected light for 6 s also. For the fusion protein IL6Y82F the SpectroScan CCD exposure time was set to 19 s with a 6 s delay and the Polarstar Optima collected light from 6-25 s in a 25 s collection window. The intensity at 452 nm for IL8F113W and 504 nm for IL1βY82F and IL6Y82F were plotted when analyzing SpectroScan data.

Individual Interleukin Dose-Response Plots. Anti-mouse IgG coated plates were employed for all experiments. Before use each well was washed three times with 200 µL of buffer D. An aliquot of 50 µL of the respective antibody at the specified concentration (diluted with buffer C) was added to each well and allowed to incubate with shaking at ~100 rpm at 4 $^{\circ}$C for 1.5 h. The antibody concentrations used were as follows: 0.005 µg/mL for anti-human IL1β and anti-human IL6 and 0.05 µg/mL for anti-human IL6. The antibody solution from each

well was removed and again washed three times with 200 µL of buffer D. Human interleukin standards (Invitrogen, Carlsbad, CA) were serially diluted in buffer C and 100 µL of the varied concentrations (in triplicate) were added to the wells and allowed to incubate with shaking at ~100 rpm at 4°C for 1.5 h. The wells were emptied and washed with 200 µL of buffer D and 50 µL of the corresponding interleukin-aequorin fusion protein was added to each well and allowed to incubate with shaking at ~100 rpm at 4°C for 1 h. Fusion protein concentrations used in the study were as follows: IL1βY82F with coelenterazine f- 2.98x10^{-8} M, IL6Y82F with coelenterazine i- 5.62 x 10^{-6} M, and IL8F113W with coelenterazine cp- 2.39 x 10^{-7} M. The wells were emptied and washed with 200 µL of buffer D. Then, an aliquot of 100 µL of buffer B was added to each well, and the bioluminescent intensity was measured using both the SpectroScan and Polarstar Optima. For the SpectroScan the CCD exposure time was set to 6 s for the wells containing IL1βY82F and IL8F113W and 19 s with a 6 s delay for IL6Y82F. For the Polarstar Optima dual luminescence emission detection with two kinetic windows was utilized. Channel A contained a 410 nm filter and channel B housed a 515 nm filter (both of BMG Labtech (Cary, NC). The first kinetic window consisted of the 0-6s time frame after addition of the buffer B and the second window was 6-25s.

Simultaneous Multiplexed Interleukin Dose-Response Plots in Buffer and Human Serum. For the dose-response plots in buffer, pre-coated anti-mouse IgG plates were washed three times with 200 µL of buffer D. To each well, an aliquot of 50 µL of each of the anti-human interleukin antibodies in the same

concentrations as used for the individual dose response plots listed above was added and allowed to incubate for 1.5 h with shaking at ~100 rpm at 4 ^{o}C. The antibody solution was removed and the wells were washed three times with 300 µL of buffer D. An aliquot of 100 µL of each interleukin standard solution was then added to the wells. For each of the interleukins the response was examined in a dose-dependent manner while the concentration of the other two interleukins was held constant at 100 pg/mL. The interleukin solutions were allowed to incubate with shaking at ~100 rpm at 4 ^{o}C for 1.5 h. The solutions were then removed from the wells and the wells were washed three times with 300 µL of buffer D. An aliquot of 50 µL of each interleukin-aequorin fusion protein was then added to the wells and allowed to incubate for 1 h with shaking at ~100 rpm at 4 ^{o}C. The wells were then drained and washed three times with 300 µL of buffer D.

The same procedure was followed for the dose-response plot generated using human serum with the exception of the additions of the standard solutions. In order to establish a calibration plot, aliquots of human serum (Invitrogen, Carlsbad, CA) were spiked with the cytokines of interest to the final desired concentration. One of the cytokines was added in the varying concentrations while the other two were held constant at 100 pg/mL. A total volume of 200 µL of the human serum with the desired interleukin concentrations was added to each well and allowed to incubate with shaking at ~100 rpm at 4 ^{o}C for 1.5 h. The bioluminescent response was then observed on the Polarstar Optima after the addition of 150 µL of buffer B to each well. Dual luminescence, with the 410 nm

and 515 nm filters, was again employed in the two distinct kinetic windows of 0-6s and 6-25 s after the injections of buffer B into the well. All measurements were performed in triplicate with the mean value plotted.

RESULTS AND DISCUSSION

Three pro-inflammatory cytokines (IL-1β, IL-6 and IL-8) were chosen as biomarker candidates for the proof of principle multiplex detection system based on the fact that they are present in low concentrations in physiological fluids and their simultaneous detection would be beneficial in the diagnosis of a number of diseases (*140-145*). The current move towards miniaturization of many detection systems combined with low analyte concentrations in physiological samples requires extremely sensitive labels.   Multiplexing of assay systems would also prove advantageous and greatly improve the analytical and diagnostic value of the assay systems.   Bioluminescent labels can provide us with the required miniaturization potential and sensitivity however, up to now there have been few examples of their use in multiplex assays. Previously, semi-synthetic aequorin was used in a dual analyte assay based on time resolution (*100*), while obelin mutants and luciferases were applied in dual-color assays (*96, 126*).   By combining both time and wavelength resolution the bioluminescent multiplexing capabilities can be expanded even further in bioanalytical and medical applications.

The selection of semi-synthetic aequorins was centered off our previous work that studied the effect of genetic mutations and synthetic coelenterazines

61

on the observed emission maxima and decay kinetics of the semi-synthetic aequorins (*98*). Based on this work,we selected aequorin mutants Y82F and F113W as labels for the development of the current multiplex assay. This decision was based on the fact that these mutants would allow for maximal spectral and time resolution while maintaining ample bioluminescence activity. The genes for the interleukin proteins were fused to the genes of the aequorin mutants through an overlap PCR procedure and ligated into the pIN4 expression plasmid. Optimal expression of the IL1βY82F and IL6Y82F fusion proteins was achieved by introducing the plasmids into the *Escherichia coli* JM101 strain, while the IL8F113W was expressed in the TOP10F´*Escherichia coli* strain. Purity of the proteins was verified by SDS-PAGE. In addition to size, the aequorin bioluminescence activity and the visualization in a Western blot with the respective anti-interleukin antibodies confirmed that the proteins not only contained both the aequorin and interleukin portions, but also would bind as required with the antibodies employed in the assays.

Previous studies have shown that certain genetic mutations and different synthetic coelenterazines can result in altered emission characteristics of aequorin (*98*). To evaluate the effect of genetically attached interleukinson the bioluminescence emission of aequorin, each fusion protein was investigated with an array of synthetic coelenterazines with respect to the emission maxima and decay kinetics. A broad range of half lives was observed ranging from 0.10 s up to 14.2 s (Table 2b). In addition the emission maxima exhibited by the fusion proteins with same array of coelenterazines were also investigated. The

A.	IL1βY82F	IL6Y82F	IL8F113W
Coelenterazine	Emission Maximum (nm)	Emission Maximum (nm)	Emission Maximum (nm)
ntv	501	503	475
i	509	507	484
f	506	504	480
ip	480	481	453
hcp	480	483	453
h	501	501	470
cp	476	478	452
fcp	490	486	470
n	512	504	480

B.	IL1βY82F	IL6Y82F	IL8F113W
Coelenterazine	Half-life (s)	Half-life (s)	Half-life (s)
ntv	1.10	0.87	0.66
i	14.14	14.21	11.65
f	0.53	0.52	0.56
ip	0.39	0.39	0.59
hcp	0.10	0.10	0.12
h	0.20	0.19	0.19
cp	0.17	0.15	0.16
fcp	0.24	0.21	0.34
n	2.83	2.72	0.90

Table 2. A. The monitoring of the maximal emission wavelength of the different interleukin-aequorin fusion proteins with an array of synthetic coelenterazines. All measurements were performed in triplicate with the mean response used for analysis. B. The measured emission half-lives of the interleukin-aequorin fusion proteins with the same array of synthetic coelenterazines. All measurements were performed in triplicate with the mean response used for analysis.

emission profile through the entire spectra of the visible region was recorded by a liquid cooled CCD camera and the wavelength maximum was determined corresponding to the maximal bioluminescent emission intensity. A maximal wavelength separation of 57 nm was obtained ranging from 452 nm to 509 nm for the IL8F113W mutant and IL1βY82F mutant, respectively (Table 2a). Based on these results, semi-synthetic aequorin mutants with coelenterazines *cp*, *f*, and *i* were selected for theestablishment of three distinct time/wavelength windows in which the simultaneous discrimination of the three separate bioluminescent signals can be achieved. The fusion protein IL1βY82F was paired with coelenterazine *f*, IL6Y82F with coelenterazine *i* and IL8F113W with coelenterazine *cp*. This would allow IL-1β to be detected in the 0-6 s interval using a 515 nm filter. IL-6 can be detected in the 6-25 sinterval also with the 515 nm filter, and IL-8 can be distinguished in the 0-6 s interval using a 410 nm filter. Wavelength resolution between the IL1βY82F and IL8F113Wsignals was achieved using the band pass filters of 410 nm and 515 nm allowing for thedetection of both IL-1β and IL-8 in the 0-6 s kinetic window (figure 14a). After 6 s the only signal left is from the IL6Y82F emission, thus in the 6-25 s kinetic window with the 515 nm filter IL-6 can be detected as demonstrated in figure 14b.

Serial dilutions were made of each interleukin-aequorin fusion protein to determine the optimal concentration for use with the assay (figure 15). Concentrations of 2.98×10^{-8} M for IL1βY82F with coelenterazine *f*, 5.62×10^{-6} M
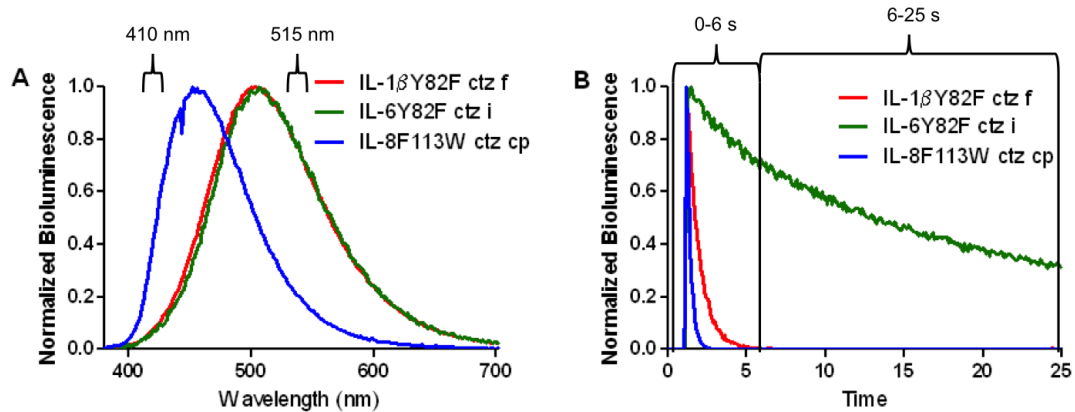
Figure 14. A. The emission spectra profiles of the three interleukin-aequorin fusion proteins with the respective ctz's combinations selected for the study. All measurements were performed in triplicate with the mean response plotted and normalized with the maximal intensity assigned the value of 1. B. The emission decay kinetics of the three fusion protein/ ctz combinations. All points are the mean of three replicates. The response was again normalized with respect to the maximal intensity which was made equal to 1.
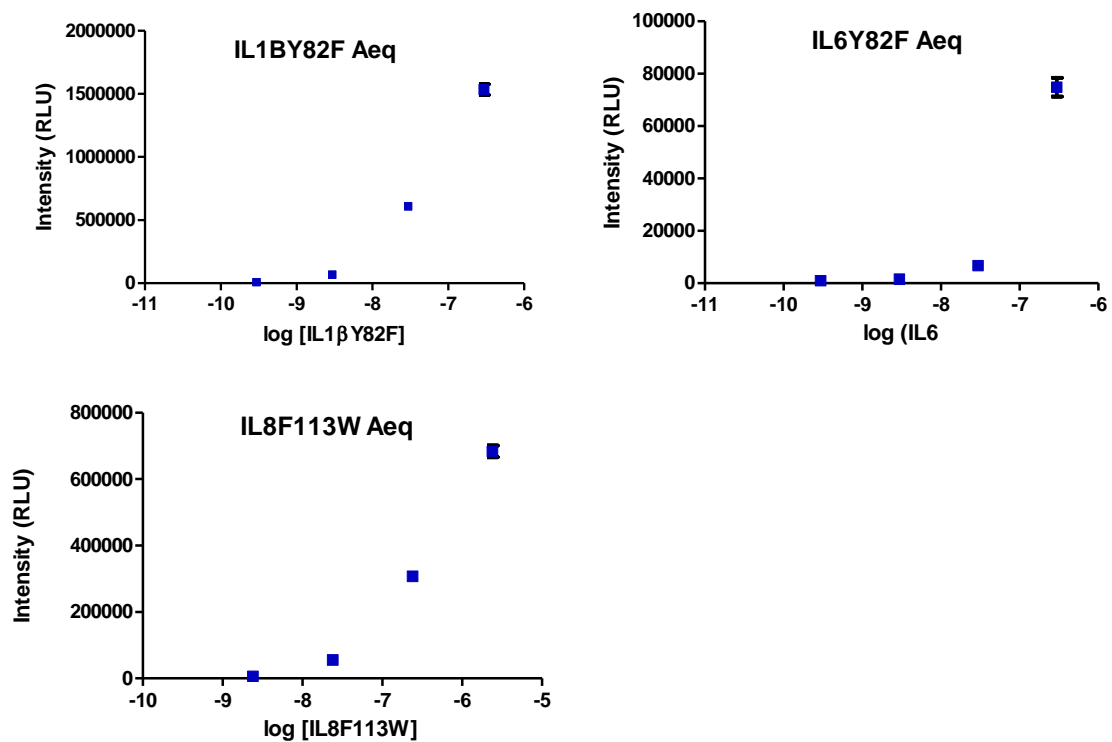
Figure 15. Concentration optimization of all three IL fusion proteins. All points are the average of triplicate measurements ± one standard deviation. Error bars not visible are concealed by the points.

for IL6Y82F with coelenterazine *i,* and 2.39 x 10^{-7} M for IL8F113W with coelenterazine *cp* were selected for the studies based on the fact that these concentrations allowed for significant amount of signal over the background while minimizing the amount of reagents used. Additionally, binder-dilution studies with the respective anti-human interleukin antibodies were performed to optimize the antibody concentration (figure 16). For that, anti-mouse IgG coated plates were utilized to allow for optimal orientation of the anti-interleukin antibodies (all mouse IgG) in the wells. An antibody concentration of 0.005 µg/mL for the anti-human IL-1β and IL-8 antibodies and a concentration of 0.05 µg/mL for the anti-human IL-6 antibody were found to be most favorable in terms of the detection range of the assay.Initially, the dose response-plots for the desired interleukins were executed individually to allow for optimization. Each of the interleukins were able to be detected through the physiologically elevated relevant concentration range (~10 pg- 1000 pg) (*146-148*) with detection limits of 0.1 pg/mL for IL-1β and IL-8 and 1.0 ng/mL for IL-6 (figure 17). Each interleukin was then assayed with all of the interleukins present in a single well (figure 18). A similar procedure was followed as for the individual dose-response plots with exception that all three of the antibodies, standards, and fusion proteins were added to each well. Two of the interleukin concentrations were held constant while the third wasincreased through the desired range to demonstrate that the observed change was only affected by the expected fusion protein signal. The concentrations of the two interleukins were held constant at a typical elevated concentration of 100 pg/mL. Even though the fixed concentration is high, it does

67
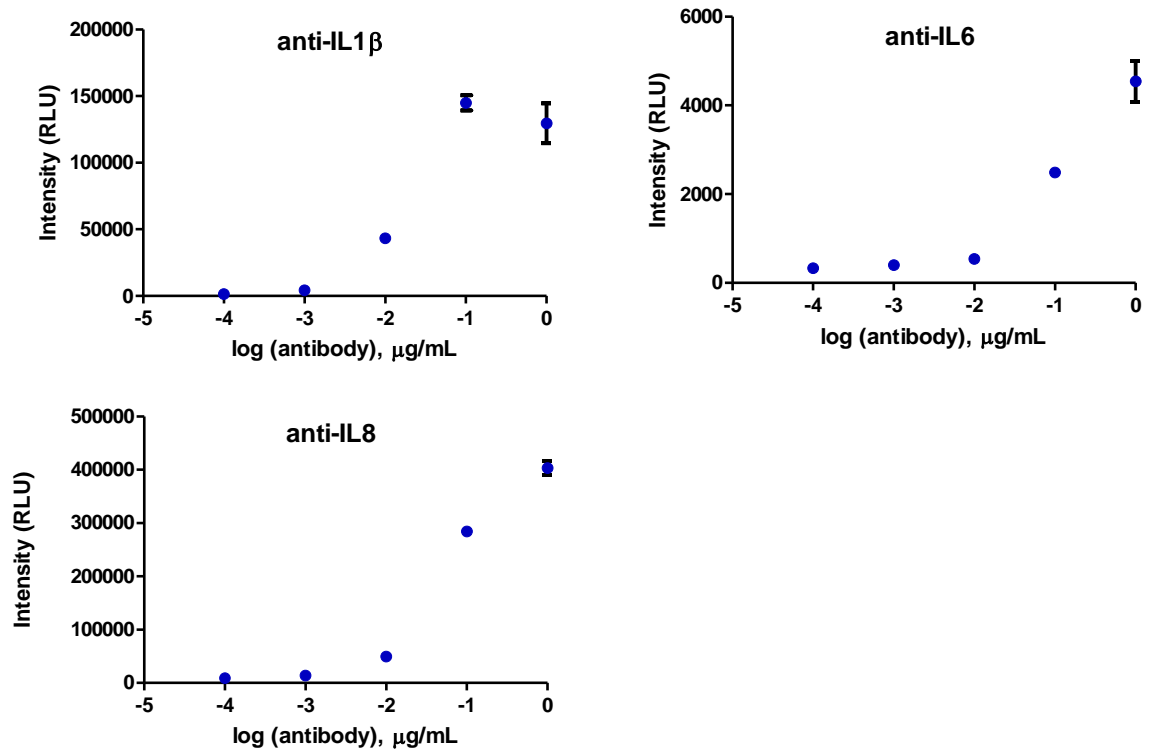
Figure 16. Binder dillution plots for all three antibodies. All points are the average of triplicate measurements ± one standard deviation. Error bars now visible are concealed by the points.
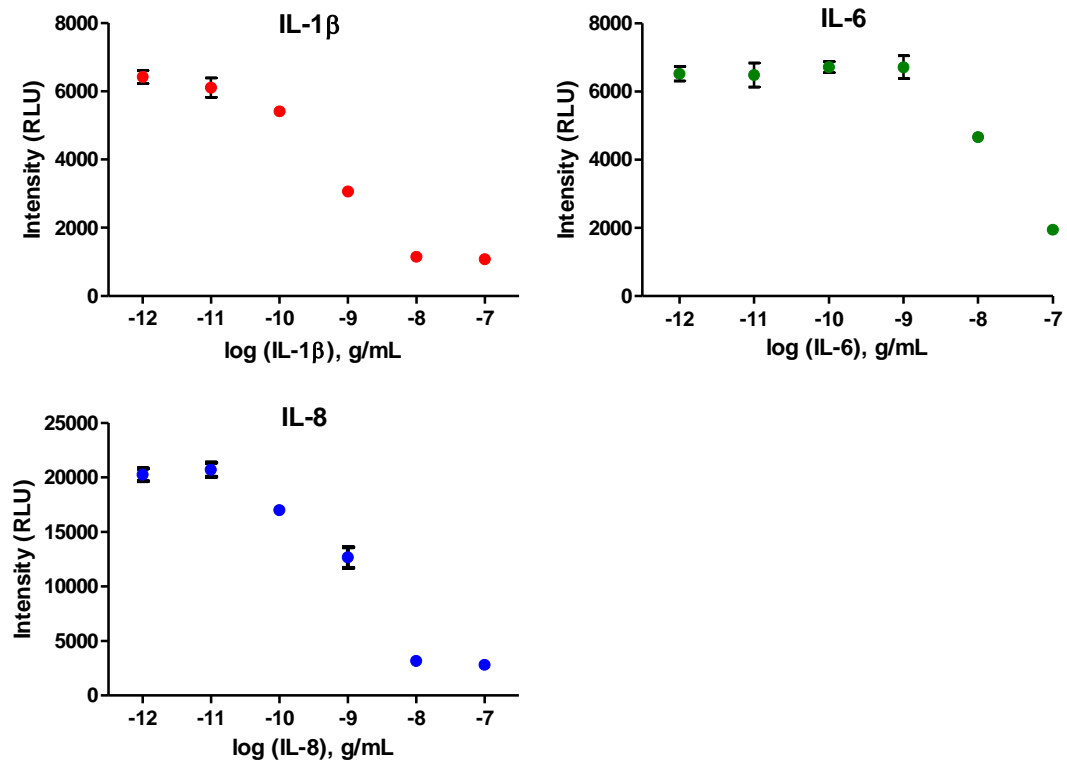
Figure 17. Individual dose response plots of the three analytes of interest in a buffered solution. All points are the mean of three measurements ± one standard deviation. Error bars that are not visible are obstructed by the points.
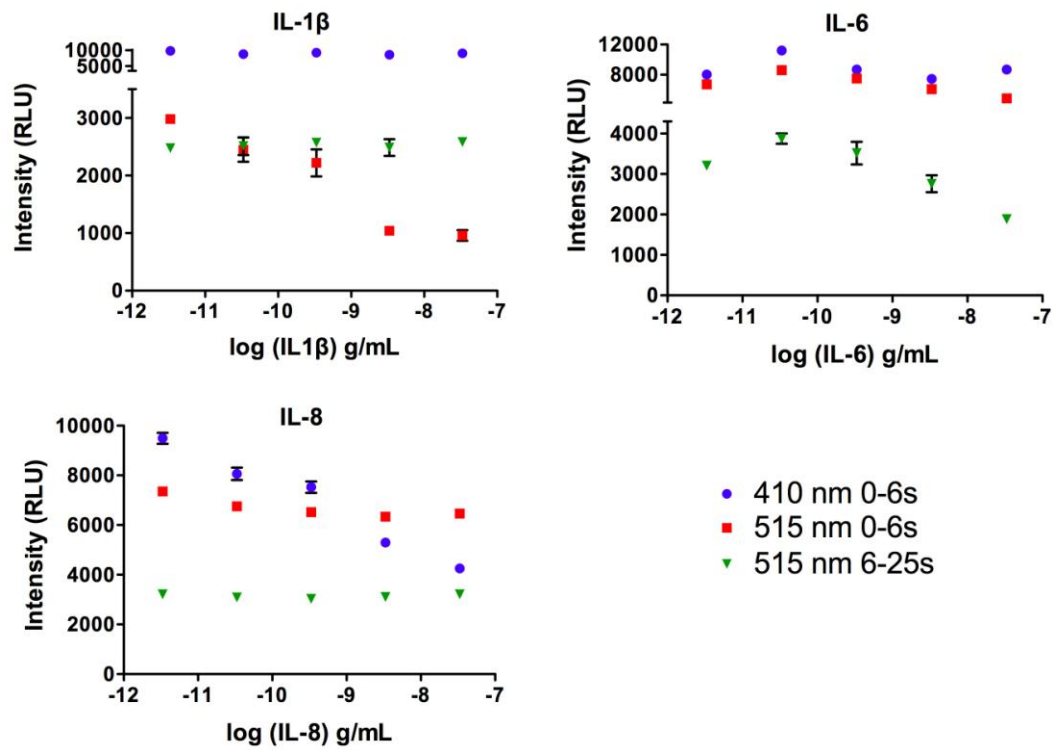
Figure 18. Simultaneous dose-response plots of all three analytes in a single well with a buffered solution. All three time/wavelength windows are plotted. The response of the IL-1β in the 515 nm, 0-6s window has been corrected for the effect of the IL6Y82F signal. All points are the mean of three measurements ± one standard deviation. Error bars that are not visible are obstructed by the point.

not interfere with the assay for the target interleukin. As expected, the response for interleukin 6 could be seen throughout both of the long and short kinetic windows. The IL6Y82F protein with coelenterazine i has a long half-life, thus the signal is not only present in the 6-25 s kinetic window but also in the 0-6 s.To resolve this issue the long decay component can be subtracted from the short decay component by the use of a signal deconvolution algorithm as described previously (*100*).Dose-response plots for the simultaneous detection of three interleukins showed a similar profile as the individual interleukins and was capable of detecting the analytes in the relevant concentration range with detection limits of 0.3 pg/mL for IL-1β and IL-8 and 0.3 ng/mL for IL-6. The response from fusion proteins with the fixed interleukin concentrations did not interfere with the target signal outside of the expected presence of the IL-6Y82F aequorin in both the long and short time intervals. Additionally, the multiplex assay was performed using human serum as the sample matrix. Being able to perform the assays directly in physiological fluids will eliminate sample preparation steps, reduce assay time, and thus allow for quicker disease diagnosis. The system again showed high sensitivity and specificity, detecting the desired analyte with a four order of magnitude dynamic range that encompass the physiological levels of interleukins. The detection limits of 3 pg/mL for IL-8, 30 pg/mL for IL-1β and 0.3 ng/mL for IL-6 (figure 19) were obtained.
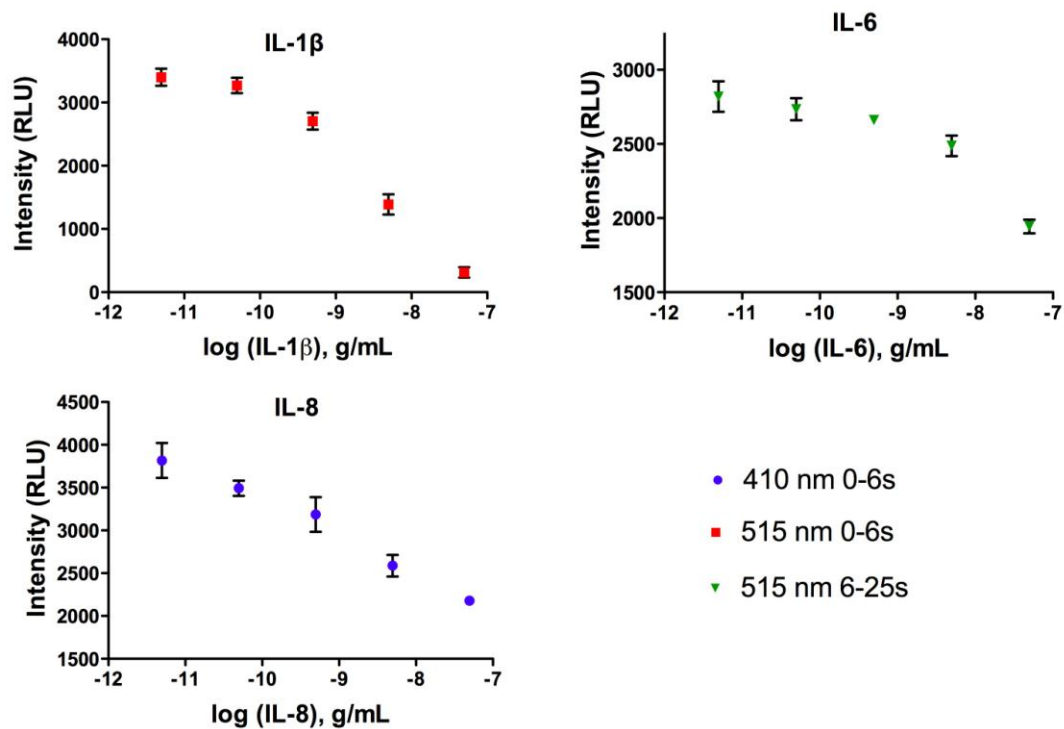
Figure 19. Simultaneous dose response plots of all three analytes in human serum in a single well. The response in the specific time/wavelength window of interest for each interleukin is plotted separately for ease of viewing. The response of the IL-1β in the 515 nm, 0-6s window has been corrected for the effect of the IL6Y82F signal. All points are the mean of three measurements ± one standard deviation. Error bars that are not visible are obstructed by the point.

Currently there are several other methods for the quantification of human interleukins including ELISA, flow cytometry, and meso scale base systems. Each system offers advantages and disadvantages, which can vary by the individual experimental needs. All require specialized equipment and space for the required instruments. The aequorin based competive assay offers similar detection limits as the alternative methods, corresponding with the physiologically relevant concentration ranges. Additionally, the unique ability of aequorin to be detected at extremely low levels with minimal background allows the potential for aequorin labels to be incorporated with miniaturized devices. Miniaturized devices offer greater prospective for point of care diagnostics and field applications where a small, portable device is required.

CONCLUSIONS

Bioluminescent labels capable of multiplex detection have the opportunity to be a key element for the advancement of detection systems as the move towards miniaturization progresses, requiring more sensitive, quick, and cost efficient labels. Herein the multiplexed detection of three analytes is presented. The system was able to respond quickly and efficiently in a dose-dependent manner over several orders of magnitude, including the physiological and elevated range for the specific interleukinprotein biomarkers of interest. Previously, dual-analyte bioluminescent assays have been reported either based on spectral or time resolved bioluminescentproteins (*96, 100, 123-126*). However, in this study we have demonstrated that a combination of both time and wavelength resolved aequorin mutants impart enhanced multiplexing

73

capabilities for the development of a bioluminescence-based detection system. In addition,both spectral and time resolved aequorin mutants need a calcium solution to trigger bioluminescence, unlike in the case of dual luciferase system where the bioluminescence is triggered using different reagents. This, in addition to the fact that band pass filters are implemented for wavelength discrimination, allows for simplifying instrumentation requirements and maintaining cost effectiveness. The high sensitivity of aequorin also allows for easy quantification even in small volumes and the microtiter plate format aids in high-throughput screening. Lab-on-a-chip and lab-on-a-CD set-ups also offer compatible platforms with which a label of this type could be utilized for the development of a more versatile detection system. As the library of semi-synthetic aequorins expands introducing a variety of emission maxima and decay kinetics, this combination of time and wavelength resolution could offer a novel pathway for the development of multiplex assays and expand the possibilities for the advancement of diagnostic and detection systems.

CHAPTER FOUR

GENETICALLY ENHANCED SEMI-SYNTHETIC AEQUORIN VARIANT WITH

IMPROVED DETECTION AND IMAGING CAPABILITIES

INTRODUCTION

Driven by its unique and attractive properties, bioluminescence continues to emerge as an alternative method of detection in many clinical and diagnostic applications. Coinciding with continuing improvements in instrumentation, bioluminescence has found utility in a variety of applications including assay development, investigation into gene expression, whole cell sensing, and intracellular analysis to name a few (*5, 10, 117-120*). Even more recently, bioluminescent proteins have started to surface as an imaging agent. Typically the imaging is achieved using genetically engineered cells to express the bioluminescent reporter, of which the bioluminescent emission can be used to analyze physio-pathological processes, disease progression, bacterial infection, and intracellular interaction (*149-153*). The bioluminescence signal is generated through a chemical reaction, which eliminates the need for an external light source and thus, avoids any background signal. This property is very useful in imaging applications compared to the imaging using green fluorescent protein, which suffers from high cellular autofluorescence background. There are a few luciferase enzymes that have been traditionally employed for bioluminescent imaging studies. The photoprotein aequorin has not been widely used in such

studies, however, due its flash type kinetics (~1 s half-life) and the extremely slow turnover rate once the bioluminescence flash has occurred. Herein we describe a genetically enhanced aequorin mutant that shows improved detection and imaging capabilities. Specifically, the Y82F mutant aequorin that displays a longer wavelength and increased half-life when paired with the coelenterazine *i* was employed as a label for the detection and imaging applications. We demonstrate the feasibility of implementing the protein aequorin as an immunolabel, able to detect a desired antigen down to the attomole range and as few as three target cells of interest.

Occurring natively in the jellyfish *Aequorea victoria*, the photoprotein aequorin consists of apo-aequorin (22 kDa) and the imidazopyrazine chromophore coelenterazine contained in the protein's hydrophobic core. Aequorin binds calcium, which induces a conformational change in the protein that, in the presence of molecular oxygen, allows the oxidation of the coelenterazine to an excited coelenteramide. Relaxation of the excited state coelenteramide results in the emission of a photon of light with a λ_{max}~ 469 nm (*25, 127*). The spent coelenteramide is still bound by the photoprotein and is slow to be released; thus, as long as excess coelenterazine is present in the initial solution the intensity of the emitted light will be directly proportional to the moles of photoprotein in the sample (*25*). Bioluminescent proteins, such as aequorin, havebeen shown to have great potential as a label in analytical applications, demonstrating very efficient quantum yields. In addition, the light emission is a direct result of a chemical reaction, eliminating the need for an

76

outside excitation source, which dramatically reduces nonspecific signal and autofluorescence from the sample solution, allowing extremely high sensitivity. Aequorin has recently been shown to yield sensitivity as an immunolabel similar to alkaline phosphatase and horseradish peroxidase (*154*). Furthermore, extensive random and site-directed mutagenesis have been performed on aequorin, which in combination with the use of synthetic coelenterazines, has greatly expanded the spectral diversity of aequorin's bioluminescence (*97-98, 128-139*).

The CD33 protein and anti-CD33 antibody were chosen as a model system to assess the engineered aequorin's analytical potential in addition to improving its imaging capabilities (figure 20). CD33 is a 67 kDa glycoprotein expressed uniquely on the surface of 80-90% of acute myeloid leukemia (AML) cells (*155-156*). CD33 has been used as a target for anti-cancer drugs. For example, Mylotarg, which couples the cytotoxic drug calicheamicin to an anti-CD33 antibody, has been shown effective for the treatment of AML patients (*157*). Additionally, cell free circulating CD33 has also been shown to be significantly higher in patients with AML and may also be important for clinical applications (*158*). It was demonstrated that by adding a unique cysteine into the sequence of the Y82F aequorin mutant, the protein can be employed as a sensitive immuno-label, allowing the detection of both free and surface attached CD33 at very low levels. Additionally, an effort towards the ability to use aequorin in novel imaging applications is also presented.
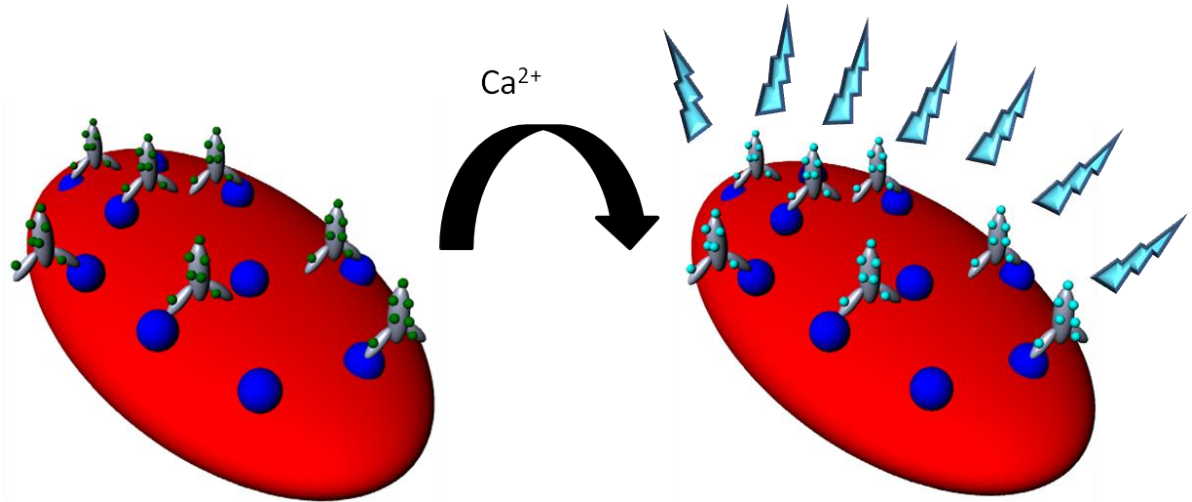
Figure 20. A schematic of the developed system for the detection of AML cells. CD33 (blue) are expressed on the surface of AML cells (red). CD33 is recognized by the anti-CD33 antibody (grey) which is conjugated to C5Y82F aequorin (small spheres on the grey structure). Upon the addition of Ca^{2+} the aequorin will emit light with the increasing intensity corresponding to an increased number of bound aequorin labeled antibodies.

EXPERIMENTAL PROCEDURES

Reagents. Disodium ethylenediaminetetraacetate (EDTA), Luria-Bertani (LB) Agar, LB Broth and Amicon Ultra 4 spin filters were purchased from Fischer Scientific (Fair Lawn, NJ). Diethylaminoethyl (DEAE) Fast Flow was obtained from GE Life Sciences. Poros 50 HQ was purchased from AB Applied Biosystems (Foster City, CA). The Bradford protein assay kit was from Bio-Rad Laboratories, Inc. (Hercules, CA). Sodium Dodecyl Sulfate (SDS) was purchased from Curtin Mathesin Scientific, Inc. (Houston, TX). Plasmid mini-prep kits and gel extraction kits were obtained from Qiagen (Valencia, CA). T4 DNA ligase, alkaline phosphatase, and *EcoR*I and HindIII restriction enzymes were purchased from Promega (Madison, WI). Pfu Ultra polymerase and Taq polymerase were obtained from Stratagene (Ceder Creek, TX). Tris(hydroxymethyl)amino methane (Tris) free base, HEPES, ampicillin, sodium phosphate, sodium chloride, potassium chloride, magnesium chloride potassium phosphate and bovine serum albumin (BSA) were purchased from Sigma Aldrich (St. Louis, MO). Top10 chemical competent cells were from Invitrogen (Carlsbad, CA). CD33 monoclonal antibody and recombinant human CD33 were purchased from R&D systems (Minneapolis, MN). CD33 polyclonal antibody was obtained from Novus Biologicals (Littleton, CO). Sulfo-LC-SPDP, DTT (Dithiothreitol), Zebra Spin desalting columns, Reacti-Bind goat anti-mouse IgG coated white 96-well plates and Reacti-Bind goat anti-rabbit IgG coated white 96-well plates were purchased from Pierce Biotechnology (St. Louis, MO). HL-60 cells, Iscove's Modified Dulbecco's Medium, and Fetal Bovine Serumwere purchased from

American Type Culture Collection (ATCC)(Manassas, VA). All chemicals were reagent grade or better and all aqueous solutions were prepared using 16 MΩ deionized distilled water produced by a Milli-Q water purification system (Millipore, Bedford, MA).

Apparatus. Polymerase chain reactions (PCR) were performed using an Eppendorf Mastercycler Personal thermocycler (AG, Hamburg). DNA electrophoresis was performed using a FB105 Fischer Biotech Electrophorese Power Supply (Pittsburgh, PA) and the gels were visualized using a UV Transilluminator (UVP, Upland, CA). OD_{600} readings were taken using a Spectronic 21D UV-Vis Spectrophotometer (Milton Roy, Ivy Land, PA). Bacteria employed for the expression of the aequorin protein were incubated in a Fisher Scientific incubating orbital shaker and Fisher Scientific open air orbital shaker (Fair Lawn, NJ) and harvested by a Beckman J2-M1 centrifuge (Palo Alto, CA). All chromatographical purifications were performed on a BioCAD SPRINT perfusion chromatography system from PerSeptive Biosciences (Framingham, MA). Purity of the fusion proteins were verified by sodium dodecyl sulfate-polyacrylamide gel electrophoresis (SDS-PAGE) using Invitrogen 10-20% Tris-glycine gels in an Invitrogen X Cell Sure Lock Mini Cell (Carlsbad, CA). Bioluminescence measurements were made on a Polarstar Optima luminometer from BMG Labtech (Cary, NC) and decay kinetics analyzed with GraphPad Prism 5.0 (San Diego, CA). Emission spectra were taken on a custom made SpectroScan instrument from Sciencewares (Farmingham, MA). Tissue cultures were maintained in a Thermo Scientific (Waltham, MA) NAPCO series 8000 DH

CO_2 Incubator at 37 $^{\circ}$C, 5% CO_2 and cellular concentrations were determined via Nexcelom Biosciences (Lawrence, MA) Cellometer Vision cell counter. Imaging experiments were performed on an Andor iXon EMCCD camera (Andor Technology, Belfast, Ireland) attached to a Nikon E600FN microscope and data acquisition and analysis were performed using Imaging Workbench 5.0 (Indec BioSystems, Santa Clara, CA, USA).

Construction of Genetically Modified Aequorin. The Y82F aequorin mutant developed previously in our lab (*98*) served as a base for the studies. To allow for site-specific conjugation of the protein to the CD33 antibody, the PCR was used to produce a Y82F mutant coding for a unique cysteine at amino acid position 5. The cysteine free Y82F aequorin coding sequence (*98*) was used as the template in the PCR and amplified with the following primers to produce the C5Y82F aequorin mutant.

Forward Primer:

GTGGAATTCCAATGGTGAAACTGACCTGCGACTTCGACAACCCAAGATGGA

Reverse Primer:

CACAAGCTTTTAGGGGACAGCTCCACCG

The position introducing the unique cysteine is highlighted in red letters. The forward and reverse primers also introduced *EcoR*I and HindIII restriction sites. The PCR product was then ligated into the *EcoR*I – HindIII sites of the ompA containing pIN4 plasmid. The plasmid containing the gene for C5Y82F aequorin was used to transform Top10 *E. coli* cells. The correct DNA sequence of the

mutant aequorin gene was confirmed by the Advanced Genetic Technologies Center at the University of Kentucky.

Expression and Purification of Aequorin. *E. coli* cells containing the plasmid encoding for C5Y82F were grown in 500 mL Luria Bertani (LB) broth containing 100 μg/mL ampicillin while shaking at 250 rpm at 37 $^{\circ}$C overnight to an OD_{600} ~ 1.5. The protein was expressed without any induction being required and was released from the cells into the culture media. The cells were then pelleted by centrifugation at 12,000 x g for 15 min and the supernatant (medium) containing the aequorin was saved. The C5Y82F aequorin was acid precipitated by adding glacial acetic acid dropwise to the medium to a final pH of 4.2 and incubating at 4 $^{\circ}$C for 2 h. The solution was then centrifuged at 12,000 x g for 20 min to isolate the precipitated protein. The protein pellet was resuspended in 30 mM Tris/HCl pH 7.5 buffercontaining 2mM EDTA. The protein was centrifuged at 12,000 x g for 15 min to remove any particulate matter and then purified by ion-exchange chromatography using a BioCAD Sprint system. The protein was loaded onto a DEAE Sepharose Fast Flow column (20 mL column volume) equilibrated with 30 mM Tris/HCl pH 7.5 buffer containing 2mM EDTA. A gradient was then run from 0-50 % of 30 mM Tris/HCl pH 7.5, 2 mM EDTA, 1 M NaCl over 10 column volumes.   Four mL fractions were collected and fractions containing the highest concentration of the aequorin, as determined by SDS-PAGE and aequorin activity, were pooled. All purified proteins were stored at 4 $^{\circ}$C until use.

Chemical conjugation of C5Y82F aequorin to CD33 monoclonal antibody. The C5Y82F aequorin mutant was chemically conjugated to the CD33

monoclonal antibody through the use of the heterobifunctional cross-linking molecule Sulfo-LC-SPDP. Sulfo-LC-SPDP is capable of conjugating two proteins through the reaction of amine groups of one protein and sulfhydryl residues of the other. First 20 µL of 20 mM Sulfo-LC-SPDP was added to 100 µg of the CD33 monoclonal antibody and allowed to incubate for 4 h at 4 ^{o}C to react the NHS ester end of the molecule with the amine groups of the antibody. A 10 mM DTT solution was added to the C5Y82F aequorin solution and allowed to incubate at 4 ^{o}C for 4 h. To remove unreacted Sulfo-LC-SPDP and DTT both solutions were passed through Zebra Spin Desalting Columns (Pierce Biotechnology) pre-equilibrated with phosphate buffered saline (PBS) pH 7.2, 2 mM EDTA (buffer A). Immediately after the buffer exchange a 10 times mole excess of the C5Y82F aequorin was added to Sulfo-LC-SPDP activated CD33 monoclonal antibody solution and incubated for 16 h at 4 ^{o}C to react the 2-pyridyldithiol group on the other end of Sulfo-LC-SPDP with the reduced sulfhydryl group on C5Y82F aequorin. Unconjugated C5Y82F aequorin was removed by centrifugation with an Amicon Ultra 4 spin filter (MWCO 50K).

Decay Half-Life of Free and Conjugated Mutant Aequorin. The decay kinetics of both the free and conjugated C5Y82F aequroin were examined with an array of coelenterazine analogues. A three molar excess of each coelenterazine analog was added to aliquots of both forms of the protein and incubated for 18 h at 4 ^{o}C. The fusion proteins were then diluted with buffer A until the maximal bioluminescent intensities were below 500,000 relative light units (RLUs) when analyzed on the Polarstar Optima luminometer. A volume of 10 µL of the

coelenterazine bound protein solution was added to the well of a microtiter plate and the bioluminescent light reaction was initiated by injecting 100 μL of 100 mM CaCl$_2$, 30 mM Tris/HCl pH 7.5 (buffer B) into the well. For all of the coelenterazines except coelenterazine i the light emission was monitored for 25 s, with readings taken every 100 ms. For coelenterazine i, the light emission was monitored for 50 s with a reading taken every 200 ms. All measurements were taken in triplicate and the mean of the three measurements used for the half-life analysis. The data was analyzed by GraphPad Prism 5.0 software using a non-linear, one phase exponential decay kinetics half-life equation. The analysis was initiated at the time interval displaying the maximal bioluminescent intensity as to only evaluate the decay of the light emission.

Bioluminescent Emission Spectra of Free and Conjugated Mutant Aequorin. The bioluminescent emission spectra profile was observed for both the free and conjugated aequorin with same array of coelenterazine analogues as used for the half-life study. The emission spectra were collected on the SpectroScan, a custom made instrument based on the Thermo-Labsystems Luminoskan Ascent luminometer. The instrument is capable of recording the spectra from flash reactions through the visible region of 400-700 nm. Again, a three molar excess of each coelenterazine was added to aliquots of each protein form and incubated for 18 h at 4 °C. A volume of 30 μL of the coelenterazine bound fusion protein solution was then added to a well on a 96 well microtiter plate. A volume of 100 μL of buffer B was then added to the well and the light

was collected for 6 s. All measurements were taken in triplicate and the mean used for emission maximum determination.

CD33 Dose Response. A dose response plot for free CD33 was first developed using C5Y82F aequorin as a label. Goat anti-rabbit IgG coated microplates (Pierce Biotechnology) were used for the study. The wells of the plate were initially washed three times with 150 µL of buffer A. A volume of 100 µL of 1 µg/mL rabbit anti-human CD33 polyclonal antibody was added to each well and allowed to incubate with shaking for 2 h at 4°C. The antibody solution was removed and the wells were then washed with 150 µL of buffer A. Next, 100 µL of each CD33 concentration was added to the wells and allowed to incubate with shaking at 4 $^{\circ}$C for 2 h. The wells were emptied and washed three times with buffer A. A volume of 100 µL of the mouse anti-human CD33 monoclonal antibody conjugated to C5Y82F aequorin was added to the wells and allowed to incubate with shaking at 4 $^{\circ}$C for 1 h. The aequorin conjugated antibody solution was removed and the microtiter plate was washed three times with buffer A to remove any unbound protein. Next, 100 µL of buffer B was added to each well and the bioluminescence intensity was measured for 4 s on the Polarstar Optima. All measurements were taken in triplicate with the mean of the set plotted for analysis.

Bioluminescent Detection of CD33 Expressing Cells. The ability for the C5Y82F aequorin-antibody conjugate to bind to CD33 expressed on the surface of HL-60 AML cells was also investigated. Goat anti-rabbit IgG pre-coated plates were again used for the study. The wells were washed three times with 150 µL

of buffer A. A volume of 100 µL of 1 µg/mL rabbit anti-human CD33 polyclonal antibody was added to each well and allowed to incubate with shaking for 2 h at 4 ^{o}C. The antibody solution was removed and the wells were then washed with 150 µL of buffer A. HL-60 cells were collected and centrifuged at 2000 g for 10 min to pellet the cells. The growth media was removed and the cells were resuspended in buffer A and then further diluted with buffer A to the desired concentration. A volume of 100 µL of HL-60 cell suspension was then added to wells and allowed to incubate with shaking at 4 ^{o}C for 16 h. The wells were emptied and washed three times with buffer A. A volume of 100 µL of the mouse anti-human CD33 monoclonal antibody conjugated to C5Y82F aequorin solution was added to the wells and allowed to incubate with shaking at 4 ^{o}C for 1 h. The aequorin conjugated antibody solution was removed and washed three times with buffer A to remove any unbound protein. Buffer B (100 µL) was added to each well and the bioluminescence intensity was measured for 4 s on the Polarstar Optima. All measurements were taken in triplicate with the mean of the set plotted for analysis.

Bioluminescent Imaging of CD33 Expressing Cells. C5Y82F aequorin was incubated for 16 h with a three molar excess of coelenterazine i. A volume of 50 µL of the C5Y82F aequorin protein was added to 1.450 mL of buffer A in a 35 mM dish. A background baseline was established and then 500 µL of buffer B was added to the dish and the time of injection noted. The bioluminescence was then captured on an Andor iXon EMCCD camera (Andor Technology, Belfast, Ireland) attached to a Nikon E600FN microscope for a total of 400 s. EM gain

was set to 4095 and a 5 s exposure time. Data acquisition and analysis were performed using Imaging Workbench 5.0 (Indec BioSystems, Santa Clara, CA, USA). For the bioluminescent measurements with the HL-60 cells the cells were incubated for two days at 37 ^{o}C, 5% CO_2 in a 35 mm*poly-L-lysine coated MatTek* Glass Bottom Culture Dishes (MatTek *Corporation,* Ashland, MA) to allow the cells to adhere to the surface. The cell media was then removed from the dish and washed 3x with 10 mM HEPES pH 7.4 containing 145 mM NaCl, 2.5 mM KCl, 10 mM glucose, 1 mM $MgCl_2$, and 5 mM EDTA (buffer C) to remove any unbound cells. A volume of 1.5 mL of C5Y82F aequorin labeled monoclonal anti-CD33 antibody with coelenterazine i in buffer C was then added to the dish and allowed to incubate on ice for 1 h. The solution was then removed from the dish and the dish was washed 2x with buffer C. Next, 1.5 mL of buffer C was added back into the dish and placed under the microscope. A stable baseline was obtained and 500 μL of buffer B was added to the dish and the addition time noted. The bioluminescence was then captured on an Andor iXon EMCCD camera (Andor Technology, Belfast, Ireland) attached to a Nikon E600FN microscope for a total of 400 s. EM gain was set to 4095 and a 5 s exposure time. Data acquisition and analysis were performed using Imaging Workbench 5.0 (Indec BioSystems, Santa Clara, CA, USA).

RESULTS AND DISCUSSION

Bioluminescence continues to emerge as a popular alternative for many of the diagnostic and bioanalytical methods. The advantages of bioluminescent proteins are low detection limits, simple instrumentation, biocompatibility, and

non-toxicityto living organisms. Aequorin, however, has been limited in applications due to its flash-type emission kinetics and extremely slow turnover rate of the bound coeleteramide after the bioluminescence occurs. To overcome these shortcomings, we have employed genetic manipulation in combination with synthetic coelenterazines to improve aequorin's labeling and imaging capabilities. In this study, we have demonstrated that a new and improved aequorin mutant can be employed as a sensitive label for bioluminescent detection and imaging applications. As a model system, the cell surface protein CD33, expressed exclusively on the surface of myeloid lineage cells, was chosen to demonstrate bioanalysis using aequorin as a label.

Our laboratory has performed extensive work with aequorin, which has resulted in the creation of several aequorin mutants and semi-synthetic aequorins exhibiting a range of both spectral and kinetic properties (*56-57, 98-100, 135*). One such aequorin mutant, Y82F, was chosen for this study. The Y82F mutant possesses a mutation at position 82 where a tyrosine has been changed to a phenylalanine. In the wild type aequorin, the hydroxyl group on the tyrosine residue is engaged with the bound coelenterazine through hydrogen bonding (*127*). Although, Tyr and Pheare very similar in size and orientation, this amino acid mutation alters the electronic environment experienced by the bound coelenterazine. In addition to this mutation, a unique cysteine was incorporated at amino acid position 5 of the protein through the use of specifically designed primers and the PCR, yielding the C5Y82F aequorin protein. This unique cysteine enablessite-specific conjugation of any target molecule to aequorin

using well established cross-linking procedures (*159*). This permits the protein to be used in a number of applications by only varying the target molecule without the need for extensive genetic modification. Furthermore, site-specific conjugation provides for a reproducible production of conjugates and in maintaining the bioluminescent activity of the protein. Commercially available aequorin labeled antibodies for thyrotropin (*160*) and digoxigenin (*161*) that employ the native protein have been made available; however, by introducing this unique cysteine, C5Y82F aequorin can be used to label essentially any antibody or other molecule of interest. Furthermore, the use of the semi-synthetic aequorin with a longer half-life expands the application of aequorin conjugates in imaging studies.

As a model system we chose the CD33 protein that is expressed on the surface of AML cells as the target biomolecule (*155-156*). The heterobifunctional sulfo-LC-SPDP crosslinker was selected to link the antibody to C5Y82F aequorin. First, the crosslinker was reacted with the antibody to allow the NHS ester portion of sulfo-LC-SPDP to react with primary amines of the lysine residues of the antibody. A 10 times mole excess of the C5Y82F aequorin was then mixed with the modified antibody so that the 2-pyridyldithio group on the other end of the crosslinker would react with the sulfhydryl group of the unique cysteine present on C5Y82F aequorin. The multiple SPDP conjugated sites on the antibody, in combination with the molar excess of aequorin available were utilized in an effort to permit each antibody molecule to be labeled by multiple

aequorin molecules, thus enhancing the detectability of the anibody-aequorin conjugate.

As reported previously by our laboratory, a combination of synthetic coelenterazines with genetic mutations to the native aequorin has yielded proteins with novel and improved bioluminescent properties (*98*). To confirm that these favorable characteristics were not compromised by the addition of a cysteine to the protein or the subsequent conjugation of the protein to an antibody of interest, the spectral properties and decay kinetics of both the free C5Y82F aequorin mutant and the antibody conjugated complex were examined with respect to the emission profile and decay kinetics. As demonstrated in table 3, both the free and conjugated proteins did show the expected spectral and kinetic characteristics. Of particular interest to our purposes is the combination of the proteins with the coelenterazine *i*. This combination resulted in an emission maximum of 506 nm, but more importantly a half-life of 16.37 s and 18.57 s for the free and conjugated forms, respectively. This significantly longer half-life compared to that of the typical aequorin bioluminescence, which is ~1 s, leads to more of a glow type of emission and can greatly improve the imaging capabilities of the protein. The increased luminescent time will allow for larger exposure times, increasing the amount of light able to be captured by the detection equipment and allowing fewer molecules to result in a distinguishable signal. The increased half-life of the proteins when paired with the coelenterazine i can be attributed to the internal heavy atom effect of the iodine which is uniquely present in this coelenterazine. As explained by Nijegorodov

C5Y82F aequorin			CD33 Antibody-C5Y82F aequorin		
coelenterazine	λ_{max} (nm)	Half-life (s)	coelenterazine	λ_{max} (nm)	Half-life (s)
ntv	501	0.95	Ntv	496	1.25
i	506	16.37	i	506	18.57
f	506	0.62	f	507	0.72
cp	478	0.18	cp	484	0.26

Table 3. The emission maxima and half-lifes of both free C5Y82F aequorin and the C5Y82F aequorin conjugated to the anti-CD33 monoclonal antibody. All measurements were performed in triplicate with the averages reported.

and Mabbs (*162*), the iodine on coelenterazine i can increase the probability of a transition from an excitedsinglet state to an excited triplet state. The forbidden triplet to singlet transition results in an increased residence time in the excited states and the longer observed bioluminescence emission. In addition to the longer half-life, both the free and conjugated proteins also continued to display the red shifted bioluminescence as compared to the native 469 nm emission. The coelenterazine *i* gave an emission maximum of 506 nm and the coelenterazine *f* an emission maximum of 507 nm. Emission maxima around 450 nm have been achieved with other aequorin mutant/coelenterazine analog pairs (*98*) and thus multiplexing through wavelength resolution would also be a future possibility with the aequorin mutants as labels.

It has recently been discovered that free CD33 circulating through the blood could serve as a marker for important clinical applications when dealing with AML patients. Free CD33 has been shown to be capable of discriminating between various pathophysiological states, to correspond with survival prognosis, and possibly be an indicator of tumor cell turnover (*158, 163-164*). In addition, with the antibody based AML treatment strategies, free CD33 would act as a major inhibitor of the antibody-drug complex reaching the desired target and play a role in the efficacy and dosing requirements of the drug. Being able to quickly and efficiently determine free CD33 concentrations in physiological fluids has the potential to be a key requirement for future dosing decisions along with a simple non-invasive method to track and monitor disease progression. Consequently, the C5Y82F aequorin labeled anti-CD33 antibody was used to

develop a microtiter plate based immunoassay. The high sensitivity of bioluminescence allowed free CD33 to be detected down to 1.87×10^{-18} moles, as shown in figure 21. The microtiter plate platform would also allow numerous samples to be investigated in a very short time.

Cell surface expressed CD33 has also shown to be a useful entity, being used as a therapeutic target by drugs such as Mylotarg (*157*). Thus we also evaluated the use of C5Y82F aequorin labeled antibody to detect CD33 expressed on the surface of AML cells (HL-60 cells, ATCC, Manassas, MA). A quantifiable bioluminescent signal, significantly above the background, was obtained from as few as three AML cells (figure 22).

As previously mentioned, current explorations with bioluminescence imaging are typically limited to luciferase based systems, as the continuous administering of D-luciferin and availability of ATP allows the bioluminescence to be produced and observed continuously. The slow turnover rate and flash-type kinetics of aequorin have not been favorable on the imaging forefront and have typically limited aequorin to the visualization of Ca^{2+} dynamics, availability, and signaling (*165-167*). In a step in the direction towards the use of aequorin outside of the typical Ca^{2+} imaging, we show that a quantifiable signal from the C5Y82F aequorin mutant was observed several minutes after the initiation of the bioluminescent reaction on a typical imaging microscope (figure 23a, 23b). This longer emission profile will allow the increased integration and camera exposure times necessary for the detection of the bioluminescent signal. The C5Y82F aequorin labeled antibody was also successful in indicating the presence of AML

93
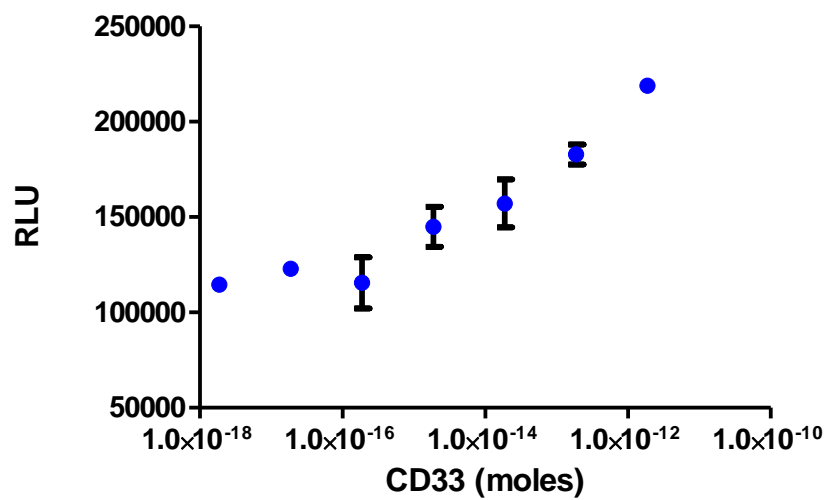
Figure 21. Dose response plot for free CD33. All points are the average of triplicate measurements ± one standard deviation. Measurements were taken in a volume of 100 μL. Error bars not visible are concealed by the points.
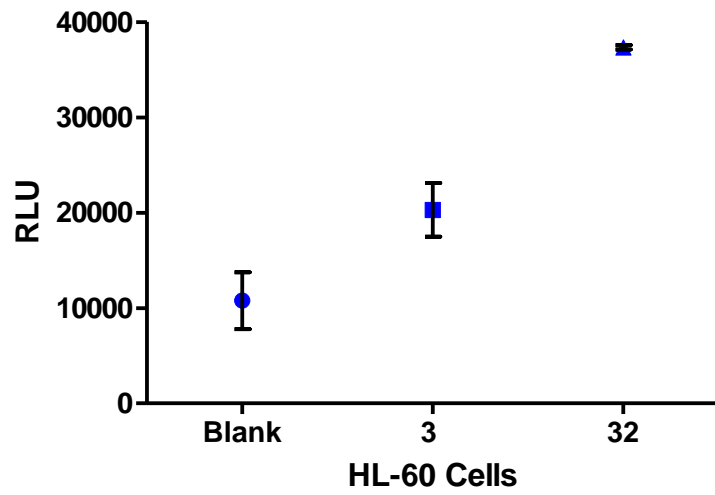
Figure 22. Bioluminescence intensity observed from differing amounts of HL-60 cells expressing the CD33 surface antigen. All points are the average of triplicate measurements ± one standard deviation. Error bars not visible are concealed by the points.
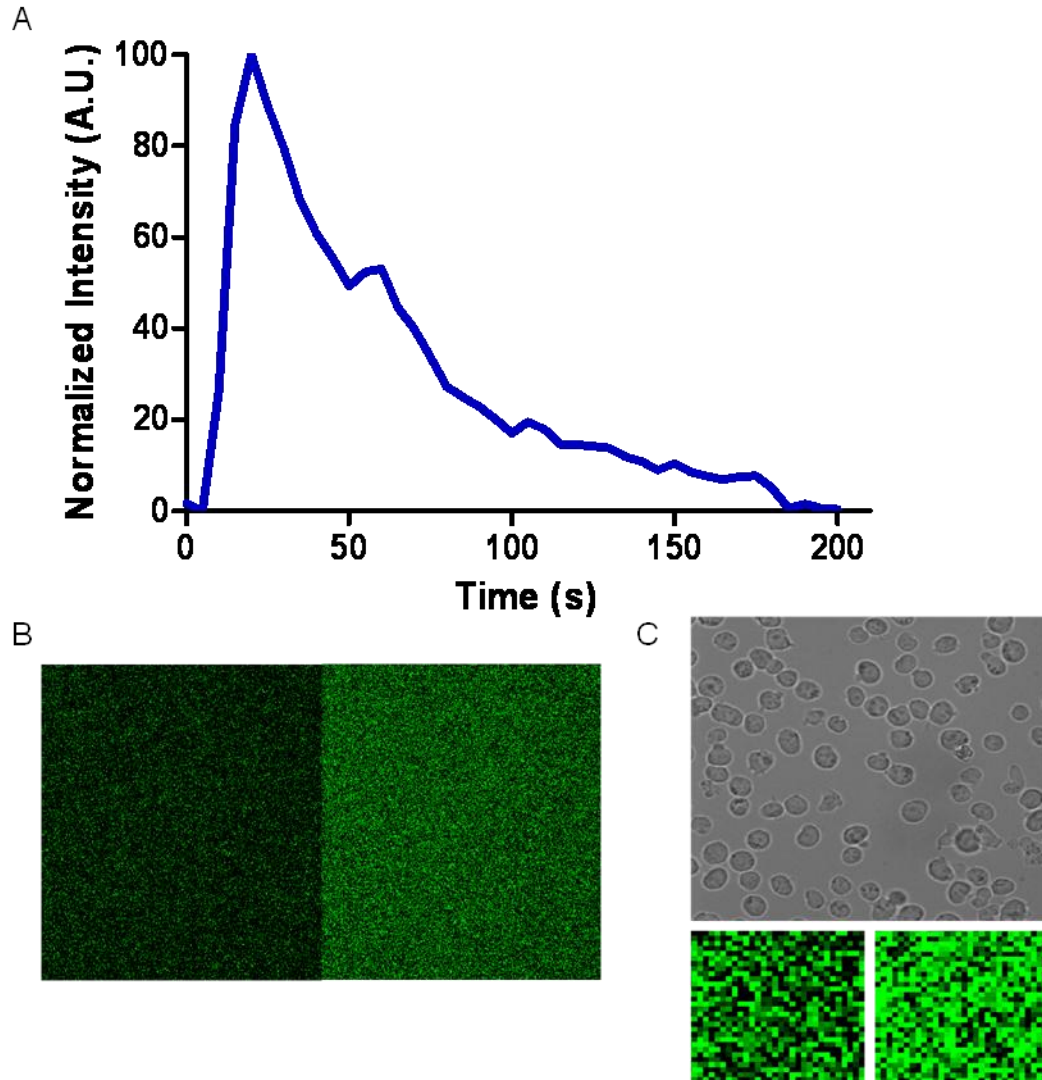
Figure 23. A. The bioluminescence response observed after the addition of Ca^{2+} to a solution containing free C5Y82F aequorin with respect to time. B. The image taken of the solution before (left) and after (right) the addition of Ca^{2+} to the free protein in solution. C. The top imager is the bright field image of the field of view of AML cells bound to the surface of dish with the aequorin conjugated antibody bound to the surface. The bottom two images are the field of view before (left) and after (right) the addition of Ca^{2+} showing the antibody was bound to the surface of the cells.

cells expressing the CD33 antigen on the cell surface (figure 23c). In addition, the unique cysteine and the ability to visualize the purified protein will allow the labeling with this protein to be tailored to specific needs that do not necessitate the genetic creation of an entirely new protein complex.

CONCLUSIONS

Bioluminescence offers a number of advantages when considering the requirement for extremely sensitive detection. The biocompatibility of bioluminescent proteins, the elimination of sample auto-fluorescence, and removal of the need for an excitation source all make bioluminescent an excellent choice as an inexpensive and efficient labeling option. Herein we describe an aequorin mutant, C5Y82F aequorin, which further expands the possibilities of using aequorin bioluminescence in a clinical and research setting. A unique cysteine was added to the protein to allow for quick and effective conjugations of any molecule of interest to aequorin. As a model system, an immunoassay for the AML surface antigen, CD33, was developed with a C5Y82F aequorin labeled monoclonal CD33 antibody. Free CD33 has recently been shown to be of clinical significance (*158*) and we were able to achieve excellent detection of the protein, down to 1.87×10^{-18} moles. We were also able to demonstrate the ability to detect as few as three individual AML cells using the aequorin-antibody conjugate. Furthermore, we were able to show that the potential for imaging with the engineered protein exists, demonstrating an observable bioluminescent signal for several minutes with a typical imaging

97

microscope. As imaging instrumentation continues to advance and improve, a versatile bioluminescent label could push the imaging capabilities forward for highly sensitive analysis.

CHAPTER FIVE

CYCLIC AMP RECEPTOR PROTEIN- AEQUORIN MOLECULAR SWITCH

FOR CYCLIC AMP

INTRODUCTION

Nature is able to produce proteins exhibiting highly desirable characteristics in terms of function, specificity, and efficiency, unmatched by synthetically developed molecules. Driven by this phenomenon, many scientists utilize and manipulate natural proteins to achieve the specificity and response that many of today's assays and detection methods strive for. But there is not always a single natural protein suitable for a task at hand. In some instances it would be advantageous to couple the functions of two completely unrelated proteins to work together as one to achieve a desired function-e.g., to quantify an analyte binding induced conformational change of a protein that naturally would be undetectable.Molecular switches can be the solution to accomplish such tasks. A protein molecular switch is defined as an entity that couples signal to functionality (*168*). For example, a protein molecular switch responds to an input signal by producing an "on/off" output signal. Such a protein could be constructed by genetically combining the coding sequence of one protein with

that of another, creating a hybrid fusion protein with a completely new function, which displays the discrete functions of the individual proteins (*168-171*). To that end, we have inserted the flexible hinge motion binding protein, cyclic AMP (cAMP) receptor protein (CRP), into the genetic sequence of the bioluminescent protein aequorin to create a functional fusion hybrid protein, CRPAEQ. The separate proteins were genetically attached in a manner so that the conformational change experienced by CRP upon binding to cAMP results in a loss of bioluminescent signal of the aequorin portion of the hybrid protein (figure 24).

Aequorin (figure 25) is a calcium dependent bioluminescent protein found naturally in the jellyfish *Aequorea victoria.* Aequorin was originally isolated in 1962 by Shimomura *et al* (*172-173*). The complete aequorin complex is composed of the apoprotein, apoaequorin, and the organic chromophore coelenterazine. Apo-aequorin contains 189 amino acids arranged to form four EF-hand sequences (*127, 174*) that fold to create the hydrophobic core for the stabilization of the coelenterazine allowing for the bioluminescence to occur. In the presence of molecular oxygen and Ca^{2+}, aequorin undergoes a conformational change that allows for the oxidation of coelenterazine to coelenteramide with the release of CO_2 and the emission of light at 469 nm (*175*). Employing aequorin as a signal generating molecule has advantages over employing chemical or protein-based fluorescent probes because since the emission of light is the result of an internal biochemical reaction there is no need for an excitation source causing negligible background signal and leading to
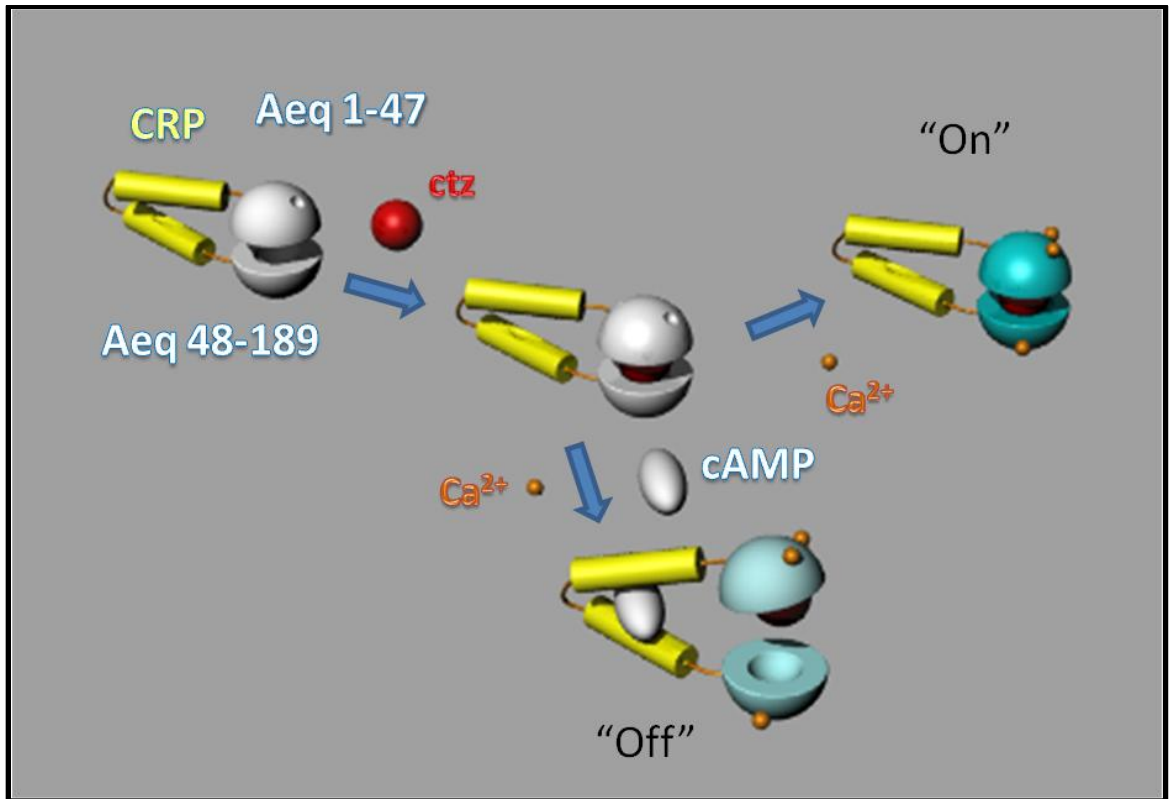
Figure 24. Schematic of the response of the CRPAEQ molecular switch to the presence of cAMP. Initially the coelenterazine free CRPAEQ complex is not bioluminescent. Upon stabilization of the chromophoric coelenterazine and the addition of Ca^{2+} the complex will emit the bioluminescent flash, characteristic of normal aequorin. Following the cAMP induced conformational change the two halves of aequorin are positioned too far apart to form the active aequorin complex and thus decreases the observed bioluminescent intensity.
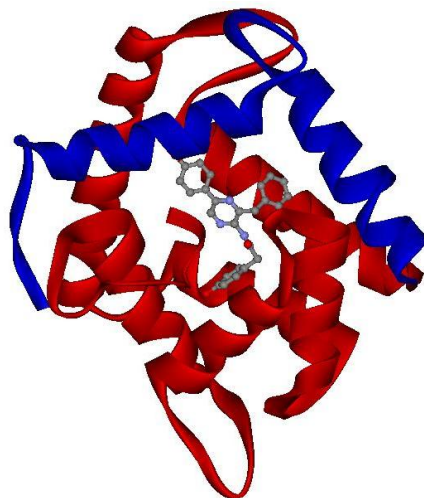
Figure 25. The crystal structure of aequorin with coelenterazine bound in the hydrophobic pocket. Amino acids 1-47 are shown in blue and amino acids 48-189 in red representing the fragments in which aequorin was split.

exceptional detection limits. In addition aequorin is environmentally friendly and thus it does not require special attention for disposal (*176-178*).

CRP regulates transcription of over 150 genes in *Escherichia coli* (*179*). It is allosterically activated by the binding of cAMP, which causes CRP to undergo a conformational change that allows for the binding of specific DNA Sequences (*180-182*). In nature CRP exists as a homodimer of two identical subunits each containing 209 amino acids (23.6 kDa molecular mass) (*182*). Each subunit folds into two domains: the N-terminal domain (residues 1-133) responsible for the dimerization of CRP and housing the higher affinity cAMP binding pocket, and the C-terminal domain (residues 139-209), which is responsible for the interaction with DNA through a helix-turn-helix motif (*179, 182-183*). Amino acids 134-138 form a flexible hinge that couples the two domains through covalent interactions (*182*). Each subunit contains two cAMP binding sites. The N-terminal domain houses the higher affinity cAMP binding site, which binds cAMP in the µM range. The second cAMP binding site is located between the hinge and the turn of the helix-turn-helix motif and only binds cAMP when it is present at mM concentrations. Thus, the CRP protein is believed to exist in three states: free CRP with no cAMP bound, CRP-(cAMP)$_2$ when each subunit contains one bound cAMP molecule in the higher affinity binding site, and CRP-(cAMP)$_4$ when each subunit has two cAMP molecules bound, one each in the higher and lower affinity binding sites (*179, 184-185*). The binding of cAMP by the higher affinity binding site is what induces the first conformational change in the N-terminal

domain, which is then conveyed to the C-terminal domain resulting in a further conformational adjustment allowing the binding of DNA (*179*).

The large diversity of biological molecules exhibiting high specificity and affinity for analytes of interest has lead to the increasing use of these molecules for the development of novel biosensing systems. Molecular switches have been created to translate the binding induced conformational change of many of the protein biomolecular recognition elements into a quantifiable signal in the forms of altered fluorescence emissions, electron transfer, and biochemical activity among others. Examples of analytes targeted by such switches include a number of different sugars, secondary messengers, drug molecules, and proteins to name a few (*186*). Molecular switches have also been developed based on DNA-base mispairing to monitor changes in the pH of the local environment (*187*). However very rarely has bioluminescence, with the advantages mentioned previously, been employed for the evolution of a molecular switch. Examples can be seen with the molecular switches created for glucose using the bioluminescent proteins AEQ (*170*) and firefly luciferase (*188*), but are limited beyond these examples.

Herein, we have employed CRP and aequorin in the construction of a molecular switch hybrid protein, CRPAEQ capable of the detection of cAMP. In cells, cAMP is an omnipresent secondary messenger with a plethora of functions including the regulation of cellular events (*189-193*). The ability to monitor cellular cAMP should provide insight into many cellular processes and responses from external stimuli. CRP is a favorable candidate for use in a molecular switch

given that its hinge region allows for the protein to move in a clamping-type of motion when binding to cAMP, allowing for the possibility of a molecule attached to the ends of the protein to experience a greater change in position when the motion caused by the conformational change occurs. In our "on/off" molecular switch, cAMP provides the input signal when it selectively binds to CRP and induces the conformational change in the native protein, while aequorin provides the output signal in the form of the bioluminescence emission. To prepare the hybrid protein, aequorin was split in two fragments and attached to the N and C terminal ends of CRP to take advantage of this characteristic. We had previously observed that that there is a flexible loop between the EF hands I and II of aequorin, corresponding to amino acids 46-51, that allow for insertion of another protein without significantly disrupting the rest of the tertiary structure of the protein (*170*). We, therefore, hypothesized that by inserting CRP between amino acids 47 and 48 in addition to adding a linker sequence to both ends of the CRP molecule the aequorin fragments would have enough flexibility and freedom to reunite and reassemble to form the active bioluminescent aequorin complex.

EXPERIMENTAL PROCEDURES

Materials. Tris free base–Tris(hydroxymethyl)amino methane was purchased from Serva (Heidelburg, Germany). Disodium ethylenediaminetetraacetate (EDTA), Luria-Bertani (LB) Agar, and LB Broth were purchased from Fischer Scientific (Fair Lawn, NJ). Urea, glucose, albumin from bovine serum (BSA), calcium chloride, 3'-5'-cyclic adenosine monophosphate, 3'-5'-cyclic guanosine monophosphate, 3'-5'-cyclic inosine monophosphate, 3'-5'-cyclic uridine

monophosphate, 3'-5'-cyclic cytosine monophosphate, ampicillin sodium salt, chloramphenicol, kanamycin monosulfate, and ethidium bromide were purchased from Sigma-Aldrich (St. Louis, MO). Sodium Dodecyl Sulfate (SDS) was purchased from Curtin Mathesin Scientific, Inc. (Houston, TX). Isopropyl-β-D-thiogalactoside (IPTG) was purchased from Gold Biotechnology, Inc. (St. Louis, MO). DEAE Fast Flow was purchased from GE Life Sciences. Poros 50 HQ was purchased from AB Applied Biosystems (Foster City, CA). The Bradford protein assay kit was purchased from Bio-Rad Laboratories, Inc. (Hercules, CA). Mini-prep kits and gel extraction kits were purchased from Qiagen (Valencia, CA). Top10 and Top10F' chemical competent cells were purchase from Invitrogen (Carlsbad, CA). The plasmid, pET28(a)+, BL21(DE3)pLysS chemical competent cells, and BL21(DE3) cells were purchased from Novagen (Madison, WI). JM109(DE3) chemical competent cells were purchased from Promega (Madison, WI). Gel code blue stain was purchased from Pierce (Rockford, IL). T4 DNA ligase, alkaline phosphatase, and EcoRI, HindIII, and NheI, restriction enzymes were purchased from Promega (Madison, WI). Pfu Ultra polymerase and Taq polymerase were purchase from Strategene (Ceder Creek, TX). All chemicals were reagent grade or better and all aqueous solutions were prepared using 16 mΩ deionized distilled water produced by a Milli-Q water purification system (Millipore, Bedford, MA).

Apparatus. Polymerase chain reactions (PCR) were performed using an Eppendorf Mastercycler Personal (AG, Hamburg). DNA electrophoresis was performed using a FB105 Fischer Biotech Electrophorese Power Supply

106

(Pittsburgh, PA) and the gels were visualized using a UV Transilluminator (UVP, Upland, CA). OD$_{600}$ readings were taken using a Spectronic 21D (Milton Roy, Ivy Land, PA). Cells were sonicated using a Fischer Scientific 550 Sonic Dismembrator (Pittsburg, PA). Proteins were expressed by incubating bacteria at 37°C on a Forma Scientific Orbital Shaker (Waltham, MA) and harvested using a Beckman J2MI centrifuge (Palo Alto, CA). Fusion proteins were purified using a BioCad Sprint Perfusion Chromatography System (Perseptive Biosystems, Framingtion, MA). Purity of the fusion proteins were verified by sodium dodecyl sulfate-polyacrylamide gel electrophoresis (SDS-PAGE) using Invitrogen 10-20% Tris-glycine gels in an Invitrogen X Cell Sure Lock Mini Cell (Carlsbad, CA). Bioluminescence measurements were made on an Optocomp I test tube luminometer (MGM Instruments, Inc., Hamden, CT) using Fischer borosilicate 12x75mm disposable glass tubes (Pittsburg, PA). Emission spectra were taken on a custom made SpectroScan instrument from Sciencewares (Farmingham, MA). Circular dichroism measurements were performed on a Jasco J-810 circular dichroism system (Easton, MD).

Construction, Expression, and Purification of CRPAEQ fusion protein. The CRPAEQ gene was produced by an overlap PCR method as shown in figure 26. More specifically the PCR was used to amplify the coding sequence for amino acids 1-47 of aequorin and to introduce an EcoRI restriction site on the 5' end of the coding sequence along with a sequence coding for a linker region with the sequence SGGGGS followed by the restriction sites for PstI and SacI at the 3' end. The coding sequence for amino acids 48-189 of aequorin was amplified
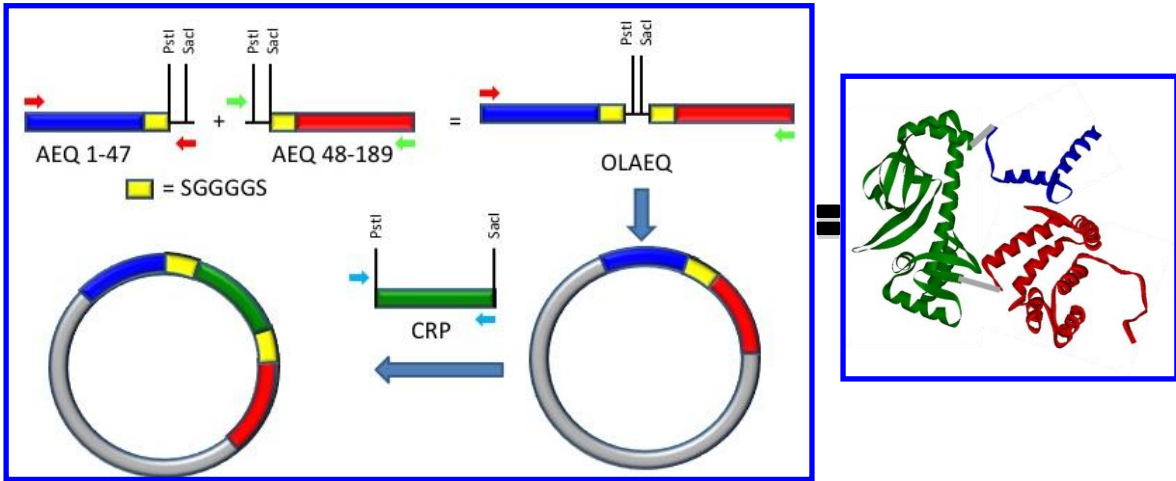
Figure 26. Schematic of the stepwise design of the plasmid containing the gene for the CRPAEQ fusion protein. Briefly; the individual fragments of AEQ (amino acids 1-47 and 48-189) and CRP are PCR amplified while introducing unique restriction sites. Overlap PCR is then used to attach to two AEQ fragments followed by the ligation into the expression vector achieved through the cutting of unique restriction sites and ligated back together. The CRP gene is then inserted into the middle of the AEQ gene through the same restriction and ligation method. A schematic of how the fusion protein could potentially appear if crystalized is shown on the right.

separately introducing PstI and SacI restriction sites and the linker region at the 5'end and a HindIII restriction site 3' end of the coding sequence. By utilizing the aequorin 1-47 forward primer and the aequorin 48-189 reverse primer in an overlap PCR reaction the complete aequorin gene was reassembled with the linker region followed by the PstI and SacI restriction sites followed by another linker region inserted between amino acids 47 and 48 of aequorin. The overlap aequorin product was ligated into the EcoRI and HindIII sites of pIN4 to yield pOLAEQ. The gene for CRP was then amplified with PstI and SacI restriction sites introduced on 5´ and 3´ ends of the gene, respectfully, and inserted into the PstI and SacI sites of the aequorin gene in pIN4 to yield pCRPAEQ. The resultant fusion protein gene encodes for the split aequorin protein attached to the ends of CRP as follows: AEQ1-47-linker-CRP-linker-AEQ 48-189. After unsuccessful expression attempts were performed it was decided to remove the CRPAEQ fusion protein gene from the pIN4 plasmid and insert it into the pET28(a)+ plasmid. The PCR was used to introduce a NheI restriction site at the 5´ end of the coding sequence while conserving the HindIII restriction site on the 3´ end. The CRPAEQ gene was then ligated into pET28(a)+ to produce pCRPAEQ2. The DNA was then transformed into competent BL21(DE3) cells. Sequencing to confirm the correct DNA orientation was performed by the University of Kentucky Advanced Genetics Technology Center (AGTC).

Overnight cultures of the bacteria cells were grown at 37°C at 250 rpm in 5 mL LB broth containing 30 µg/mL Kanamycin. This culture was used to inoculate 500 mL of LB broth containing 30 µg/mL Kanamycin and grown at 37°C at 250

rpm. Once the OD_{600} reached 0.4 the cells were induced with IPTG to a concentration of 1 mM and the bacteria were allowed to grow overnight. The cells were collected by centrifugation at 12,000 rpm, 4°C for 15 minutes.

The CRPAEQ protein was only found to be expressed in inclusion bodies under a number of different conditions and thus required to be purified from the inclusion bodies. The cell pellet was dissolved in 20 mL of 30 mM Tris/HCl pH 7.5 2 mM EDTA buffer and lysed by two, 5 minute cycles of sonication alternating 10 s on/ 10 s off. The lysis mixture was then centrifuged for 10 min at 12,000 rpm and 4°C to collect the inclusion bodies. The pellet was then washed consecutively with 30 mM Tris/HCl pH 7.5, 2 mM EDTA, 150 mM NaCl; 30 mM Tris/HCl, pH 7.5, 2 mM EDTA, 1% Triton X-100; and then 30 mM Tris/HCl, pH 7.5, 2 mM EDTA, 5 mM $CaCl_2$ with the protein collected in between the washes by centrifugation at 12,000 rpm and 4°C for 10 minutes. The pellet was then re-suspended in 3 mL/g of pellet of 30 mM Tris/HCl, pH 7.5, 2 mM EDTA, 6 M Urea and allowed to rotate overnight at 4 $^{\circ}$C. The mixture was then centrifuged at 12,000 rpm and 4 $^{\circ}$C for 20 minutes and the supernatant, which contained the denatured CRPAEQ protein, was reserved. The denatured protein was purified using a DEAE Sepharose Fast Flow ion exchange column on a BioCAD Sprint Perfusion Chromatography System. The column was equilibrated with 4 column volumes of equilibration buffer (30 mM Tris/HCl, pH 7.5, 2 mM EDTA, 6 M urea). The denatured protein supernatant was loaded onto the column and the column was washed with 3 column volumes of equilibration buffer. The protein was then eluted with elution buffer (30 mM Tris/HCl, pH 7.5, 2 mM EDTA, 6 M urea, 1 M

110

NaCl) using a 0 to 50% elution buffer gradient over 10 column volumes. Five mL fractions were collected and a SDS-PAGE was used to confirm the fractions containing the CRPAEQ protein, which were then pooled together. The urea was removed through dialysis in 30 mM Tris/HCl, pH 7.5, 2 mM EDTA to allow the protein to refold. Protein refolding in the correct orientation was verified by bioluminescent activity of the aequorin portion of the protein. The protein concentration was determined to be 1.784 mg/mL using a Bradford protein assay.

Bioluminescent Half-life Determination. A final concentration of 1 µg/mL of coelenterazine was added to the apoCRPAEQ fusion protein and left for 18 h at 4 ^{o}C. Ten µL of the coelenterazine charged CRPAEQ mixture was added to a glass culture tube and the bioluminescence was measured using the Optocomp I test tube luminometer and the signal was collected for 10 s. The half life was determined using the one phase exponential decay kinetics equation from GraphPad Prism. The same procedure was followed for the half life determination of the CRPAEQ fusion protein in the presence of 0.1 mM cAMP.

Emission spectra. The CRPAEQ protein was charged with several native coelenterazine for 18 h at 4 ^{o}C. The emission spectra of the protein with the native coelenterazine was then measured on the SpectroScan instrument from ScienceWares (Framingham, MA, USA).

cAMP Detection by CRPAEQ Fusion Protein. The CRPAEQ fusion protein was diluted to 1×10^{-5}M in 30 mM Tris/HCl, pH 7.5, 2 mM EDTA and coelenterazine was added to a final concentration of 1 µg/ml. Ninety µl of the

CRPAEQ/coelenterazine mixture was placed in a 1.5 ml polypropylene microcentrifuge tube and 10 µl of the corresponding cAMP standard was added to achieve the desired concentration and allowed to charge at 4°C for 18 h. Ten µl of the charged mixture was added to a disposable glass tube and the bioluminescence was measured using the Optocomp I luminometer as described above. The bioluminescent signal was integrated over six s.

Selectivity Study. To determine the selectivity of the CRPAEQ fusion protein the stock apoCRPAEQ fusion protein was diluted to 1×10^{-5} M and coelenterazine added to a final concentration of 1 µg/ml. Ninety µl of this mixture was added to 1.5 ml polypropylene microcentrifuge tubes along with 10 µl of a cyclic nucleotide corresponding to a final concentration of 0.1 mM. The cyclic nucleotides tested consisted of cyclic guanosine monophosphate (cGMP), cyclic cytidine monophosphate (cCMP), cyclic uridine monophosphate (cUMP), cyclic inosine monophosphate (cIMP) and were prepared in 30 mM Tris/HCl, pH 7.5, 2 mM EDTA. The tubes were allowed to charge 18 h at 4°C then 10 µl of each tube was added to a disposable glass tube. Bioluminescence was measured using the Optocomp I luminometer as described above.

Cellular cAMP Monitoring. Three separate BL21(DE3) *E. coli* cell cultures were grown at 37 °C in 8 mL LB broth at 250 rpm to an O.D.$_{600}$ ~ 0.5. One culture was grown in the presence of 100 µM glucose, another in the presence of 50 mM inorganic phosphate, and the third without any additions. Once the O.D.$_{600}$ of 0.5 was reached the cell cultures were distributed into 1 mL aliquots. Two µL of toluene was added to each aliquot and shaken at room temperature

for 10 minutes at ~200 rpm. Fifty µL of the cell solution was then added to 100 µL of a solution of CRPAEQ in 30 mM Tris/HCl, pH 7.5, 2 mM EDTA with 1 µL coelenterazine and allowed to charge 18 h at 4 ^{o}C. Ten µL of each solution was then added to a disposable glass tube and the bioluminescent activity was observed using the Optocomp I as described above and integrating the signal over 6 s.

RESULTS AND DISCUSSION

Bioluminescence has a number of advantages over fluorescence as a bioanalytical tool including extremely low background, highly sensitive detection and the ability to be used in the absence of an external excitation light source. Exhibiting these quality characteristics aequorin and has been shown to be a very sensitive label for a variety of applications (*176-178*). CRP is natively found in *Escherichia coli* and is used to regulate transcription of over 150 genes in the organism. CRP is allosterically activated by cAMP binding and upon binding cAMP undergoes a conformational change (*181-182, 194*). This conformation change combined with the bioluminescent activity of aequorin can be integrated in the form of a fusion protein to create a very efficient and biologically relevant molecular switch to be implemented in a cAMP sensing system.

Much care, however, must be exhibited when genetically engineering the two proteins to be expressed together as a fusion protein. Aequorin consists of four EF hands, three of which bind calcium (EF-hand I, III, and IV). It also has three triads consisting of the amino acids tryptophan, tyrosine, and histidine that are involved in the detainment of the chromophoric coelenterazine in the active

113

site of the protein (*170*). These components are very important to the function of aequorin and must be conserved to preserve bioluminescent activity. Disrupting any of the structural components by inserting CRP would render the resulting protein bioluminescently inactive and thus useless for the designed function. However, there is a flexible loop on the exterior of the protein between EF-hand I and EF-hand II corresponding to amino acids 46-51 that has the ability to house a large sequence without disturbing the functional components of aequorin mentioned previously (*170*). Thus CRP was inserted between amino acids 47 and 48 of aequorin. A linker region was also included in between the aequorin and CRP fragments to allow for extra flexibility and aid in the correct folding of the individual portions of the protein. The gene encodes for the split aequorin protein sequence attached to the ends of the CRP sequence as follows: AEQ1-47-linker-CRP-linker-AEQ 48-189 (figure 26). The fusion protein coding gene was then ligated into the pET28(a)+ expression plasmid. Following the transformation of the plasmid into BL21(DE3) cells an acceptable level of expression was achieved, however the protein was expressed in inclusion bodies. Several changes to the expression of the protein were attempted in order to avoid the formation of inclusion bodies including growth at a lower temperature and inducing with decreased amounts of IPTG with no avail resulting in the need to purify the protein as inclusion bodies followed by refolding of the protein. The inclusion bodies were solubilized through the use of urea and purified on a DEAE Sepharose ion exchange column also in the presence of urea. Refolding of the fusion protein was achieved by removing the urea through

114

dialysis with 30 mM Tris/HCl, pH 7.5, 2 mM EDTA buffer. The purity of the protein was confirmed by a single prominent band at ~46 kDa on a SDS-PAGE gel, corresponding to the size of the CRP monomer added to that of aequorin. The protein also exhibited bioluminescent activity when charge with the coelenterazine and exposed to a Ca^+ containing solution. The purified CRPAEQ was found to have a final concentration of 1.784 mg/ml as determined by a Bradford Assay.

The molecular switch showed a reproducible, decrease in signal corresponding to an increase in cAMP concentration from about $1x10^{-7}$ M to $1x10^{-3}$ M (figure 27). It has been reported that CRP contains two cAMP binding sites, one higher affinity site located in the N-terminal domain and also a lower affinity site contained between the hinge region and turn of the helix-turn-helix motif of the protein (*182, 185*). The higher affinity cAMP binding site binds cAMP in the µM range, and the lower affinity site is bound when cAMP is in the mM range (*179*) keeping the observed response consistent with previous studies and permitting the sensor to be suitable for measuring cAMP levels of biologically relevant samples (*195*). As reported above, as the cAMP concentration increases, the bioluminescent signal from the aequorin portion of the fusion protein decreases. It has been shown previously that CRP undergoes a hinge type conformational change upon the binding of cAMP (*182*). This leads to the presumption that upon binding of cAMP, the conformation change experienced by CRP occurs in a manner which causes the two halves of aequorin to move in

115
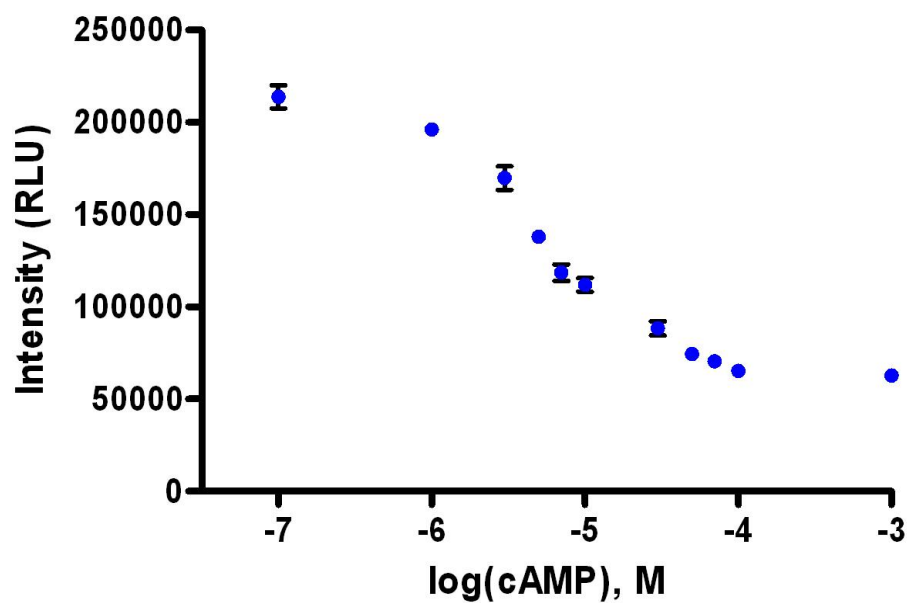
Figure 27. Dose-response plot of the observed response of the CRPAEQ fusion protein to varying concentrations of cAMP. Data points are the mean of three samples in triplicate ± one standard deviation. Error bars not visible are concealed by the data point.
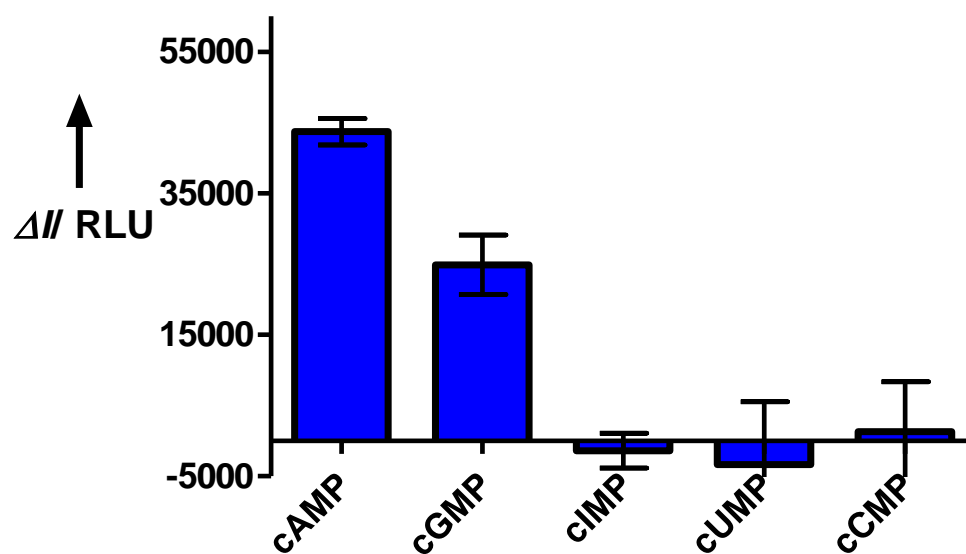
Figure 28. Selectivity study results.*ΔI* represents the intensity change from the control in relative light units (RLU) after the addition of the respective cyclic nucleotides.   Data represent the mean of three samples in triplicate ± one standard deviation.

opposite directions from each other based on their original position. With the spatial separation increased between the two halves, the bioluminescently active complex is unable to be reformed thus inhibiting the production of light upon the binding of Ca^{2+} by the aequorin portion of the protein as shown above in figure 24.

A selectivity study was performed to determine the effect other cyclic nucleotides would have on the activity of the fusion protein. The data show CRPAEQ to be selective for cAMP (figure 28). Cyclic UMP (cUMP), cyclic CMP (cCMP), and cyclic IMP (cIMP) were found to be negligible in affecting the bioluminescent signal. cGMP, the most similar to cAMP in terms of structure, was found to affect the signal, but to a lower extent than that of cAMP. cAMP decreased the bioluminescent signal from CRPAEQ by 47% while, cGMP only caused a 26% decrease in the signal.

The spectral properties of the fusion protein were compared to that of the individual aequorin. The half-life of the bioluminescence from the aequorin of the CRPAEQ fusion protein was found to be 1.5 s without cAMP and 1.9 s with cAMP bound, similar to the 1 s half-life of the cysteine free mutant of aequorin (*196*). The emission maximum was slightly blue shifted to 480 nm, but still similar to the 471 nm emission shown by the cysteine free aequorin (*196*). This shows that although the CRP protein has been inserted in between the two halves of aequorin, the kinetics of the protein have not been greatly affected.

To test the switches potential in cAMP monitoring applications *Escherichia coli* was used as a model system. It has been shown previously in *Escherichia*

coli that inorganic orthophosphate is able to increase the amount of intracellular cAMP via two separate mechanisms. The inorganic orthophosphate not only stimulates adenylyl cyclase, the enzyme responsible for cAMP synthesis, but also slows down the degradation of cAMP by inhibiting cAMP phosphodiesterase, the enzyme responsible for the degradation, consequently elevating the cAMP levels in the cell (*197*). Glucose has been shown to possess a reverse effect on adenylyl cyclase, decreasing its activity, resulting in lower intracellular cAMP concentrations (*198*). Thus in an effort to allow for changes in cellular cAMP levels Escher*ichia coli* cultures were grown in the presence of either inorganic orthophosphate or glucose in hopes of increasing and decreasing cellular cAMP levels respectively. Previous studies also indicate the use of toluene to increase cellular permeability is an effective and more efficient method to allow for the quantification of intracellular cAMP (*197-198*). After allowing cultures to grow in the presence of the specified molecules, the CRPAEQ molecular switch was utilized to detect changes in cellular cAMP levels. As shown in figure 29 the molecular switch provides a very reliable method to monitor increases and/or decreases in cellular levels of cAMP in response to different external stimuli without the need to lyse the cells. Although aequorin has traditionally been employed as a Ca^{2+} probe, in our experiments we employ EDTA buffered solutions to prevent uncontrolled bioluminescence emission triggered by endogenous Ca^{2+}. This made sure the change in the bioluminescent signal was due solely to the changes in cAMP levels and not Ca^{2+} fluctuation.
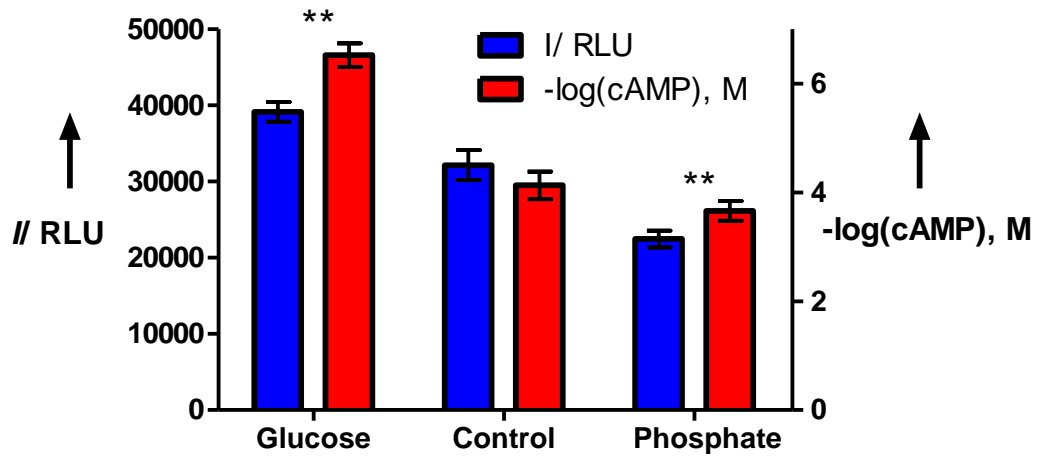
Figure 29. The bioluminescent signal observed from the CRPAEQ molecular switch when exposed to cell cultures grown in the presence of either glucose, inorganic orthophosphate, or with no additions (Control). Concentrations were calculated from dose response plot of known concentrations. Points are mean of three samples in triplicate ± standard deviation. (** P value < 0.05 as determined via ANOVA compared to the Control culture).

There are currently a variety of cAMP detection methods that have been developed and explored, including radiometric and antibody based assay systems (*199*). The radiometric systems pose the safety issues and disposal problems while the antibody based systems require expensive antibodies. Among those, we can cite the commercially available cAMP-Glo[TM] Assay from Promega (Promega Coorporation, Madison, WI, www.promega.com) and the LANCE[®]*Ultra* cAMP detection kit from PerkinElmer (PerkinElmer, Waltham, MA, www.perkinelmer.com). The cAMP-Glo[TM] assay uses a luciferase and protein kinase A to indirectly monitor the cAMP levels. cAMP binds to protein kinase A, releasing its catalytic subunits, which then catalyze the transfer of a terminal phosphate from ATP to the protein kinase A substrate, reducing the levels of ATP in the solution. The remaining ATP is then quantified with luciferase. Therefore, as the amount of cAMP increases, more ATP is consumed by the protein kinase A reaction, causing a decrease in the luminescence observed. The LANCE[®]*Ultra* cAMP detection kit is a competitive binding assay between europium chelate labeled cAMP molecules and free cAMP in the sample. The two cAMP forms compete for binding sites on a fluorescently labeled anti-cAMP antibody. When the europium chelate molecule is excited, if it is bound to the antibody it transfers non-radatively energy to the attached fluorescent label, which, in turn, is excited and emits a distinct fluorescence signal.   However, when the free cAMP is bound to the labeled antibody, there is no europium chelate capable of transfering energy to the fluorescent label, and therefore the fluorescence emission observed corresponds to that of the europium on the

labeled cAMP molecules.   Thus, the intensity of the emission from the fluorescently labeled antibody is inversely proportional to the amount of free cAMP in the solution. Our CRPAEQ molecular switch offers a unique alternative to the available methods and creates a more direct detection method than those of the existing technologies. The ability of our switch to directly translate the binding of cAMP to a change in the bioluminescence intensity without requirement for the addition of reagents at different steps, results in a faster method of detection.   Moreover, our switch is also eliminates the need for expensive labeled cAMP molecules and antibodies.   This direct detection also reduces the possibility of the results being inaccurate due to potential changes in the concentration of the complementary assay molecules, such as ATP, that could be caused by unrelated cellular events or responses.   In addition, bioluminescence offers the advantage of eliminating background interference from autofluorescent molecules commonly present in cellular and physiological samples. The CRPAEQ molecular switch provides a reagentless detection method saving resources while offering a safer and more environmentally friendly system.   The hybrid protein which is the basis of the molecular switch, is expressed as a single protein.   Thus, if the apoprotein is expressed and reconstituted *in vivo*, it could potentially find applications in cellular detection.

CONCLUSIONS

In summary, it has been demonstrated that the functions of two unrelated proteins, each with desirable characteristics can be successfully coupled in the development of a bioluminescent molecular switch which can be used for

detection and monitoring of a specific analytes. CRP, a cAMP selective binding protein, was fused with a split aequorin, a photoprotein that generates a bioluminescent signal. When combined, the fusion hybrid protein results in a molecular switch capable of highly sensitive cAMP detection. This switch offers a number of advantages over currently employed methods in terms of simplicity, safety, and environmental friendliness. Moreover, it is envisioned that it would find a host of applications in a number of fields, such as biomedicine, biotechnology, medicinal chemistry, pharmacology, etc. Finally, CRPAEQ joins a very short list of bioluminescent molecular switches. Very rarely has a protein been able to be split, and re-united under desired conditions to give a reliable response able to be used for quantification of a specific analyte. This could open the doors to a whole new class of detection molecules to be implemented in various monitoring applications, allowing for a better understanding of mechanisms and behavior of complex biological and cellular systems as well as for elucidating the interactions and mechanisms of not-well characterized naturally occurring proteins.

CHAPTER SIX

A PORTABLE, REAGENTLESS, OPTICAL SENSOR CATHETER FOR REAL TIME *IN VIVO* POTASSIUM DETECTION

INTRODUCTION

The potassium ion, K^+, plays a critical role in many physiological processes and can be a valuable marker for a variety of applications, including postoperative monitoring, signaling of ischemia, and renal failure, among others (*200-203*). However, there is no commercially available sensor that can monitor *in vivo* the variations of potassium ion concentrations in real time. Thus the need for a fast and reliable *in vivo* potassium ion sensing system, capable of real time monitoring would be valuable for many clinical applications, providing instant feedback, allowing for immediate action, and efficient monitoring, management and treatment of patients. Current methods of choice for potassium detection include flame emission spectroscopy and ion-selective electrodes (*204*). Although very accurate with regard to potassium analysis, the possibility of *in vivo* detection with these methods is difficult. Although previously, there have been claims of real time K^+ detection systems (*205*), they did not demonstrate their ability for *in vivo* monitoring and were never commercialized (*206*). More recently, selective ionophore optodes incorporated into polymeric membranes have been employed for the quantification of potassium (*207-208*). A variety of potassium sensing optodes have been implemented previously for use in

analytical assays (*207-208*), including integration into microfluidic platforms (*209*), microspheres and microspots (*210-211*), to name a few. Coupling of these optodes with fiber optics may provide an avenue by which a real time potassium sensor could be developed. The deposition of a fluorescent optode membrane onto the tip of a custom made fiber optic system has lead to the development of a sensor suitable for integration into a catheter-based system for the *in vivo* detection of K$^+$ ions in a variety of clinical settings.

Herein, we prepared a potassium ion-selective optode that was employed in the development of the sensor. Potassium ionophore III (BME 44) has been shown to be a reliable and selective potassium ionophore (*208, 212*), and hence, was chosen as the sensing element for our catheter sensor. In addition, we decided to employ PVC as the polymeric material for the preparation of the sensor given its chemical inertness, strength, and ease of use with ionophores (*213*).

Due to the harsh and suboptimal *in vivo* conditions, suitable materials play a key role in the development of an *in vivo* sensor. Fiber optics can be manufactured in a variety of diameters and lengths while exhibiting great flexibility and maintaining functionality, thus offering a strong foundation for such a sensor. In addition, the development of an optimal *in vivo* detection device would require a small, durable, and biocompatible components (*206*), all of which are met by a fiber optic. By uncasing a typical optical fiber to leave only the cladding and core, the fiber diameters can be fabricated on the order of micrometers, allowing for dimensions to be tuned for *in vivo* use, more

125

specifically able to be introduced through a small heart catheter. As catheter based systems, such as the Transpac® IV Monitoring Kit (Hospira, Lake Forest, IL), are already currently used for invasively measuring the patients hemodynamic and cardiovascular status, the potassium sensor could be easily integrated into a typical point-of-care monitoring setup.

Along with cooperation from Ocean Optics Inc. (Dunedin, FL) a custom made portable instrumental set-up was developed. Using a miniature fiber optic spectrometer, small light source, and a laptop computer the system can be moved and set-up with ease. The small size of the system makes its use possible even in tight spaces and areas which are already crowded with other instruments. This allows for easy accommodation for point-of-care, operating rooms or other situations requiring immediate potassium monitoring and detection.

EXPERIMENTAL PROCEDURES

Materials. 9-(Diethylamino)-5-(2-octadecylamino)benzo[a]phenoxazine (proton chromoionophore III, ETH 5350), 2-dodecyl-2-methyl-1,3-propanediylbis[N-[5'-nitro(benzo-15-crown-5)-4'-yl]carbamate] (BME 44, potassium ionophore III), valinomycin (Cyclo(L-Val-D-HyIva-D-Val-L-Lac-)$_3$: HyIva = α-Hydroxyisovaleric acid, Lac = Lactic acid), potassium tetrakis[3,5-bis-(trifluoromethyl)phenyl]borate (KTFPB), high molecular weight poly(vinyl chloride) (PVC), bis(2-ethylhexyl)-sebacate (DOS), and Selectophore-grade tetrahydrofuran (THF) were obtained from Fluka (Milwaukee, WI). Tris(hydroxymethyl)aminomethane, molecular biology grade was obtained from Serva Chemicals (Heidelberg, Germany).

126

Potassium Chloride and Human Serum type AB (Male) were obtained from Sigma (St. Louis, MO). Swine whole blood was obtained from Innovative Research (Southfield, MI). A Transpac® IV Monitoring Kit was obtained from Hospira (Forrest Park, IL). All aqueous solutions were prepared using 16 MΩ deionized distilled water produced by a Milli-Q water purification system (Millipore, Bedford, MA). Solutions were kept at 37 °C by an 8000 series heating circulator from Polyscience (Niles, IL). Potassium standards were prepared in 0.500 M Tris/HCl pH 7.4. A custom made fiber optic system consisting of Spectrasuite software, a one meter long, 300 μm in diameter fiber optic cable, a two meter long, 200 μm in diameter bifurcated fiber optic cable, 1 meter uncased, a 400 μm in diameter fiber optic cable, filter holder, PX-2 Xenon light source, and USB4000 miniature fiber optic spectrometer were obtained from Ocean Optics Inc. (Dunedin, FL). 600 nm optical filter was obtained from Chroma Technology Corp. (Rockingham, VT).

Preparation of Optode Membranes and Immobilization on Fiber Optic. Membrane cocktails were prepared with the following composition: 0.5 mg Chromoionophore III, 0.81 mg KTFPB, 1.74 mg BME 44, 19.04 mg PVC, 38.10 mg DOS dissolved in 357 μl THF (*214*)and vortexed to dissolve. Prior to the deposition of the optode membrane on the fiber optic tip, the tip was functionalized with silanol groups to provide for the covalent linkage of the membrane to the fiber optic. The fiber optic was soaked in 1.0 M NaOH for one hr and then soaked in 3-(trimethoxysilyl)propyl methacrylate for 3 hrs. The tip of the uncased, 400 μm in diameter, fiber optic cable was then dip coated in the

membrane cocktail by dipping the fiber optic in the cocktail for 2 s, removing to allow to dry, and then repeating this dipping/drying process for a total of 10 times. The membrane cocktail was allowed to dry for one hr and then the fiber was dipped a second series of times.

Experimental Setup. A one meter long, 300 μm in diameter fiber optic cable connected the xenon source to the filter holder which housed a 600 ± 10 nm filter. One arm of the two meter long, 200 μm in diameter bifurcated fiber optic cable connects the filter holder to the single uncased 400 μm fiber optic that is used to measure the potassium in solutions. The other arm of the bifurcated cable is attached to the portable spectrometer connected through an USB port to a computer. The experiments requiring a temperature of 37 $^\circ$C were held constant at the desired temperature by a water circulator. Smaller vials containing the solution of interest were positioned inside the circulating vial maintained at the desired temperature. The solutions to be measured and the end of 400 μm uncased fiber optic on which the optode membrane was immobilized were covered with a black sheet to avoid influence on the measurements from outside light sources. The settings for the Spectrasuite software were as follows: 200 ms integration time, 75 scans to average, and boxcar of 100. The dark reading was cancelled out using the scope minus dark mode.

Response Time Measurements. The response time of the sensor was determined in order to ensure adequate time was allotted for the sensor to respond before the reading was taken. The tip of the sensor was submerged in

20 mL, stirred solution of 0.05 M Tris/HCl pH 7.4 and allowed to equilibrate. Readings were taken continuously. Then this buffer solution was spiked with two mL of 0.1 M KCl, 0.05 M Tris/HCl pH 7.4, corresponding to 9.1 mM change in the potassium concentration. Readings were monitored until the fluorescent reading was constant.

Potassium Dose Response. The sensor was used to monitor changes in potassium concentrations in 0.05 M Tris/HCl pH 7.4, artificial serum, human serum and swine whole blood. All calibrations were carried out in identical fashion substituting only the solution in which the calibration was taken. The temperature of designated experiments was also controlled with the previously mentioned water circulator. Artificial serum was prepared with the following concentrations: 5×10^{-4} M $NaHSO_4$, 8×10^{-4} M $MgCl_2$, 3×10^{-2} M $NaHCO_3$, 9.5×10^{-4} M NaH_2PO_4, 1.4×10^{-1} M NaCl, and 2.5×10^{-3} M $CaCl_2$. One mL of the solution of interest was added to each of three small glass vials while being stirred continuously. After the solution was at the desired temperature the initial reading was taken in the solution in triplicate. The sensor was briefly removed from the solution and each vial was then spiked with 20µL of 0.1 M KCl 0.05 M Tris/HCl pH 7.4. The sensor was then replaced and allowed to equilibrate for 2 min, and the measurement with the new concentration was taken. This procedure was repeated until the desired concentration was reached. An excitation light of 600 ±10 nm was used and the emission was measured at 683 nm. Initial potassium concentrations of biological fluids were determined by a K^+ specific ion-selective electrode (*205*).

Sensor stability and conditioning. The sensor was left in human serum for 5.5 hrs to demonstrate the sensors reliability for a significant length of time. The sensing optode was placed in the human serum at 37 ^{o}C, while stirring, and the fluorescent response to the initial potassium concentration was recorded. The sensor was then removed from the initial solution and placed in a new serum solution spiked with the potassium concentration corresponding to a 2 mmol/L increase. This process was repeated to a final concentration 6 mmol/L higher than the initial potassium concentration and through the physiological range of potassium. After completion of a series of concentrations the sensor was left in the serum at 37^0 C until the next dose-response was to be evaluated with the same prepared standards. The conditioning of the sensor was performed in the same serum solution used for the dose-response. The sensor was incubated in the potassium containing serum solution at 37 ^{o}C for one hr before the first dose-response was evaluated.

RESULTS AND DISCUSSIONS

We have developed a potassium sensor based on a lipophilic optode membrane, containing a potassium ionophore (BME 44) and a proton chromoionophore (ETH 5350). The electron neutrality condition of the membrane promotes an ion-exchange mechanism where potassium ions bound by the potassium ionophore exchange with the hydrogen ions bound by the proton chromoionophore in the membrane. KTFPB, an anionic lipophilic additive is present to assist in the partition of the ions in and out of the membrane while DOS is used as a plasticizer for the PVC membrane. The capture of potassium

ions from the sample by the membrane results in the release of protons of the same total charge out of the bulk of the membrane. The resultant pH change occurring in the membrane can be monitored by observing the intensity of the fluorescent emission peak of the protonated form of the chromoionophore at ~683 nm, and thus, allowing for the quantification of the potassium ions in the solution of interest. As stated, the emission spectra of the protonated form of the chromoionophore is monitored, therefore as the potassium concentration increases, the fluorescent intensity of the emission peak decreases. The equilibrium reaction is represented as follows:

$$K^+_{(aq)} + L_{(org)} + CH^+_{(org)} + R^-_{(org)} \rightleftarrows LK^+_{(org)} + C_{(org)} + H^+_{(aq)} + R^-_{(org)}$$
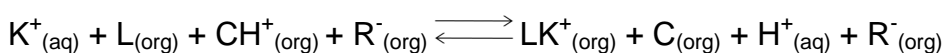
where L represents the potassium ionophore, C represents the chromoionophore, and R^- represents the anionic lipophilic additive (*210*). A more descriptive explanation of this mechanism has been described previously (*215-216*). BME 44 has been shown to be sensitive and selective for potassium (*212*), while PVC provides optimal mechanical characteristics for use in the sensing membrane (*213*).

An uncased 400 µL in diameter fiber optic cable with the optode membrane immobilized on the tip was used for potassium detection. The fact that the fiber is uncased allows the diameter of the fiber optic to be small enough in dimension to allow for incorporation of the sensor into an existing commercially available heart catheter making possible its use for *in vivo* detection of whole blood potassium concentrations at or near the heart (figure 30). For the

A
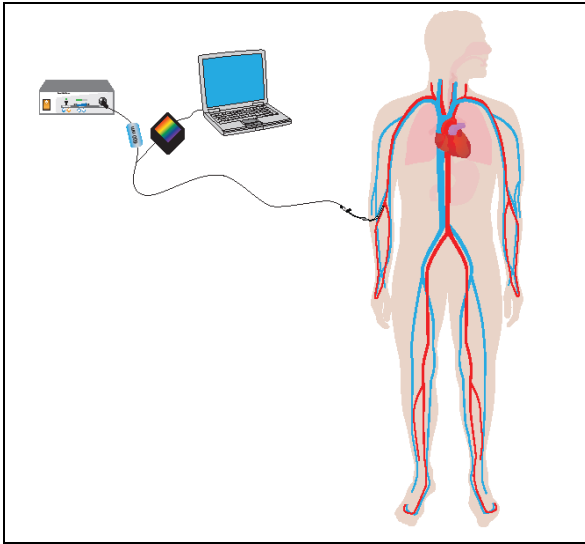
B
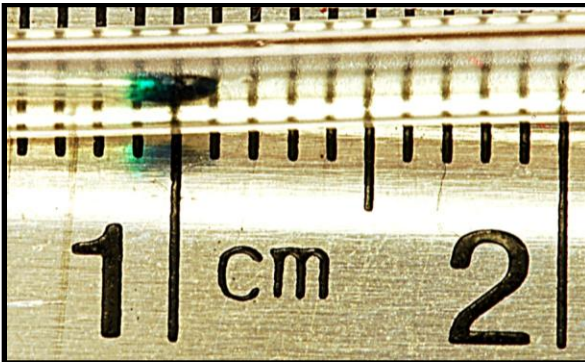
Figure 30. A is a schematic for the experimental setup of the portable, fiber optic potassium sensor as the system could easily be incorporated with currently used heart catheters. B is the potassium sensing optode membrane immobilized on the tip of an uncased fiber optic is shown inside a Hospira Transpac IV Monitoring Kit.

characterization of the system *in vitro*, the tip of the fiber optic cable with the immobilized membrane was submerged in the solution of interest while being constantly stirred. In order to perform experiments at physiological temperature we employed a water bath circulator to keep the solutions at 37 °C.

Initially, the custom made, uncased, 400 µm in diameter, fiber optics intended for the optode immobilization were obtained with one inch of exposed, uncladded fiber optic core at the tip of the fiber. It was hypothesized that this longer uncladded portion, on which the sensing membrane was immobilized would increased the surface area available for the deposition of the membrane and would allow for an amplified fluorescent signal, which should lead to a sensitive response. However, upon further investigation it was discovered that a shorter uncladded portion of roughly one mm to even a completely cladded fiber optic allowed for a more sensitive response to the potassium ions as shown in figure 31. It has been shown previously that removing cladding from a fiber optic and immersing in an aqueous solution can result in a loss of the fluorescent intensity measured. This is not only due to a loss of the fluorescence light emitted as a response to potassium present, but also because there is a loss of excitation light traveling through the fiber (*217*). In our case, with the one inch of exposed fiber optic, a large amount of the excitation and fluorescent emission was lost through the uncladded sides of the fiber optic therefore, the potential gain due to the increased surface area of the uncladded fiber optic did not contribute it the manner that we had expected. Once the shorter fiber was

133
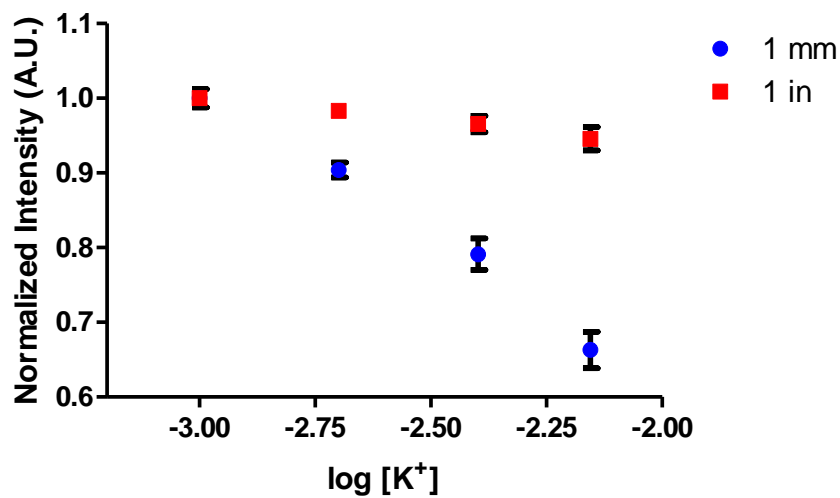
Figure 31.Dose-response comparing the difference in emission intensity of the

optode at 683 nm with respect to the different potassium concentrations

experience by a fiber possessing either a one inch or 1 mm uncladded core at

the tip. Points are the average of 3 readings ± 1 standard deviation and

normalized with maximum value being equal to 1. Error bars not visible are

concealed by the points of the graph.

employed, the light could be focused more efficiently to the tip of the fiber optic where the subsequent fluorescence resulting from the excitation of the membrane could be more efficiently detected, leading to a more sensitive response than that obtained with the longer, one inch uncladded fibers.

We also evaluated the time required for the sensing membrane to reach equilibrium to assess the system's capability for real time blood potassium level monitoring. For that, the sensor was exposed to an initial artificial serum solution and then spiked with 0.1 M KCl, 0.05 M Tris/HCl solution corresponding to roughly a one order of magnitude change in the potassium concentration of the solution. The fluorescent emission at 683 nm was monitored continuously as the optode responded.The response time of the optode membrane was found to be very fast. Roughly, 100% of the change in fluorescence intensity was observed after 60 s of exposure of the optode to the solution of interest, as it can be seen in figure 32. This fast response times allows for the sensor to provide physicians with real time feedback in the detection of small changes of a patient's potassium levels.

The normal physiological range of serum potassium ranges from 3.5-5.5 mmol/L (log[K^+]= (-2.45)- (-2.26)) and even minor deviations from this range can lead to severe conditions (*218*). Hypokalemia, or decreased serum potassium levels, less than 3.0 mmol/L, are an indication of a high level of intracellular
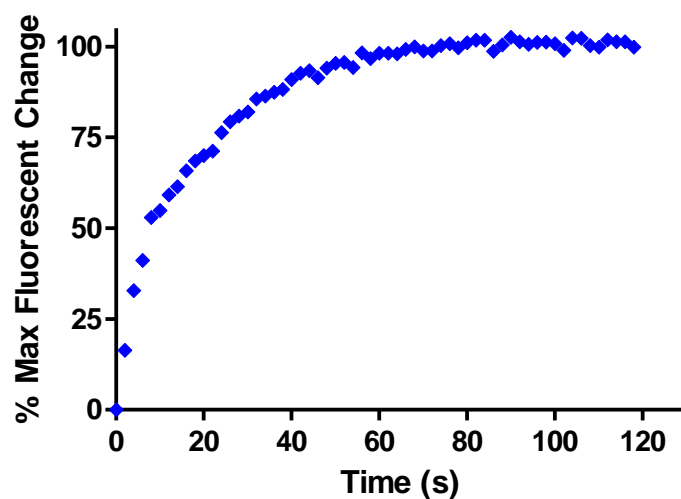
Figure 32. The response time of the sensor was measured by continuously monitoring the change in emission at 683 nm after the addition of potassium to a final increase in concentration of 9.1 mM.

Depletion, and can result in acute neuromuscular symptoms (*204*). Elevated serum potassium level or hyperkalemia, presents potassium levels greater than 7.5 mmol/L, and also has serious effects with symptoms ranging from mental confusion, weakness, slowed heart rate, flaccid paralysis of the extremities, andeventually cardiac arrest, among others. Levels greater than 10 mmol/L typically result in death of the individual (*204*). In order to investigate our system's ability to respond in a linear fashion with respect to changes in potassium concentration through the desired concentration range, the fluorescent emission at 683 nm was monitored as the solution was spiked with 0.1 M KCl, 0.5 M Tris/HCl pH 7.4. The sensor was shown to be effective in monitoring changes in potassium levels of a buffered solution, artificial serum, human serum and swine whole blood within a large dynamic range. When the buffer solution was spiked with known concentrations of potassium ions the response of the sensor was linear, decreasing as the concentration of potassium ions increased over several orders of magnitude well beyond the normal, elevated, or depleted physiological serum potassium levels (figure 33). The sensor was then observed through the potassium range of interest using the artificial serum described previously to study the effect of any possible interfering ions. Again, the sensor responded in a linear fashion as a result of the changes in potassium concentration. The response of the sensor was bidirectional and was not affected by whether the change in potassium concentration happened in an increasing or a decreasing manner (figure 34). The performance of the sensor was also not affected by temperature, as changing the temperature from room

137
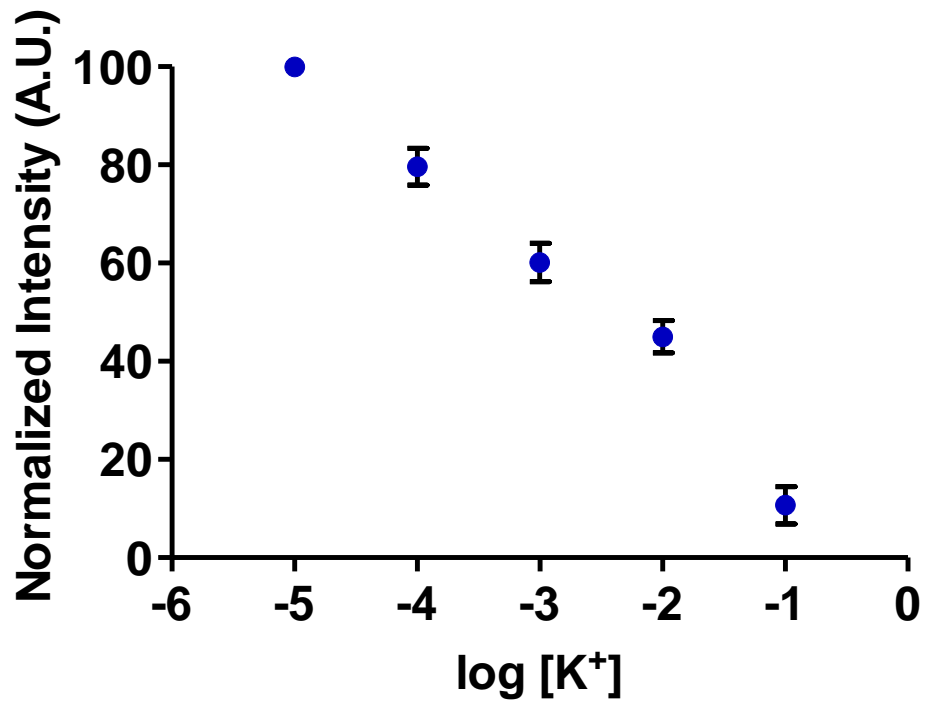
Figure 33. Fiber optic optode sensor response to different potassium concentrations in a Tris/HCl pH 7.4 buffered solution. All points are the average of 3 measurements ± 1 standard deviation. Error bars not visible are concealed by the points of the graph.
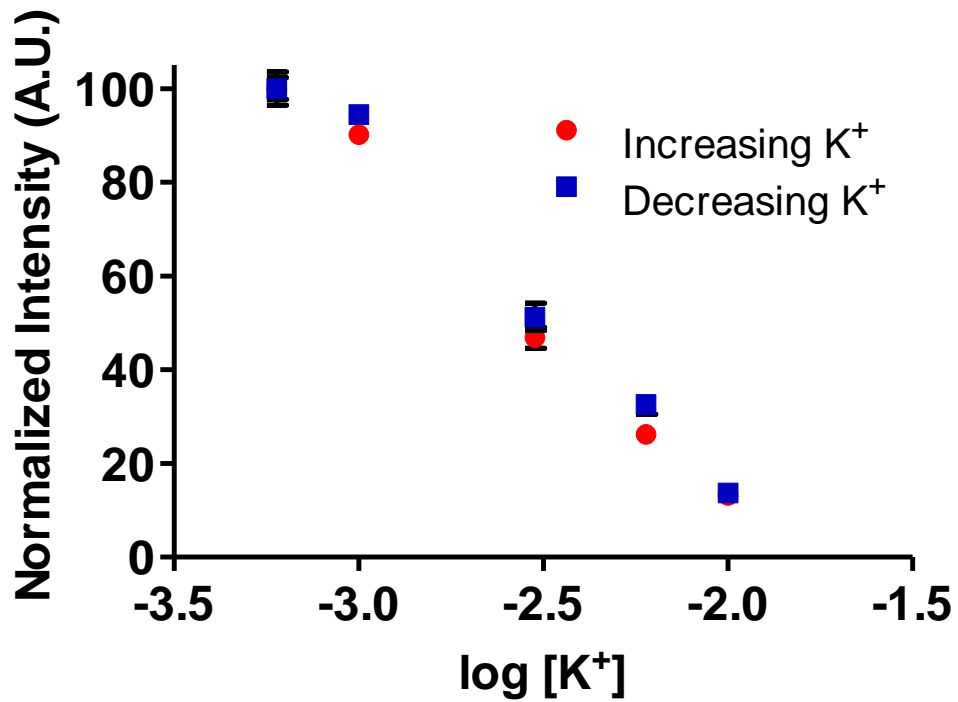
Figure 34. Fiber optic optode sensor response to different potassium concentrations in artificial serum at room temperature, with changes occurring both in an increasing and decreasing fashion. All points are the average of 3 measurements ± 1 standard deviation. Error bars not visible are concealed by the points of the graph.

temperature to 37 ^{o}C did not adversely affect the performance of the system (figure 35). While human serum and blood introduce several other possible interfering substances with the presence of a diverse range of proteins and complex matrix constituents, the sensor was able to maintain the precise linear response to potassium as in buffer. Moreover, it did not exhibit any deviation from the expected performance when employed in human serum (figure 36) or swine whole blood at physiological temperature (figure 37).   As shown, the physiological range of potassium concentrations is encompassed by the dynamic range of the sensor, indicating that this sensor is practical for the detection of potassium in clinically relevant physiological fluids.

Given that the sensor could be potentially used for *in vivo* monitoring of potassium levels in situations such as surgery, the long term stability needed to be investigated. Since the sensor would need to be inserted in or near the heart and in contact with blood, it was postulated that biofouling may become an issue of concern. To test the long-term stability and reproducibility of the sensor, the sensor was placed in human serum at 37 ^{o}C and a dose-response plot was obtained. Then, the sensor was kept in this serum for up to 5.5 hrs and the sensor's performance was evaluated at several points throughout the time period with respect to the response to the different serum potassium concentrations. It was observed that the initial sensor response to potassium was roughly 9.3% higher than the subsequent sensor response after the optode had been exposed to serum (figure 38). We believe that this may be due to the non-specific binding of serum proteins on the sensing optode surface and the resultant interference in
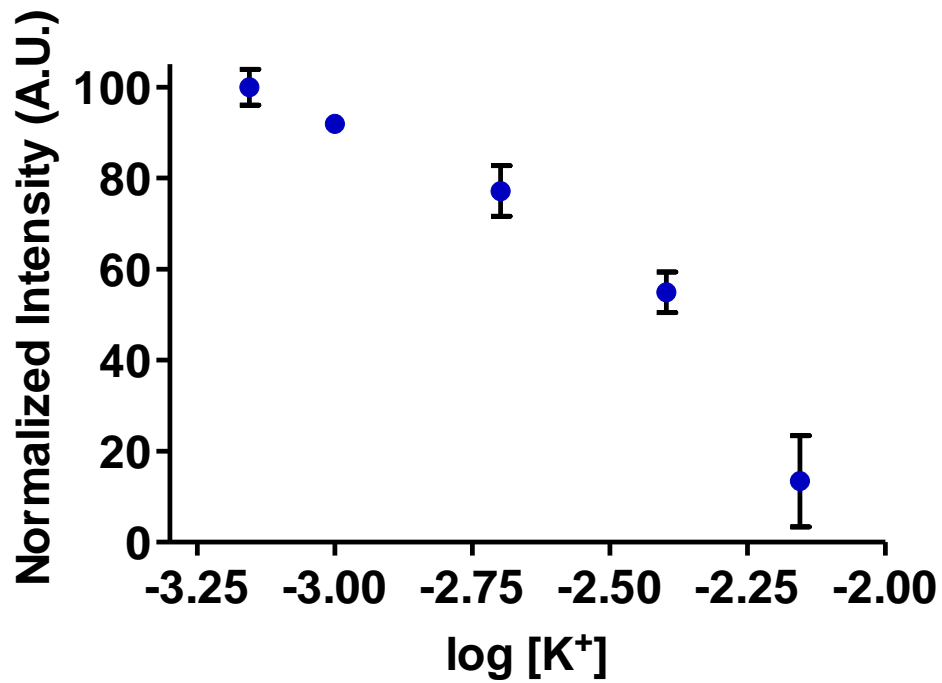
Figure 35. Fiber optic optode sensor response to different potassium concentrations in artificial serum at 37 ^{o}C. All points are the average of 3 measurements ± 1 standard deviation. Error bars not visible are concealed by the points of the graph.

Figure 36. Fiber optic optode sensor response to different potassium concentrations in human serum at 37 $^{\circ}$C. All points are the average of 3 measurements ± 1 standard deviation. Error bars not visible are concealed by the points of the graph.
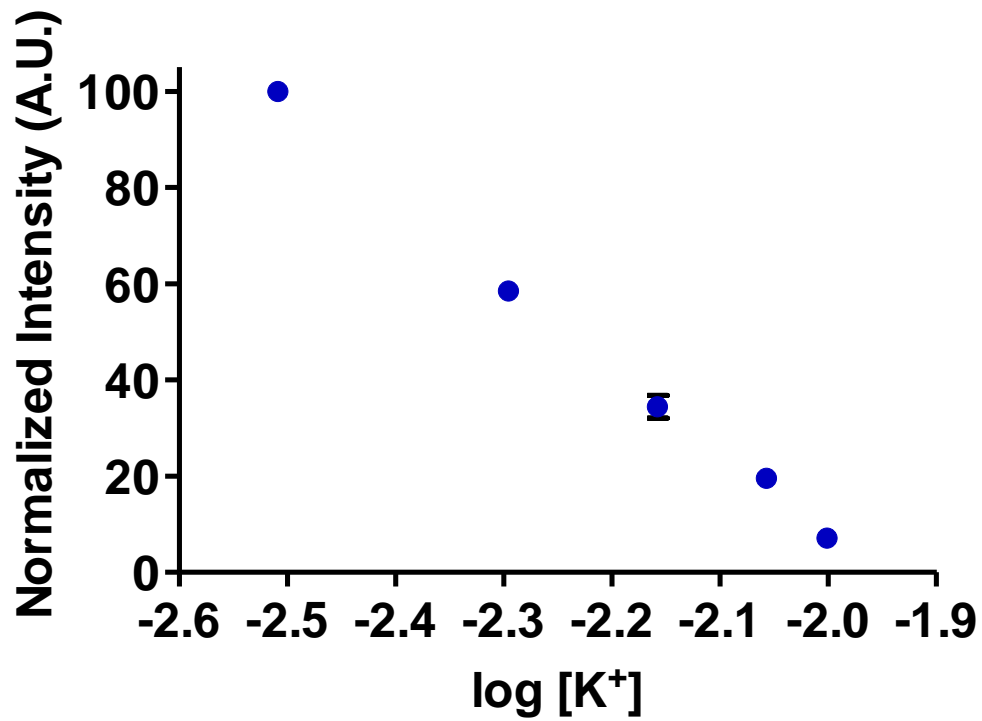
Figure 37. Fiber optic optode sensor response to different potassium concentrations in swine whole blood at 37 ^{o}C. All points are the average of 3 measurements ± 1 standard deviation. Error bars not visible are concealed by the points of the graph.
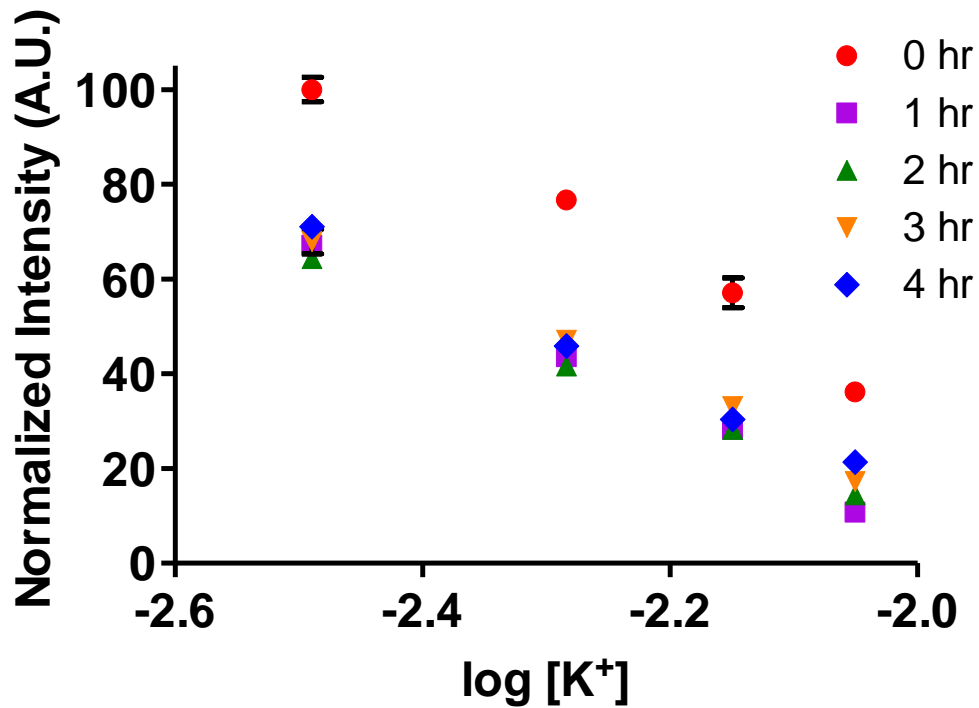
Figure 38. The response of the sensor with respect to time over an extended period of time with the sensing membrane exposed to human serum. The sensing membrane was not exposed to serum prior to the initial potassium measurements. All points are the average of 3 measurements ± 1 standard deviation. Error bars not visible are concealed by the points of the graph.
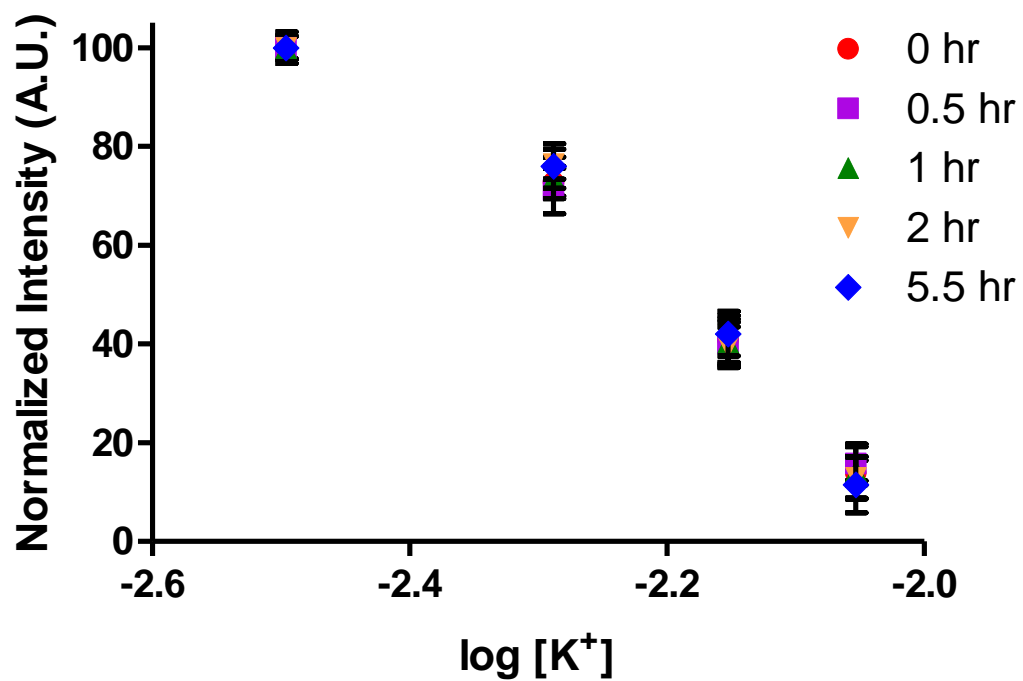
Figure 39. The response of the sensor is shown over an extended period of time in human serum. The first measurement was recorded after a brief conditioning of the sensing optode to human serum. All points are the average of 3 measurements ± 1 standard deviation. Error bars not visible are concealed by the points of the graph.

the binding of the potassium by the optode's ionophores. However, after a brief exposure of the optode to the serum most of the available non-specific sensing surface was blocked by the serum proteins, consequentially allowing a reproducible sensor response to potassium to be observed as shown in figure 39. The sensor was consistently able to produce reproducible readings corresponding to the potassium concentration in the human serum over the extended period of time the sensor was in the solution. Knowing this, for practical purposes, we can incorporate an algorithm in the calibration system to account for this difference or pre-condition the sensor before use.

CONCLUSIONS

We have demonstrated the design and development of a portable, real-time, *in vivo* potassium monitoring sensor that could greatly benefit patients in variety of clinical settings. Furthermore, the sensor, based on an optode membrane immobilized on the tip of a fiber optic has suitable dimensions for integration with a heart catheter. The fast response time allows for changes in potassium levels to be monitored in real-time as they occur. The sensor reacts reproducibly and reversibly at normal physiological blood potassium levels as well as in hypo- and hyperkalemia conditions (*206*), hence exhibiting the necessary characteristics for clinical use. The stability of the sensor over time also shows promise for monitoring potassium levels in a variety of medical procedures, such as those related to interventional cardiology and surgery where real time monitoring of potassium may be crucial.

CHAPTER SEVEN

CONCLUSIONS AND FUTURE PERSPECTIVES

As advancements in molecular engineering techniques and improvements in instrumentation continue to evolve, so too will the use of bioluminescent proteins in analytical applications. Over the past ten years, the sensitivity of CCD cameras and other luminescent detectors has greatly improved.Their cost has also decreased, making systems capable of detecting only a few light emitting molecules readily available for investigators (*219*). This, along with the miniaturization of instruments, has allowed for the integration of the luminescent detectors into miniaturized detection systems such as lab-on-a-chip and lab-on-a-CD type devices (*220*). As the push for faster, portable, and more robust detection capabilities continues for point-of-care and on-site analysis, these systems provide many of the desired characteristics. The ability for multiplexed analysis of samples in these miniaturized devices would further increase the versatility and value of these systems to the scientific community.

To that end, Chapter Three describes the simultaneous multiplexed detection of three pro-inflammatory cytokines in physiological fluids through the clinical range of interest. Previous multiplexed detection with bioluminescent labels has been reported and there are several methods which have allowed more than one analyte to be detected in a single sample. These include separating the emission spectra by using two different, individual luminescent proteins (*123-125*), using genetically engineered proteins to achieve spectrally

diverse emission profiles (*96, 126*), orallowing the differentiation of the signals through time resolution (*100*).   All of the previous studies, although very innovative and important, are limited to two analytes. Our study combines time and wavelength resolution to create three distinct time/wavelength windows to allow the successful resolution of three separate bioluminescent signals in a single solution. This is the first time that a single bioluminescent protein has been able to quantify three separate analytes simultaneously. The cytokines of interest (IL-1β, IL-6, and IL-8) were each individually genetically fused to a selected aequorin mutant to create three new proteins. The resultant proteins were expressed in *E. coli* and purified. Each interleukin-aequorin fusion protein was characterized with respect to emission profile and decay kinetics with nine different coelenterazine analogs.   The selected semi-synthetic interleukin-aequorin fusion proteins gave a spectral separation of 54 nm in their emission maximum and a half-life difference of 13.68 s, sufficient to resolute all three signals simultaneously.   An assay was then developed that was capable of detecting all three targeted proteins in a single well with detection in the clinically relevant range.

Future work to extend the findings presenting inChapter Three would focus on several areas. The first would be to incorporate the use of aequorin and multiplexed detection into a miniaturized device. Aequorin has previously been shown to be compatible with miniaturized device platforms (*220*). Thus the initial next step would be to transfer the developed microtiter plate assay to a miniaturized lab-on-a-CD platform. A CD mold with the desired microchannels,

reservoirs, and burst valves would need to be constructed and tested, and then the assay scaled down to appropriate volumes and incubation times. Again as a proof of concept the multiplexed cytokine detection would serve as an excellent template to start with as the fusion protein constructs and purification procedure are already established. Further extension and new applications could also include other clinically relevant diagnostic tests such as DNA hybridization assays able to quickly and efficiently differentiate unique influenza strains. As new influenza strains continue to emerge, the ability to quickly determine which strain a patient has contracted could offer valuable information that would determine the subsequent treatment and physicians recommendations. The bioluminescent labels would offer the sensitivity to label the DNA probes efficiently and allow detection in the μL or less volume required for the miniaturized devices.

Additional attention should also be directed towards the continued identification and synthesis of new aequorin mutants and coelenterazine analogues with favorable characteristics. The development of a coelenterazine analogue that shifted the aequorin emission to the higher energy, shorter wavelength region while maintaining the longer half-life would allow the current multiplexed assay to immediately be expanded to four analytes. Currently, the spectral overlap of the shortest wavelength and long half-life semi-synthetic aequorin (F113W mutant with coelenterazine *i*, 484 nm emission max and 11.65 s half-life) make to resolving the signal from either the longer or shorter wavelength peaks obtained with the interleukin fusion proteins extremely difficult.

One potential option would be if a coelenterazine analogue was constructed that combined the iodine substitution in the C2 position to retain the longer half-life with one of the alterations at the C8 position that has lead to the higher energy emission with previous coelenterazines. Pairing this coelenterazine with one of the current aequorin mutants that show a more blue shifted emission, such as the F113W mutant, could possibly result in a semi-synthetic mutant with an emission maximum near 450 nm while still possessing a long half-life. Further investigation into aequorin mutants with multiple mutations and continued random mutagenesis could also lead to variants capable of filling this void and/or shifting the emission further towards the red region to allow even more targets to be labeled simultaneously with aequorin.

Chapter Four outlines the use of a new semi-synthetic aequorin mutant that was shown to improve the labeling and imaging capabilities of aequorin. Instead of a genetic conjugation, a chemical conjugation through a unique cysteine created in the protein was employed. The cysteine was usedto attach the protein to an anti-CD33 monoclonal antibody capable of recognizing the CD33 antigen expressed on the surface of AML cells. Excellent detection of free CD33 was achieve, well below the limits necessary to detect the recently discovered, clinically relevant concentrations (*158*), with the aequorin labeled antibody complex. Whole AML cells could also to be detected by the complex down to three cells. Both of these assays were developed on a microtiter plate format in order to allow quick screening of a large number of samples. Additionally, the ability to image with this new semi-synthetic aequorin was also

investigated. A distinguishable signal was observed from the protein for up to approximately three minutes after the initiation of the bioluminescent reaction on an imaging microscope. Light emitted from the antibody-aequorin complex bound to the surface of AML cells could also be visualized with the setup.

Future considerations for this project have several potential pathways for investigation. Initially cellular imaging with this and similar aequorin molecules would benefit greatly from custom instrumentation. All of the reported imaging results were obtained on an imaging microscope typically used with fluorescence imaging, and thus the setup was not optimal for bioluminescence imaging. The sample platform was not isolated from outside light, and while the microscope was located in a small room with no windows, inherent light from the computer monitor and light leaking underneath the door was evident. Although they did not completely eliminate the problem, black sheets covering the door and computer and a custom black box placed on the observation platform did aid with this issue. Additionally, a very rough injection system was created from available materials and was not completely conducive to the experimental procedure. Dislodging of the immobilized cells was continually observed with the injection of the Ca^{2+} solution, which made it extremely difficult to focus on a specified point to collect light, as many times the cells and bioluminescence attached to their surface were not completely stationary throughout the camera exposure. It is speculated that a custom instrumental setup with a sample platform isolated from outside light and an injection system would allow high quality images to be collected. With this new instrumental setup or a similar one, *in vivo* imaging with

the aequorin labeled antibody for the detection of AML in a laboratory animal could be examined. As stated previously, aequorin bioluminescence imaging has been limited with respect to imaging outside of Ca^{2+} applications; thus, the ability to label an antibody and image the location with aequorin would provide the necessary incentive to move forward with future imaging applications of aequorin.

Once successful with the *in vivo* imaging, multiple surface antigens or complementary analytes could be targeted through the use of several semi-synthetic aequorins, similarly to the multiplexed cytokine detection above. The confirmation that aequorin immunolabels can bind and quantify surface antigens allows a similar system to be employed for other disease prognoses and monitoring applications. This application extends beyond the imaging and could also be simplified to a microtiter plate platform as seen with the preliminary CD33 on AML cells monitoring. For example, the literature has shown that the cell surface antigens CD25+ levels ofCD19 expressing cells can provide important information with regard to HIV infection disease stage and activity (*221*). The ability to monitor these levels on the cell surfacequickly and efficiently could provide valuable information in terms of evaluating the activation and course of the disease, patient prognosis, and therapeutic options. A multiplexed microtiter plate assay could be developed to screen cells for the levels of these two important surface markers on the whole cells, without the need to separate different cellular components. Similarly, cell surface sialic acid presentations have recently been shown to be effective indicators for a number of disease

infections, states, and susceptibility including influenza and malaria (*222*). Thus by targeting these surface antigens with aequorin immunolabels, not only can the physical state of the disease be addressed, but also the possibility of examining processes such as infection pathways and mechanisms in an effort to create new therapeutic options.

Chapter Five discusses the creation of a bioluminescent molecular switch capable of monitoring cAMP. The switch was constructed by genetically splitting and subsequently attaching the two fragments of aequorin to the N- and C-termini of cAMP receptor protein (CRP). CRP undergoes a conformational change upon the selective binding of cAMP which causes the repositioning of the attached aequorin fragments, resulting in a loss of bioluminescent signal. The molecular switch was shown to be capable of monitoring changes in cAMP concentration over several orders of magnitude, in addition to the ability to detect changes in cellular cAMP concentrations due to external conditions. Future extension of this work could include the use of the molecular switch to monitor the cellular movement and presence of both cAMP and CRP during specific cellular processes or in response to external stimuli. CRP levels have been shown to correlate to disease states of certain cancers (*223*). The ability to monitor where these proteins are and at what stages they are binding cAMP could lead to valuable insight into the disease progression and signaling pathways. Additionally, cAMP has been associated with the regulation of Ca^{2+} channels and Ca^{2+} entry into the cell (*224*). Consequently, a complex capable of

responding to both cAMP and Ca^{2+} could offer previously unavailable information as to some of the specifics of the cellular signaling cascade.

Chapter Six offers a glance into the versatility of fluorescent based systems as well. A fluorescent fiber optic potassium sensor was customdesigned and developed to allow a patient's potassium concentration to be monitored in real time at the point of interest. The system is comprised of a custom made, portable instrumental setup consisting of an undersized light source and spectrophotometer run by a laptop computer, allowing the system to be easily moved and positioned in a crowded working area. The sensing membrane is immobilized on the tip of an uncased fiber optic, the dimensions of which easily allow for the incorporation of the sensor through a typical heart catheter. The potassium sensor was able to response linearly, reversibly, and consistently through the relevant range of potassium concentrations in both serum and whole blood. In addition, the ability to monitor potassium concentrations over an extended period of time was also demonstrated. The future of this project lies in the clinical testing and use of the sensor. The sensor would first need to be tested with laboratory animals and could easily be incorporated into an existing catheter laboratory procedure. The exposure time and positioning of the sensor would need to be optimized. A possible method to extend the stability of the sensor further would be to engineer the tip of the sensor to rest in an isolated chamber at the end of the catheter. When a reading was desired, the blood could be drawn in and exposed to the sensor for the necessary amount of time and then flushed back out of the chamber. This would

prolong the lifetime of the sensing membrane and discourage biofouling. After the initial testing and optimization of the sensor, this work could be expanded by the development of similar sensors for other ions of interest. There are several commercially available ionophores for other ions such as sodium, hydrogen, calcium, and iron. The incorporation of these ionophores into similar membrane cocktails would allow the sensor to be tailored to these other clinically relevant ions. Once the individual sensors have been developed and optimized, the nature of the fiber optics would allow the bundling of the individual fibers to create a single, insertable fiber that could monitor all of the desired ions simultaneously. This could greatly simplify the task of patient monitoring in a clinical setting and allow real time, *in vivo* measurements that would improve the physician's therapeutic considerations and diagnostic abilities, and in turn improve patient care.

As the work presented in this dissertation is expanded upon, new obastacles to overcome and issues to consider will undoubtedly arise. In the case of *in vivo* imaging with any aequorin based system, the presence and requirement of Ca^{2+} throughout the body will require special attention to prevent the spontaneous emission of light as soon as the aequorin complex is introduced into the body. If a fixed cell population were to be used to model *in vivo* response, an EDTA containing media could be employed to prevent premature light emission. However, if actual, *in vivo* investigation is desired, other considerations must be examined. One possible avenue around this would be to introduce the apo form of the protein that does not have the coelenterazine

already bound in the hydrophobic pocket. Thus, when Ca^{2+} is bound by aequorin, the coelenterazine will not be excited before the aequorin complex has arrived at the desired location. Once the aequorin has been targeted to the required location, coelenterazine can be introduced into the subject to allow the production of light. The introduction of coelenterazine into the organism to be examined also brings new issues into the equation. Coelenterazine is very expensive, thus injecting enough to circulate throughout the blood stream of an animal or human to trigger the bioluminescent reaction with aequorin would not be very cost efficient. To overcome this problem, the investigation could be localized to a contained area that was readily accessible to an injection. Thus, the need to inject a mass amount of coelenterazine could be eliminated. The aequorin complex could be introduced into the localized area and allowed to bind the targeted molecules and then coelenterazine injected to trigger the bioluminescence reaction.

Overall progress in the area of luminescent monitoring and detection has greatly advanced as exemplified by many novel technologies. Other examples include antibody coated magnetic beads that have been used to capture specific bacteria on a microfluidic device, which were then quantified indirectly with firefly luciferase (*225*). Whole cell biosensors with engineered *E. coli* cells have been incorporated into lab-on-a-chip setups that have shown their ability to rapidly monitor environmental and water pollutants in samples (*226-227*). Firefly luciferase has also been employed in a lab-on-a-chip metabolic profiling system able to detect ATP down to sub-micromolar ranges (*228*).

The work presented in this dissertation illustrates how luminescent molecules can be tailored to enhance and progress detection capabilitiesfurther. These types of demonstrations will continue to expand the boundriesof what is thoughtpossible with regard to understanding of molecular and cellular events and to their applications in the detection of biomedical samples.In addition, as the discovery and characterization of new bioluminescent proteins and the genetic modification of current bioluminescent proteins continues to expand the spectral diversity and favorable characteristics, the employment of bioluminescent proteins will also grow. Above all, luminescent molecules are a fascinating natural phenomenon that when coupled with modern instrumentation and reagents results in bioanalytical methods with exceptionally low detection limits. Recent discoveries of bioluminescent organisms and plants living in the depths of the Antarctic waters and in the rain forests will undoubtedly provide researchers with a myriad of new proteins that will have many applications in bioanalysisin the near future.

REFERENCES

1. Harvey, E. N. (1957) *A history of luminescence from the earliest times until 1900*, American Philosophical Society, Philadelphia,.

2. Lee, J. (2008) Bioluminescence: the First 3000Years (Review), *Journal of Siberian Federal University. Biology 1*, 194-205.

3. Hastings, J. W. (1983) Biological diversity, chemical mechanisms, and the evolutionary origins of bioluminescent systems, *J Mol Evol 19*, 309-321.

4. Shimomura, O., Johnson, F. H., and Saiga, Y. (1962) Extraction, purification and properties of aequorin, a bioluminescent protein from the luminous hydromedusan, Aequorea, *J Cell Comp Physiol 59*, 223-239.

5. Chalfie, M., Tu, Y., Euskirchen, G., Ward, W. W., and Prasher, D. C. (1994) Green fluorescent protein as a marker for gene expression, *Science 263*, 802-805.

6. Shaner, N. C., Campbell, R. E., Steinbach, P. A., Giepmans, B. N., Palmer, A. E., and Tsien, R. Y. (2004) Improved monomeric red, orange and yellow fluorescent proteins derived from Discosoma sp. red fluorescent protein, *Nat Biotechnol 22*, 1567-1572.

7. Weiss, P. S. (2008) 2008 Nobel Prize in Chemistry: green fluorescent protein, its variants and implications, *ACS Nano 2*, 1977.

8. Roda, A., Guardigli, M., Michelini, E., and Mirasoli, M. (2009) Bioluminescence in analytical chemistry and in vivo imaging, *TrAC Trends in Analytical Chemistry 28*, 307-322.

9. Hastings, J. W. (1996) Chemistries and colors of bioluminescent reactions: a review, *Gene 173*, 5-11.

10. Daunert, S., and Deo, S. K., (Eds.) (2006) *Photoproteins in Bioanalysis*, Wiley-VCH, Weinheim, Germany.

11. Widder, E. A. (2010) Bioluminescence in the ocean: origins of biological, chemical, and ecological diversity, *Science 328*, 704-708.

12. Fraga, H. (2008) Firefly luminescence: a historical perspective and recent developments, *Photochem Photobiol Sci 7*, 146-158.

13. Viviani, V. R., and Ohmiya, Y. (2006) Beetle Luciferases: Colorful Lights on Biological Processes and Diseases, In *Photoproteins in Bioanalysis* (Daunert, S., and Deo, S. K., Eds.), pp 51-54, WILEY-VCH Verlag GmbH & Co. KGaA, Weinheim.

14. Haddock, S. H. D., Moline, M. A., and Case, J. F. (2010) Bioluminescence in the Sea, *Annual Review of Marine Science 2*, 443-493.

15. Roda, A., Guardigli, M., Michelini, E., and Mirasoli, M. (2009) Nanobioanalytical luminescence: Forster-type energy transfer methods, *Anal Bioanal Chem 393*, 109-123.

16. Gottschalk, M., Bach, A., Hansen, J. L., Krogsgaard-Larsen, P., Kristensen, A. S., and Stromgaard, K. (2009) Detecting protein-protein interactions in living cells: development of a bioluminescence resonance energy transfer assay to evaluate the PSD-95/NMDA receptor interaction, *Neurochem Res 34*, 1729-1737.

17. Laursen, L. S., and Oxvig, C. (2005) Real-time measurement in living cells of insulin-like growth factor activity using bioluminescence resonance energy transfer, *Biochem Pharmacol 69*, 1723-1732.

18. Tannous, B. A., Kim, D. E., Fernandez, J. L., Weissleder, R., and Breakefield, X. O. (2005) Codon-optimized Gaussia luciferase cDNA for mammalian gene expression in culture and in vivo, *Mol Ther 11*, 435-443.

19. Dunlap, P., and Kita-Tsukamoto, K. (2006) Luminous Bacteria, In *The Prokaryotes* (Dworkin, M., Falkow, S., Rosenberg, E., Schleifer, K.-H., and Stackebrandt, E., Eds.) 3rd ed., p 864, Springer, New York.

20. Kumari, A., Pasini, P., Deo, S. K., Flomenhoft, D., Shashidhar, H., and Daunert, S. (2006) Biosensing systems for the detection of bacterial quorum signaling molecules, *Anal Chem 78*, 7603-7609.

21. Meighen, E. A. (1993) Bacterial bioluminescence: organization, regulation, and application of the lux genes, *FASEB J 7*, 1016-1022.

22. Ramanathan, S., Shi, W., Rosen, B. P., and Daunert, S. (1997) Sensing antimonite and arsenite at the subattomole level with genetically engineered bioluminescent bacteria, *Anal Chem 69*, 3380-3384.

23. Ripp, S., Daumer, K. A., McKnight, T., Levine, L. H., Garland, J. L., Simpson, M. L., and Sayler, G. S. (2003) Bioluminescent bioreporter integrated-circuit sensing of microbial volatile organic compounds, *J Ind Microbiol Biotechnol 30*, 636-642.

24. Turner, K., Xu, S., Pasini, P., Deo, S., Bachas, L., and Daunert, S. (2007) Hydroxylated polychlorinated biphenyl detection based on a genetically

engineered bioluminescent whole-cell sensing system, *Anal Chem 79*, 5740-5745.

25. Prendergast, F. G. (2000) Bioluminescence illuminated, *Nature 405*, 291-293.

26. Kendall, J. M., and Badminton, M. N. (1998) Aequorea victoria bioluminescence moves into an exciting new era, *Trends Biotechnol 16*, 216-224.

27. Chiesa, A., Rapizzi, E., Tosello, V., Pinton, P., de Virgilio, M., Fogarty, K. E., and Rizzuto, R. (2001) Recombinant aequorin and green fluorescent protein as valuable tools in the study of cell signalling, *Biochem J 355*, 1-12.

28. Stanley, P. E. (1997) Commercially available luminometers and imaging devices for low-light level measurements and kits and reagents utilizing bioluminescence or chemiluminescence: Survey update 5, *Journal of Bioluminescence and Chemiluminescence 12*, 61-78.

29. Sarter, S., and Zakhia, N. (2004) Chemiluminescent and bioluminescent assays as innovative prospects for mycotoxin determination in food and feed, *Luminescence 19*, 345-351.

30. Alhanout, K., Malesinki, S., Vidal, N., Peyrot, V., Rolain, J. M., and Brunel, J. M. (2010) New insights into the antibacterial mechanism of action of squalamine, *J Antimicrob Chemother 65*, 1688-1693.

31. Urata, M., Iwata, R., Noda, K., Murakami, Y., and Kuroda, A. (2009) Detection of living Salmonella cells using bioluminescence, *Biotechnol Lett 31*, 737-741.

32. Lafond, M., Vidal, N., Letourneux, Y., and Brunel, J. M. (2010) A comparison of three rapid and accurate bioluminescent antibiotic susceptibility tests, *J Pharmacol Toxicol Methods 61*, 16-19.

33. Corbitt, A. J., Bennion, N., and Forsythe, S. J. (2000) Adenylate kinase amplification of ATP bioluminescence for hygiene monitoring in the food and beverage industry, *Lett Appl Microbiol 30*, 443-447.

34. Noah, J. W., Severson, W., Noah, D. L., Rasmussen, L., White, E. L., and Jonsson, C. B. (2007) A cell-based luminescence assay is effective for high-throughput screening of potential influenza antivirals, *Antiviral Res 73*, 50-59.

35. Slater, K. (2001) Cytotoxicity tests for high-throughput drug discovery, *Curr Opin Biotechnol 12*, 70-74.

36. Brini, M. (2008) Calcium-sensitive photoproteins, *Methods 46*, 160-166.

37. Michelini, E., Cevenini, L., Mezzanotte, L., and Roda, A. (2009) Luminescent probes and visualization of bioluminescence, *Methods Mol Biol 574*, 1-13.

38. Villalobos, C., Alonso, M. T., and Garcia-Sancho, J. (2009) Bioluminescence imaging of calcium oscillations inside intracellular organelles, *Methods Mol Biol 574*, 203-214.

39. Rink, T. J. (1990) Receptor-mediated calcium entry, *FEBS Lett 268*, 381-385.

40. Menon, V., Ranganathn, A., Jorgensen, V. H., Sabio, M., Christoffersen, C. T., Uberti, M. A., Jones, K. A., and Babu, P. S. (2008) Development of an aequorin luminescence calcium assay for high-throughput screening using a plate reader, the LumiLux, *Assay Drug Dev Technol 6*, 787-793.

41. Cissell, K. A., Shrestha, S., and Deo, S. K. (2007) MicroRNA detection: challenges for the analytical chemist, *Analytical Chemistry (Washington, DC, United States) 79*, 4754-4761.

42. Deo, S. K. (2008) *Essentials of nucleic acid analysis. A robust approach, edited by Jacquie T. Keer and Lyndsey Birch*, Vol. 392.

43. Hassibi, A., Contag, C., Vlad, M. O., Hafezi, M., Lee, T. H., Davis, R. W., and Pourmand, N. (2005) Bioluminescence regenerative cycle (BRC) system: theoretical considerations for nucleic acid quantification assays, *Biophys Chem 116*, 175-185.

44. Toubanaki, D. K., Christopoulos, T. K., Ioannou, P. C., and Gravanis, A. (2008) Dry-reagent disposable biosensor for visual genotyping of single nucleotide polymorphisms by oligonucleotide ligation reaction: application to pharmacogenetic analysis, *Hum Mutat 29*, 1071-1078.

45. Zerefos, P. G., Ioannou, P. C., Traeger-Synodinos, J., Dimissianos, G., Kanavakis, E., and Christopoulos, T. K. (2006) Photoprotein aequorin as a novel reporter for SNP genotyping by primer extension-application to the variants of mannose-binding lectin gene, *Hum Mutat 27*, 279-285.

46. Arakawa, H., Karasawa, K., Munakata, E., Obinata, R., Maeda, M., Suzuki, S., Kamahori, M., and Kambara, H. (2008) Development of bioluminescent pyrophosphate assay using pyruvate phosphate dikinase and its application to single-nucleotide polymorphism analysis, *Anal Biochem 379*, 86-90.

47. Cissell, K. A., Campbell, S., and Deo, S. K. (2008) Rapid, single-step nucleic acid detection, *Analytical and Bioanalytical Chemistry 391*, 2577-2581.

48. Elenis, D. S., Kalogianni, D. P., Glynou, K., Ioannou, P. C., and Christopoulos, T. K. (2008) Advances in molecular techniques for the detection and quantification of genetically modified organisms, *Anal Bioanal Chem 392*, 347-354.

49. Nagatsugi, F., Nakahara, R., Inoue, K., and Sasaki, S. (2008) Synthesis and evaluation of the luciferase-oligodeoxynucleotide for the sequence-selective detection of nucleic acids, *Arch Pharm (Weinheim) 341*, 562-567.

50. Doleman, L., Davies, L., Rowe, L., Moschou, E. A., Deo, S., and Daunert, S. (2007) Bioluminescence DNA Hybridization Assay for Plasmodium falciparum Based on the Photoprotein Aequorin, *Analytical Chemistry 79*, 4149-4153.

51. Frank, L. A., Borisova, V. V., and Vysotski, E. S. (2005) Calcium-regulated photoprotein obelin as a label in immunoassay: an outlook for applications, *Bioluminescence & Chemiluminescence: Progress and*

Perspectives, [International Symposium on Bioluminescence & Chemiluminescence], 13th, Yokohama, Japan, Aug. 2-6, 2004, 463-466.

52.   Roda, A., Guardigli, M., Michelini, E., Mirasoli, M., and Pasini, P. (2006) Luminescent Proteins in Binding Assays, In *Photoproteins in Bioanalysis* (Daunert, S., and Deo, S. K., Eds.), pp 165-166, WILEY-VCH Verlag GmbH & Co. KGaA, Weinheim.

53.   Roda, A., Guardigli, M., Mirasoli, M., and Michelini, E. (2006) Bioluminescence meets analytical biotechnology, *BIOforum Europe 10*, 54-56.

54.   Wu, C., Kawasaki, K., Ogawa, Y., Yoshida, Y., Ohgiya, S., and Ohmiya, Y. (2007) Preparation of Biotinylated Cypridina Luciferase and Its Use in Bioluminescent Enzyme Immunoassay, *Analytical Chemistry 79*, 1634-1638.

55.   Inouye, S., and Sato, J. (2008) Recombinant aequorin with a reactive cysteine residue for conjugation with maleimide-activated antibody, *Anal Biochem 378*, 105-107.

56.   Rowe, L., Dikici, E., and Daunert, S. (2009) Engineering bioluminescent proteins: expanding their analytical potential, *Anal Chem 81*, 8662-8668.

57.   Qu, X., Deo, S. K., Dikici, E., Ensor, M., Poon, M., and Daunert, S. (2007) Bioluminescence immunoassay for angiotensin II using aequorin as a label, *Analytical Biochemistry 371*, 154-161.

58.   Kim, S. B., Sato, M., and Tao, H. (2009) Split Gaussia Luciferase-Based Bioluminescence Template for Tracing Protein Dynamics in Living Cells, *Analytical Chemistry (Washington, DC, United States) 81*, 67-74.

59.   Misawa, N., Kafi, A. K. M., Hattori, M., Miura, K., Masuda, K., and Ozawa, T. (2010) Rapid and High-Sensitivity Cell-Based Assays of Protein-Protein Interactions Using Split Click Beetle Luciferase Complementation: An Approach to the Study of G-Protein-Coupled Receptors, *Analytical Chemistry (Washington, DC, United States) 82*, 2552-2560.

60.   Ozawa, T. (2005) Methods of analysis for protein dynamics in living cells based on protein splicing, *Bulletin of the Chemical Society of Japan 78*, 739-751.

61.   Porter, J. R., Stains, C. I., Jester, B. W., and Ghosh, I. (2008) A General and Rapid Cell-Free Approach for the Interrogation of Protein-Protein, Protein-DNA, and Protein-RNA Interactions and their Antagonists Utilizing Split-Protein Reporters, *Journal of the American Chemical Society 130*, 6488-6497.

62.   Ozawa, T., Kaihara, A., Sato, M., Tachihara, K., and Umezawa, Y. (2001) Split Luciferase as an Optical Probe for Detecting Protein−Protein Interactions in Mammalian Cells Based on Protein Splicing, *Analytical Chemistry 73*, 2516-2521.

63.   Kim, S. B., Ozawa, T., Watanabe, S., and Umezawa, Y. (2004) High-throughput sensing and noninvasive imaging of protein nuclear transport by using reconstitution of split Renilla luciferase, *Proceedings of the*

National Academy of Sciences of the United States of America 101, 11542-11547.

64.   Kaihara, A., Kawai, Y., Sato, M., Ozawa, T., and Umezawa, Y. (2003) Locating a Protein−Protein Interaction in Living Cells via Split Renilla Luciferase Complementation, *Analytical Chemistry 75*, 4176-4181.

65.   Paulmurugan, R., and Gambhir, S. S. (2005) Novel fusion protein approach for efficient high-throughput screening of small molecule-mediating protein-protein interactions in cells and living animals, *Cancer Res 65*, 7413-7420.

66.   Teasley Hamorsky, K., Ensor, C. M., Wei, Y., and Daunert, S. (2008) A bioluminescent molecular switch for glucose, *Angew Chem Int Ed Engl 47*, 3718-3721.

67.   Song, Y., Li, G., Thornton, S. F., Thompson, I. P., Banwart, S. A., Lerner, D. N., and Huang, W. E. (2009) Optimization of Bacterial Whole Cell Bioreporters for Toxicity Assay of Environmental Samples, *Environmental Science & Technology 43*, 7931-7938.

68.   Ivask, A., Kahru, A., and Virta, M. (2007) Recombinant whole-cell bioreporter systems based on beetle luciferases, *Handbook of Biosensors and Biochips 1*, 163-172.

69.   Michelini, E., Guardigli, M., Magliulo, M., Mirasoli, M., Roda, A., Simoni, P., and Baraldini, M. (2006) Bioluminescent biosensors based on genetically engineered living cells in environmental and food analysis, *Analytical Letters 39*, 1503-1515.

70.   Polyak, B., and Marks, R. S. (2007) Bioluminescent whole-cell optical fiber sensors, *Handbook of Biosensors and Biochips 1*, 495-509.

71.   Belkin, S. (2003) Microbial whole-cell sensing systems of environmental pollutants, *Current Opinion in Microbiology 6*, 206-212.

72.   Hansen, L. H., and Sorensen, S. J. (2000) Detection and quantification of tetracyclines by whole cell biosensors, *FEMS Microbiol Lett 190*, 273-278.

73.   Layton, A. C., Muccini, M., Ghosh, M. M., and Sayler, G. S. (1998) Construction of a bioluminescent reporter strain To detect polychlorinated biphenyls, *Appl Environ Microbiol 64*, 5023-5026.

74.   Phoenix, P., Keane, A., Patel, A., Bergeron, H., Ghoshal, S., and Lau, P. C. (2003) Characterization of a new solvent-responsive gene locus in Pseudomonas putida F1 and its functionalization as a versatile biosensor, *Environ Microbiol 5*, 1309-1327.

75.   Riether, K. B., Dollard, M. A., and Billard, P. (2001) Assessment of heavy metal bioavailability using Escherichia coli zntAp::lux and copAp::lux-based biosensors, *Appl Microbiol Biotechnol 57*, 712-716.

76.   Selifonova, O., Burlage, R., and Barkay, T. (1993) Bioluminescent sensors for detection of bioavailable Hg(II) in the environment, *Appl Environ Microbiol 59*, 3083-3090.

77.   Shetty, R. S., Deo, S. K., Shah, P., Sun, Y., Rosen, B. P., and Daunert, S. (2003) Luminescence-based whole-cell-sensing systems for cadmium and lead using genetically engineered bacteria, *Anal Bioanal Chem 376*, 11-17.

78. Tauriainen, S., Karp, M., Chang, W., and Virta, M. (1998) Luminescent bacterial sensor for cadmium and lead, *Biosens Bioelectron 13*, 931-938.

79. Date, A., Pasini, P., and Daunert, S. (2007) Construction of spores for portable bacterial whole-cell biosensing systems, *Anal Chem 79*, 9391-9397.

80. Date, A., Pasini, P., Sangal, A., and Daunert, S. (2010) Packaging Sensing Cells in Spores for Long-Term Preservation of Sensors: A Tool for Biomedical and Environmental Analysis, *Analytical Chemistry 82*, 6098-6103.

81. Xia, Z., and Rao, J. (2009) Biosensing and imaging based on bioluminescence resonance energy transfer, *Curr Opin Biotechnol 20*, 37-44.

82. De, A., Ray, P., Loening, A. M., and Gambhir, S. S. (2009) BRET3: a red-shifted bioluminescence resonance energy transfer (BRET)-based integrated platform for imaging protein-protein interactions from single live cells and living animals, *FASEB Journal 23*, 2702-2709.

83. Kenworthy, A. K. (2001) Imaging Protein-Protein Interactions Using Fluorescence Resonance Energy Transfer Microscopy, *Methods 24*, 289-296.

84. Paulmurugan, R., Ray, P., De, A., Chan, C. T., and Gambhir, S. S. (2005) Imaging protein-protein interactions in living animals, *Protein-Protein Interactions (2nd Edition)*, 695-713.

85.   Audet, N., Gales, C., Archer-Lahlou, E., Vallieres, M., Schiller, P. W., Bouvier, M., and Pineyro, G. (2008) Bioluminescence Resonance Energy Transfer Assays Reveal Ligand-specific Conformational Changes within Preformed Signaling Complexes Containing delta -Opioid Receptors and Heterotrimeric G Proteins, *Journal of Biological Chemistry 283*, 15078-15088.

86.   Marcellino, D., Navarro, G., Sahlholm, K., Nilsson, J., Agnati, L. F., Canela, E. I., Lluis, C., Aarhem, P., Franco, R., and Fuxe, K. (2010) Cocaine produces D2R-mediated conformational changes in the adenosine A2AR-dopamine D2R heteromer, *Biochemical and Biophysical Research Communications 394*, 988-992.

87.   Cissell, K. A., Hunt, E. A., and Deo, S. K. (2009) Resonance energy transfer methods of RNA detection, *Analytical & Bioanalytical Chemistry 393*, 125-135.

88.   Xia, Z., and Rao, J. (2009) Biosensing and imaging based on bioluminescence resonance energy transfer, *Current Opinion in Biotechnology 20*, 37-44.

89.   Ma, N., Marshall, A. F., and Rao, J. (2010) Near-Infrared Light Emitting Luciferase via Biomineralization, *Journal of the American Chemical Society*.

90.   Branchini, B. R., Southworth, T. L., Khattak, N. F., Michelini, E., and Roda, A. (2005) Red- and green-emitting firefly luciferase mutants for

bioluminescent reporter applications, *Analytical Biochemistry 345*, 140-148.

91. Nakatsu, T., Ichiyama, S., Hiratake, J., Saldanha, A., Kobashi, N., Sakata, K., and Kato, H. (2006) Structural basis for the spectral difference in luciferase bioluminescence, *Nature 440*, 372-376.

92. Fahmi, N. E., Dedkova, L., Wang, B., Golovine, S., and Hecht, S. M. (2007) Site-Specific Incorporation of Glycosylated Serine and Tyrosine Derivatives into Proteins, *Journal of the American Chemical Society 129*, 3586-3597.

93. So, M.-K., Loening, A. M., Gambhir, S. S., and Rao, J. (2006) Creating self-illuminating quantum dot conjugates, *Nature Protocols 1*, 1160-1164.

94. So, M.-K., Xu, C., Loening, A. M., Gambhir, S. S., and Rao, J. (2006) Self-illuminating quantum dot conjugates for in vivo imaging, *Nature Biotechnology 24*, 339-343.

95. Ito, K., Nishimura, W., Maeda, M., Gomi, K., Inouye, S., and Arakawa, H. (2007) Highly sensitive and rapid tandem bioluminescent immunoassay using aequorin labeled Fab fragment and biotinylated firefly luciferase, *Analytica Chimica Acta 588*, 245-251.

96. Frank, L. A., Borisova, V. V., Markova, S. V., Malikova, N. P., Stepanyuk, G. A., and Vysotski, E. S. (2008) Violet and greenish photoprotein obelin mutants for reporter applications in dual-color assay, *Anal Bioanal Chem 391*, 2891-2896.

171

97. Shimomura, O., Musicki, B., and Kishi, Y. (1988) Semi-synthetic aequorin. An improved tool for the measurement of calcium ion concentration, *Biochem J 251*, 405-410.

98. Dikici, E., Qu, X., Rowe, L., Millner, L., Logue, C., Deo, S. K., Ensor, M., and Daunert, S. (2009) Aequorin variants with improved bioluminescence properties, *Protein Eng Des Sel 22*, 243-248.

99. Rowe, L., Ensor, M., Mehl, R., and Daunert, S. (2010) Modulating the Bioluminescence Emission of Photoproteins by in Vivo Site-Directed Incorporation of Non-Natural Amino Acids, *ACS Chemical Biology*.

100. Rowe, L., Combs, K., Deo, S., Ensor, C., Daunert, S., and Qu, X. (2008) Genetically Modified Semisynthetic Bioluminescent Photoprotein Variants: Simultaneous Dual-Analyte Assay in a Single Well Employing Time Resolution of Decay Kinetics, *Analytical Chemistry 80*, 8470-8476.

101. Alivisatos, A. P. (1996) Semiconductor Clusters, Nanocrystals, and Quantum Dots, *Science 271*, 933-937.

102. Vivian, J. T., and Callis, P. R. (2001) Mechanisms of Tryptophan Fluorescence Shifts in Proteins, *80*, 2093-2109.

103. Valeur, B. (2008) From Well-Known to Underrated Applications of Fluorescence, In *Fluorescence of Supermolecules, Polymers, and Nanosystems* (Berberan-Santos, M. N., Ed.), pp 21-43, Springer Berlin Heidelberg.

104. Labas, Y. A., Gurskaya, N. G., Yanushevich, Y. G., Fradkov, A. F., Lukyanov, K. A., Lukyanov, S. A., and Matz, M. V. (2002) Diversity and

evolution of the green fluorescent protein family, *Proceedings of the National Academy of Sciences of the United States of America 99*, 4256-4261.

105. Matz, M. V., Lukyanov, K. A., and Lukyanov, S. A. (2002) Family of the green fluorescent protein: Journey to the end of the rainbow, *BioEssays 24*, 953-959.

106. Likhtenshtein, G. I. (2009) Novel fluorescent methods for biotechnological and biomedical sensoring: assessing antioxidants, reactive radicals, NO dynamics, immunoassay, and biomembranes fluidity, *Appl Biochem Biotechnol 152*, 135-155.

107. Culshaw, B. (2005) Fiber-Optic Sensors: Applications and Advances, *Opt. Photon. News 16*, 24-29.

108. Ahn, S., Kulis, D. M., Erdner, D. L., Anderson, D. M., and Walt, D. R. (2006) Fiber-optic microarray for simultaneous detection of multiple harmful algal bloom species, *Appl Environ Microbiol 72*, 5742-5749.

109. Basu, B. J. (2007) Optical oxygen sensing based on luminescence quenching of platinum porphyrin dyes doped in ormosil coatings, *Sensors and Actuators B: Chemical 123*, 568-577.

110. Fritzsche, M., Barreiro, C. G., Hitzmann, B., and Scheper, T. (2007) Optical pH sensing using spectral analysis, *Sensors and Actuators B: Chemical 128*, 133-137.

111. Ivask, A., Green, T., Polyak, B., Mor, A., Kahru, A., Virta, M., and Marks, R. (2007) Fibre-optic bacterial biosensors and their application for the

analysis of bioavailable Hg and As in soils and sediments from Aznalcollar mining area in Spain, *Biosens Bioelectron 22*, 1396-1402.

112. Lai, N. S., Wang, C. C., Chiang, H. L., and Chau, L. K. (2007) Detection of antinuclear antibodies by a colloidal gold modified optical fiber: comparison with ELISA, *Anal Bioanal Chem 388*, 901-907.

113. Pasic, A., Koehler, H., Schaupp, L., Pieber, T. R., and Klimant, I. (2006) Fiber-optic flow-through sensor for online monitoring of glucose, *Anal Bioanal Chem 386*, 1293-1302.

114. Tiwari, V. S., Kalluru, R. R., Yueh, F. Y., Singh, J. P., Cyr, W. S., and Khijwania, S. K. (2007) Fiber optic Raman sensor to monitor the concentration ratio of nitrogen and oxygen in a cryogenic mixture, *Appl Opt 46*, 3345-3351.

115. Wei, H., Guo, Z., Zhu, Z., Tan, Y., Du, Z., and Yang, R. (2007) Sensitive detection of antibody against antigen F1 of Yersinia pestis by an antigen sandwich method using a portable fiber optic biosensor, *Sensors and Actuators B: Chemical 127*, 525-530.

116. Zalvidea, D., Diez, A., Cruz, J. L., and Andres, M. V. (2006) Hydrogen sensor based on a palladium-coated fibre-taper with improved time-response, *Sensor Actuat B-Chem 114*, 268-274.

117. Contag, C. H., and Bachmann, M. H. (2002) Advances in in vivo bioluminescence imaging of gene expression, *Annu Rev Biomed Eng 4*, 235-260.

118. DiPilato, L. M., Cheng, X., and Zhang, J. (2004) Fluorescent indicators of cAMP and Epac activation reveal differential dynamics of cAMP signaling within discrete subcellular compartments, *Proc Natl Acad Sci U S A 101*, 16513-16518.

119. Gonzalez, J. E., and Negulescu, P. A. (1998) Intracellular detection assays for high-throughput screening, *Curr Opin Biotechnol 9*, 624-631.

120. Heim, R., and Tsien, R. Y. (1996) Engineering green fluorescent protein for improved brightness, longer wavelengths and fluorescence resonance energy transfer, *Curr Biol 6*, 178-182.

121. Kain, S. R. (1999) Green fluorescent protein (GFP): applications in cell-based assays for drug discovery, *Drug Discov Today 4*, 304-312.

122. Lewis, J. C., and Daunert, S. (2000) Photoproteins as luminescent labels in binding assays, *Fresenius J Anal Chem 366*, 760-768.

123. Adamczyk, M., Moore, J. A., and Shreder, K. (2002) Dual Analyte Detection Using Tandem Flash Luminescence, *Bioorganic & Medicinal Chemistry Letters 12*, 395-398.

124. Ito, K., Nishimura, W., Maeda, M., Gomi, K., Inouye, S., and Arakawa, H. (2007) Highly sensitive and rapid tandem bioluminescent immunoassay using aequorin labeled Fab fragment and biotinylated firefly luciferase, *Anal Chim Acta 588*, 245-251.

125. Laios, E., Obeid, P. J., Ioannou, P. C., and Christopoulos, T. K. (2000) Expression Hybridization Assays Combining cDNAs from Firefly and

Renilla Luciferases as Labels for Simultaneous Determination of Two Target Sequences, *Analytical Chemistry 72*, 4022-4028.

126. Ohkuma, H., Abe, K., Kosaka, Y., and Maeda, M. (2000) Detection of luciferase having two kinds of luminescent colour based on optical filter procedure: application to an enzyme immunoassay, *Luminescence 15*, 21-27.

127. Head, J. F., Inouye, S., Teranishi, K., and Shimomura, O. (2000) The crystal structure of the photoprotein aequorin at 2.3 A resolution, *Nature 405*, 372-376.

128. Ohmiya, Y., Ohashi, M., and Tsuji, F. I. (1992) Two excited states in aequorin bioluminescence induced by tryptophan modification, *FEBS Lett 301*, 197-201.

129. Ohmiya, Y., and Tsuji, F. I. (1993) Bioluminescence of the Ca(2+)-binding photoprotein, aequorin, after histidine modification, *FEBS Lett 320*, 267-270.

130. Stepanyuk, G. A., Golz, S., Markova, S. V., Frank, L. A., Lee, J., and Vysotski, E. S. (2005) Interchange of aequorin and obelin bioluminescence color is determined by substitution of one active site residue of each photoprotein, *FEBS Lett 579*, 1008-1014.

131. Tricoire, L., Tsuzuki, K., Courjean, O., Gibelin, N., Bourout, G., Rossier, J., and Lambolez, B. (2006) Calcium dependence of aequorin bioluminescence dissected by random mutagenesis, *Proc Natl Acad Sci U S A 103*, 9500-9505.

132. Tsuzuki, K., Tricoire, L., Courjean, O., Gibelin, N., Rossier, J., and Lambolez, B. (2005) Thermostable mutants of the photoprotein aequorin obtained by in vitro evolution, *J Biol Chem 280*, 34324-34331.

133. Hirano, T., Ohmiya, Y., Maki, S., Niwa, H., and Ohashi, M. (1998) Bioluminescent properties of fluorinated semi-synthetic aequorins, *Tetrahedron Letters 39*, 5541-5544.

134. Inouye, S., Ogawa, H., Yasuda, K., Umesono, K., and Tsuji, F. I. (1997) A bacterial cloning vector using a mutated Aequorea green fluorescent protein as an indicator, *Gene 189*, 159-162.

135. Rowe, L., Rothert, A., Logue, C., Ensor, C. M., Deo, S. K., and Daunert, S. (2008) Spectral tuning of photoproteins by partnering site-directed mutagenesis strategies with the incorporation of chromophore analogs, *Protein Eng Des Sel 21*, 73-81.

136. Shimomura, O., Inouye, S., Musicki, B., and Kishi, Y. (1990) Recombinant aequorin and recombinant semi-synthetic aequorins. Cellular Ca2+ ion indicators, *Biochem J 270*, 309-312.

137. Shimomura, O., Musicki, B., and Kishi, Y. (1989) Semi-synthetic aequorins with improved sensitivity to Ca2+ ions, *Biochem J 261*, 913-920.

138. Shimomura, O., Musicki, B., Kishi, Y., and Inouye, S. (1993) Light-emitting properties of recombinant semi-synthetic aequorins and recombinant fluorescein-conjugated aequorin for measuring cellular calcium, *Cell Calcium 14*, 373-378.

139. Zheng, J. L., Chen, F. Q., Hirano, T., Ohmiya, Y., Maki, S., Niwa, H., and Ohashi, M. (2000) Synthesis, Chemi- and Bioluminescence Properties, and Photolysis of a Coelenterazine Analogue Having a Photoreactive Azido Group. , *Bulletin of the Chemical Society of Japan 73*, 465-469.

140. Kristiansen, O. P., and Mandrup-Poulsen, T. (2005) Interleukin-6 and Diabetes, *Diabetes 54*, S114-S124.

141. Morgan, M. M., Clayton, C. C., and Heinricher, M. M. (2004) Dissociation of hyperalgesia from fever following intracerebroventricular administration of interleukin-1[beta] in the rat, *Brain Research 1022*, 96-100.

142. Nishimoto, N. (2006) Interleukin-6 in rheumatoid arthritis, *Curr Opin Rheumatol 18*, 277-281.

143. Smith, P. C., Hobisch, A., Lin, D.-L., Culig, Z., and Keller, E. T. (2001) Interleukin-6 and prostate cancer progression, *Cytokine & Growth Factor Reviews 12*, 33-40.

144. Tackey, E., Lipsky, P. E., and Illei, G. G. (2004) Rationale for interleukin-6 blockade in systemic lupus erythematosus, *Lupus 13*, 339-343.

145. Utgaard, J. O., Jahnsen, F. L., Bakka, A., Brandtzaeg, P., and Haraldsen, G. (1998) Rapid Secretion of Prestored Interleukin 8 from Weibel-Palade Bodies of Microvascular Endothelial Cells, *J. Exp. Med. 188*, 1751-1756.

146. Ko, Y. C., Mukaida, N., Ishiyama, S., Tokue, A., Kawai, T., Matsushima, K., and Kasahara, T. (1993) Elevated interleukin-8 levels in the urine of patients with urinary tract infections, *Infect Immun 61*, 1307-1314.

147. Lyke, K. E., Burges, R., Cissoko, Y., Sangare, L., Dao, M., Diarra, I., Kone, A., Harley, R., Plowe, C. V., Doumbo, O. K., and Sztein, M. B. (2004) Serum Levels of the Proinflammatory Cytokines Interleukin-1 Beta (IL-1{beta}), IL-6, IL-8, IL-10, Tumor Necrosis Factor Alpha, and IL-12(p70) in Malian Children with Severe Plasmodium falciparum Malaria and Matched Uncomplicated Malaria or Healthy Controls, *Infect. Immun. 72*, 5630-5637.

148. Malamitsi-Puchner, A., Protonotariou, E., Boutsikou, T., Makrakis, E., Sarandakou, A., and Creatsas, G. (2005) The influence of the mode of delivery on circulating cytokine concentrations in the perinatal period, *Early Human Development 81*, 387-392.

149. Welsh, D. K., and Kay, S. A. (2005) Bioluminescence imaging in living organisms, *Curr Opin Biotechnol 16*, 73-78.

150. Luker, K. E., and Luker, G. D. (2008) Applications of bioluminescence imaging to antiviral research and therapy: multiple luciferase enzymes and quantitation, *Antiviral Res 78*, 179-187.

151. Prinz, A., Reither, G., Diskar, M., and Schultz, C. (2008) Fluorescence and bioluminescence procedures for functional proteomics, *Proteomics 8*, 1179-1196.

152. Rabinovich, B. A., Ye, Y., Etto, T., Chen, J. Q., Levitsky, H. I., Overwijk, W. W., Cooper, L. J., Gelovani, J., and Hwu, P. (2008) Visualizing fewer than 10 mouse T cells with an enhanced firefly luciferase in

immunocompetent mouse models of cancer, *Proc Natl Acad Sci U S A 105*, 14342-14346.

153. Sanz, P., Teel, L. D., Alem, F., Carvalho, H. M., Darnell, S. C., and O'Brien, A. D. (2008) Detection of Bacillus anthracis spore germination in vivo by bioluminescence imaging, *Infect Immun 76*, 1036-1047.

154. Inouye, S., and Sato, J. (2008) Comparison of luminescent immunoassays using biotinylated proteins of aequorin, alkaline phosphatase and horseradish peroxidase as reporters, *Biosci Biotechnol Biochem 72*, 3310-3313.

155. Griffin, J. D., Linch, D., Sabbath, K., Larcom, P., and Schlossman, S. F. (1984) A monoclonal antibody reactive with normal and leukemic human myeloid progenitor cells, *Leuk Res 8*, 521-534.

156. Scheinberg, D. A., Tanimoto, M., McKenzie, S., Strife, A., Old, L. J., and Clarkson, B. D. (1989) Monoclonal antibody M195: a diagnostic marker for acute myelogenous leukemia, *Leukemia 3*, 440-445.

157. Larson, R. A., Sievers, E. L., Stadtmauer, E. A., Lowenberg, B., Estey, E. H., Dombret, H., Theobald, M., Voliotis, D., Bennett, J. M., Richie, M., Leopold, L. H., Berger, M. S., Sherman, M. L., Loken, M. R., van Dongen, J. J., Bernstein, I. D., and Appelbaum, F. R. (2005) Final report of the efficacy and safety of gemtuzumab ozogamicin (Mylotarg) in patients with CD33-positive acute myeloid leukemia in first recurrence, *Cancer 104*, 1442-1452.

158. Abdool, A., Yeh, C. H., Kantarjian, H., O'Brien, S., Bruey, J., Giles, F., and Albitar, M. (2010) Circulating CD33 and its clinical value in acute leukemia, *Exp Hematol 38*, 462-471.

159. Hermanson, G. T. (1996) *Bioconjugate Techniques*, Academic Press, Inc., San Diego, CA.

160. Sgoutas, D. S., Tuten, T. E., Verras, A. A., Love, A., and Barton, E. G. (1995) AquaLite bioluminescence assay of thyrotropin in serum evaluated, *Clin Chem 41*, 1637-1643.

161. Verhaegen, M., and Christopoulos, T. K. (1998) Quantitative polymerase chain reaction based on a dual-analyte chemiluminescence hybridization assay for target DNA and internal standard, *Anal Chem 70*, 4120-4125.

162. Nijegorodov, N., and Mabbs, R. (2001) The influence of molecular symmetry and topological factors on the internal heavy atom effect in aromatic and heteroaromatic compounds, *Spectrochim Acta A Mol Biomol Spectrosc 57*, 1449-1462.

163. Zwaan, C. M., Reinhardt, D., Jurgens, H., Huismans, D. R., Hahlen, K., Smith, O. P., Biondi, A., van Wering, E. R., Feingold, J., and Kaspers, G. J. (2003) Gemtuzumab ozogamicin in pediatric CD33-positive acute lymphoblastic leukemia: first clinical experiences and relation with cellular sensitivity to single agent calicheamicin, *Leukemia 17*, 468-470.

164. Jilani, I., Estey, E., Huh, Y., Joe, Y., Manshouri, T., Yared, M., Giles, F., Kantarjian, H., Cortes, J., Thomas, D., Keating, M., Freireich, E., and

Albitar, M. (2002) Differences in CD33 intensity between various myeloid neoplasms, *Am J Clin Pathol 118*, 560-566.

165. Chaerle, L., and Van Der Straeten, D. (2001) Seeing is believing: imaging techniques to monitor plant health, *Biochimica et Biophysica Acta (BBA) - Gene Structure and Expression 1519*, 153-166.

166. Fonteriz, R. I., de la Fuente, S., Moreno, A., Lobatón, C. D., Montero, M., and Alvarez, J. (2010) Monitoring mitochondrial [Ca2+] dynamics with rhod-2, ratiometric pericam and aequorin, *Cell Calcium 48*, 61-69.

167. Leung, C. F., Miller, A. L., Korzh, V., Chong, S. W., Sleptsova-Freidrich, I., and Webb, S. E. (2009) Visualization of stochastic Ca2+ signals in the formed somites during the early segmentation period in intact, normally developing zebrafish embryos, *Dev Growth Differ 51*, 617-637.

168. Guntas, G., and Ostermeier, M. (2004) Creation of an Allosteric Enzyme by Domain Insertion, *J Mol Biol. 336*, 263-273.

169. Baird, G. S., Zacharias, D. A., and Tsien, R. Y. (1999) Circular permutation and receptor insertion within green fluorescent proteins, *Proceedings of the National Academy of Sciences of the United States of America 96*, 11241-11246.

170. Hamorsky, K. T., Ensor, C. M., Wei, Y., and Daunert, S. (2008) A bioluminescent molecular switch for glucose, *Angew Chem Int Ed 47*, 3718-3721.

171. Ostermeier, M. (2005) Engineering allosteric protein switches by domain insertion, *Protein Eng Des Sel 18*, 359-364.

172. Shimomura, O. (2006) The photoproteins, *Photoproteins in Bioanalysis*, 1-23.

173. Shimomura, O., Johnson, F. H., and Saiga, Y. (1962) Extraction, purification, and properties of aequorin, a bioluminescent protein from the luminous hydromedusan, Aequorea, *J Cell Comp Physiol. 59*, 223-239.

174. Charbonneau, H., Walsh, K. A., McCann, R. O., Prendergast, F. G., Cormier, M. J., and Vanaman, T. C. (1985) Amino acid sequence of the calcium-dependent photoprotein aequorin, *Biochemistry 24*, 6762-6771.

175. Shimomura, O., and Johnson, F. H. (1973) Chemical nature of the light emitter in bioluminescence of Aequorin, *Tetrahedron Lett.*, 2963-2966.

176. Deo, S. K., and Daunert, S. (2001) An Immunoassay for Leu-enkephalin Based on a C-Terminal Aequorin-Peptide Fusion, *Analytical Chemistry 73*, 1903-1908.

177. Lewis, J. C., and Daunert, S. (2001) Bioluminescence immunoassay for thyroxine employing genetically engineered mutant aequorins containing unique cysteine residues, *Anal Chem 73*, 3227-3233.

178. Mirasoli, M., Deo, S. K., Lewis, J. C., Roda, A., and Daunert, S. (2002) Bioluminescence Immunoassay for Cortisol Using Recombinant Aequorin as a Label, *Anal Biochem. 306*, 204-211.

179. Gang, J., Chung, H.-J., Park, G.-G., Park, Y.-S., and Choi, S.-J. (2005) Stability and structural change of cAMP receptor protein at low and high cAMP concentrations, *J Microbiol Biotechnol 15*, 1392-1396.

180. De Crombrugghe, B., Busby, S., and Buc, H. (1984) Cyclic AMP receptor protein: role in transcription activation, *Science 224*, 831-838.

181. Harman, J. G. (2001) Allosteric regulation of the cAMP receptor protein, *Biochimica et Biophysica Acta, Protein Structure and Molecular Enzymology 1547*, 1-17.

182. Polit, A., Blaszczyk, U., and Wasylewski, Z. (2003) Steady-state and time-resolved fluorescence studies of conformational changes induced by cyclic AMP and DNA binding to cyclic AMP receptor protein from Escherichia coli, *Eur J Biochem 270*, 1413-1423.

183. Reznikoff, W. S. (1992) Catabolite gene activator protein activation of lac transcription, *J Bacteriol. 174*, 655-658.

184. Malecki, J., Polit, A., and Wasylewski, Z. (2000) Kinetic studies of cAMP-induced allosteric changes in cyclic AMP receptor protein from Escherichia coli, *J Biol Chem 275*, 8480-8486.

185. Passner, J. M., and Steitz, T. A. (1997) The structure of a CAP-DNA complex having two cAMP molecules bound to each monomer, *Proc Natl Acad Sci U S A. 94*, 2843-2847.

186. VallÈe-BÈlisle, A., and Plaxco, K. W. (2010) Structure-switching biosensors: inspired by Nature, *Current Opinion in Structural Biology 20*, 518-526.

187. Jissy, A. K., and Datta, A. (2010) Designing Molecular Switches Based on DNA-Base Mispairing, *The Journal of Physical Chemistry B 114*, 15311-15318.

188. Taneoka, A., Sakaguchi-Mikami, A., Yamazaki, T., Tsugawa, W., and Sode, K. (2009) The construction of a glucose-sensing luciferase, *Biosensors and Bioelectronics 25*, 76-81.

189. Beavo, J. A., and Brunton, L. L. (2002) Cyclic nucleotide research -- still expanding after half a century, *Nat Rev Mol Cell Biol 3*, 710-718.

190. Holz, G. G. (2004) Epac: A new cAMP-binding protein in support of glucagon-like peptide-1 receptor-mediated signal transduction in the pancreatic beta-cell, *Diabetes 53*, 5-13.

191. Morozov, A., Muzzio, I. A., Bourtchouladze, R., Van-Strien, N., Lapidus, K., Yin, D., Winder, D. G., Adams, J. P., Sweatt, J. D., and Kandel, E. R. (2003) Rap1 couples cAMP signaling to a distinct pool of p42/44MAPK regulating excitability, synaptic plasticity, learning, and memory, *Neuron 39*, 309-325.

192. Torgersen, K. M., Vang, T., Abrahamsen, H., Yaqub, S., and Tasken, K. (2002) Molecular mechanisms for protein kinase A-mediated modulation of immune function, *Cell Signal 14*, 1-9.

193. Zagotta, W. N., Olivier, N. B., Black, K. D., Young, E. C., Olson, R., and Gouaux, E. (2003) Structural basis for modulation and agonist specificity of HCN pacemaker channels, *Nature 425*, 200-205.

194. Busby, S., and Ebright, R. H. (1999) Transcription activation by catabolite activator protein (CAP), *J Mol Biol 293*, 199-213.

195. Ohsawa, H., Nakayama, K., and Okada, M. (1992) Adenylate cyclase and phosphodiesterase activities in relation to a rapid increase in cellular

cAMP concentration by hypotonic shock in Dunaliella viridis, *Botanical Magazine, Tokyo 105*, 393-404.

196. Lewis, J. C., Lopez-Moya, J. J., and Daunert, S. (2000) Bioluminescence and secondary structure properties of aequorin mutants produced for site-specific conjugation and immobilization, *Bioconjug Chem 11*, 65-70.

197. Amin, N., and Peterkofsky, A. (1995) A dual mechanism for regulating cAMP levels in Escherichia coli, *J Biol Chem 270*, 11803-11805.

198. Harwood, J. P., and Peterkofsky, A. (1975) Glucose-sensitive adenylate cyclase in toluene-treated cells of Escherichia coli B, *J Biol Chem 250*, 4656-4662.

199. Williams, C. (2004) cAMP detection methods in HTS: selecting the best from the rest, *Nat Rev Drug Discov 3*, 125-135.

200. Leier, C. V., Dei Cas, L., and Metra, M. (1994) Clinical relevance and management of the major electrolyte abnormalities in congestive heart failure: hyponatremia, hypokalemia, and hypomagnesemia, *Am Heart J 128*, 564-574.

201. Johnson, R. G., Shafique, T., Sirois, C., Weintraub, R. M., and Comunale, M. E. (1999) Potassium concentrations and ventricular ectopy: A prospective, observational study in post-cardiac surgery patients, *Critical Care Medicine 27*, 2430-2434.

202. Fenn, W. O. (1940) The Role of Potassium in Phyisological Processes, *Physiol. Rev. 20*, 377-415.

203. Jennings, R. B., Crout, J. R., and Smetters, G. W. (1957) Studies on distribution and localization to potassium in early myocardial ischemic injury, *AMA Arch Pathol 63*, 586-592.

204. Burtis, C. A. A., Edward R., (Ed.) (1994) *Tietz Textbook of Clinical Chemistry, 2nd edition*, W.B. Saunders Company, Philidelphia, Pennsylvania.

205. Osswald, H. F. A., R.; Dimai, W.; Simon, W. (1979) On-line continuous potentiometric measurement of potassium concentration in whole blood during open-heart surgery., *Clinical Chemistry 25*, 39-43.

206. Collison, M. E., and Meyerhoff, M. E. (1990) Chemical sensors for bedside monitoring of critically ill patients, *Analytical chemistry 62*, 425A-437A.

207. Garcia, R. P., Moreno, F. A., Garcia, M. E. D., Sanz-Medel, A., and Narayanaswamy, R. (1992) Serum analysis for potassium ions using a fibre optic sensor, *Clinica Chimica Acta 207*, 31-40.

208. Shortreed, M. R., Dourado, S., and Kopelman, R. (1997) Development of a fluorescent optical potassium-selective ion sensor with ratiometric response for intracellular applications, *Sensors and Actuators B: Chemical 38*, 8-12.

209. Johnson, R. D., Badr, I. H., Barrett, G., Lai, S., Lu, Y., Madou, M. J., and Bachas, L. G. (2001) Development of a fully integrated analysis system for ions based on ion-selective optodes and centrifugal microfluidics, *Analytical chemistry 73*, 3940-3946.

210. Watts, A. S., Urbas, A. A., Finley, T., Gavalas, V. G., and Bachas, L. G. (2006) Decyl methacrylate-based microspot optodes, *Analytical chemistry 78*, 524-529.

211. Wygladacz, K., and Bakker, E. (2005) Imaging fiber microarray fluorescent ion sensors based on bulk optode microspheres, *Analytica Chimica Acta 532*, 61-69.

212. Wang, K. S., K.; Morf, W. E.; Spichiger, U. E.; Simon, W.; Lindner, E.; Pungor, E. . (1990) Characterization of potassium-selective optode membranes based on neutral ionophores and application in human blood plasma. , *Analytical Sciences 6*, 715-720.

213. Ambrose, T. M. M., Mark E. (1996) Characterization of photopolymerized decyl methacrylate as a membrane matrix for ion-selective electrodes. , *Electroanalysis 8*, 1095-1100.

214. Badr, I. H. A., Johnson, R. D., Madou, M. J., and Bachas, L. G. (2002) Fluorescent Ion-Selective Optode Membranes Incorporated onto a Centrifugal Microfluidics Platform, *Analytical Chemistry 74*, 5569-5575.

215. Bakker, E., Buhlmann, P., and Pretsch, E. (1997) Carrier-Based Ion-Selective Electrodes and Bulk Optodes. 1. General Characteristics, *Chem. Rev. 97*, 3083-3132.

216. Bakker, E., and Simon, W. (1992) Selectivity of ion-sensitive bulk optodes, *Analytical Chemistry 64*, 1805-1812.

217. Golden, J. P., Anderson, G. P., Rabbany, S. Y., and Ligler, F. S. (1994) An evanescent wave biosensor--Part II: Fluorescent signal acquisition from tapered fiber optic probes, *IEEE Trans Biomed Eng 41*, 585-591.

218. Walker, K. H., Hall, D. W., and Hurst, W. J., (Eds.) (1990) *Clinical Methods: The History, Physical, and Laboratory Examinations*, 3rd ed., Butterworth-Heinemann Ltd.

219. Karplus, E. (2006) Advances in Instrumentation for Detecting Low-level Bioluminescence and Fluorescence, In *Photoproteins in Bioanalysis* (Daunert, S., and Deo, S. K., Eds.), pp 199-223, WILEY-VCH Verlag GmbH & Co. KGaA, Weinheim.

220. Dikici, E., Rowe, L., Moschou, E. A., Rothert, A., Deo, S. K., and Daunert, S. (2006) Luminescent proteins: applications in microfluidics and miniaturized analytical systems, *Photoproteins Bioanal.*, 179-198.

221. Plaeger, S., Bass, H. Z., Nishanian, P., Thomas, J., Aziz, N., Detels, R., King, J., Cumberland, W., Kemeny, M., and Fahey, J. L. (1999) The prognostic significance in HIV infection of immune activation represented by cell surface antigen and plasma activation marker changes, *Clin Immunol 90*, 238-246.

222. Varki, N. M., and Varki, A. (2007) Diversity in cell surface sialic acid presentations: implications for biology and disease, *Lab Invest 87*, 851-857.

223. Simpson, B. J., Ramage, A. D., Hulme, M. J., Burns, D. J., Katsaros, D., Langdon, S. P., and Miller, W. R. (1996) Cyclic adenosine 3',5'-

monophosphate-binding proteins in human ovarian cancer: correlations with clinicopathological features, *Clin Cancer Res 2*, 201-206.

224. Ishikawa, T., Hume, J., and Keef, K. (1993) Regulation of Ca2+ channels by cAMP and cGMP in vascular smooth muscle cells, *Circ Res 73*, 1128-1137.

225. Qiu, J., Zhou, Y., Chen, H., and Lin, J.-M. (2009) Immunomagnetic separation and rapid detection of bacteria using bioluminescence and microfluidics, *Talanta 79*, 787-795.

226. Daniel, R., Almog, R., Ron, A., Belkin, S., and Diamand, Y. S. (2008) Modeling and measurement of a whole-cell bioluminescent biosensor based on a single photon avalanche diode, *Biosensors and Bioelectronics 24*, 882-887.

227. Elman, N. M., Ben-Yoav, H., Sternheim, M., Rosen, R., Krylov, S., and Shacham-Diamand, Y. (2008) Towards toxicity detection using a lab-on-chip based on the integration of MOEMS and whole-cell sensors, *Biosensors and Bioelectronics 23*, 1631-1636.

228. Liu, B.-F., Ozaki, M., Hisamoto, H., Luo, Q., Utsumi, Y., Hattori, T., and Terabe, S. (2005) Microfluidic Chip toward Cellular ATP and ATP-Conjugated Metabolic Analysis with Bioluminescence Detection, *Analytical Chemistry 77*, 573-578.

VITA

Birth:
- March 11, 1983. Lexington, KY

Education:
- B.S., Chemistry (Biology minor), Georgetown College (Georgetown, KY), 2005.

Scholastic Honors:
- Integrative Graduate Education and Research Traineeship (IGERT) fellowship- NSF (2008-2010)
- Presidential Fellowship- University of Kentucky (2009-2010)
- NSF-IGERT Annual Meeting- Poster competition award winner (2009)
- Research Challenge Trust Fund (2005-2011)
- Summa Cum Laude, Georgetown College (2005)
- NAIA All-American Scholar Athlete- Baseball (2005)
- Dean's List, Georgetown College (2002-2005)
- Academic All-Conference, Mid-South Conference (2003-2005)
- Athletic Scholarship-Baseball (2002-2005)
- Christian Leadership Scholarship (2001-2005)
- Phi Kappa Phi National Honor Society, Georgetown College Chapter (2004)
- Alpha Lambda Delta National Honor Society, Georgetown College Chapter (2002)

Publications:

Scott, Daniel; Dikici, Emre; Ensor, C. Mark; Daunert, Sylvia.**Bioluminescence and its Impact in Bioanalysis**. *Annual Review of Analytical Chemistry*, 4, 297-319, 2011.

Scott, Daniel; Hamorsky, Krystal Teasley; Ensor, C. Mark; Anderson, Kim; Daunert, Sylvia. **Cyclic AMP Receptor Protein-Aequorin Protein Switch for Cyclic AMP**. *Bioconjugate Chemistry*, 22(3), 475-481, 2011.

Scott, Daniel; Moschou, Elizabeth; Daunert, Sylvia. **A portable, reagentless potassium sensor capable of real time, in vivo detection and monitoring**. *Analytical Chemistry*, Submitted, 2011.

Scott, Daniel; Ensor, C. Mark; Anderson, Kim; Daunert, Sylvia. **Simultaneous Cytokine Analysis via Semi-synthetic Aequorin Fusion Proteins.** *Analytical Chemistry*, Submitted, 2011.

Scott, Daniel; Dolci, Luisa Stella; Pancani, Tristano; Ensor, Mark; Thibault, Oliver; Daunert, Sylvia. **Genetically Enhanced Semi-Synthetic Aequorin Variant with Improved Detection and Imaging Capabilities.**To be submitted, 2011.

Ho, Vinh; Shimada, Mark; Szeto, David; Solvas, Xevi; Scott, Daniel; Dolci, Luisa Stella; Kulinsky, Lawrence; Daunert, Sylvia; Madou, Mark. **Utilization of Electroactive Polymer Actuators in Micromixing and in Extended-Life Biosensor Applications**" *Proc. of SPIE **7647**, 764735 (2010).*

Rowe, Laura; Ensor, Mark; Scott, Daniel; Deo, Sapna K.; Daunert, Sylvia.**Genetically Engineered Photoproteins in Biosensing.** *Proc. of SPIE*, 6098, 60980H1-60980H19, 2007.

Daniel Franklin Scott